AN ANALYSIS OF LINEAR INDUCTION MOTORS FOR PROPULSION AND SUSPENSION OF MAGNETICALLY LEVITATED VEHICLES

Fang-Chou Yang

Antenna Laboratory

Report No. 77

ACKNOWLEDGMENTS

This work was done under the supervision of Professor Charles H. Papas and the cognizance of Dr. Jay H. Harris of NSF.

ABSTRACT

A four-layer single-sided LIM used for propulsion and suspension of magnetically levitated vehicles is studied. The track is assumed to be made of conductors with uniaxial $\underset{\sim}{\mu}$ and $\underset{\sim}{\sigma}$. A general analysis allows us to exclude unsuitable geometries. The machine performance is given for the promising geometries. A possible way of computing the effective $\underset{\sim}{\mu}$ and $\underset{\sim}{\sigma}$ for a composite track is sketched. From the analysis of an extremely simplified geometry, the conditions for the validity of the effective $\underset{\sim}{\mu}$ and $\underset{\sim}{\sigma}$ concept are given. Finally, a three-dimensional correction is introduced.

TABLE OF CONTENTS

List of Symbols:

$\underline{A}$	vector
$\underline{\underline{A}}$	dyadic
$\tilde{A}$	Fourier component
$\bar{A}$	time average value
$A^{(c)}$	Quantity given according to Chu's formulation
A_i	i-component of vector $\underline{A}$, i = x,y,z
A^*	complex conjugate of A
ReA	real part of A
ImA	Imaginary part of A
a	$= \frac{k_y v}{\omega}$ in chapters III,IV = width of the source in the x-direction
$\underline{B}$	magnetic induction vector
d	skin depth (see 4.5c)
$\underline{E}$	electric field intensity vector
$\hat{\ell}_i$	unit vector along i-axis. i = x,y,z
$\underline{F}$	force vector
$\underline{H}$	magnetic field intensity vector
h_k	thickness of region k, k = 1,2,3,4
h	thickness of each lamination
$\underline{\underline{I}}$	identity matrix
$\underline{J}$	volume current density
$\underline{K}$	surface current density
$\underline{k}$	wave number vector
k_{yo}	wave number of the travelling wave source

L	half length of the stator covered by the travelling wave source.
P	power input
P_{mech}	mechanical power
P_{Loss}	induced current loss
PF	machine power factor
T_k	transfer matrix for region k as defined in (2.8), k=2,3
T_{ij}	ij component of the stress energy tensor, i,j=x,y,z
t_{ij}	ij component of T_3T_2 as defined in (2.13), i,j=1,2
$\underline{v}$	velocity of the track with respect to the vehicle, generally in the y-direction.
W_o	width of the reaction rail in the x-direction
$\tilde{Z}_s$	source winding impedance
$\tilde{Z}_L$	input impedance of the machine
β_k	wave number of region k as defined in (2.12), k=1,2,3,4
γ_k	wave number of region k as defined in (2.8), k=1,2,3,4
σ_{ki}	ii component of the conductivity of region k, k=2, i=x,y,z
μ_{ki}	ii component of the permeability of region k, k=1,2,3,4, i=x,y,z

CHAPTER I

INTRODUCTION

With the increasing need in traffic of people and commodities, automobiles have created serious pollution and noise problems; the airlines have also reached a high degree of saturation. Under the circumstances, it seems that the development of a rapid mass transportation system is desirable. Unfortunately, the conventional wheel-supported railways face some difficulties as the travelling speed becomes large. Not only does the noise become intolerable, but the small friction coefficient also inhibits the transmission of power between the rotating-type motor and the wheels. As a result, such non-contact systems as magnetic levitated (MAGLEV), track air cushion vehicles (TACV) are suggested as substitutions for future transportation.

Although the TACV is still a competitive candidate for high speed ground transportation (HSGT), in the following we will mainly consider the MAGLEV system.

There are two fundamental schemes for magnetic levitation, namely, attractive and repulsive schemes. The attractive system uses the attractive force between a magnetic field source and a ferromagnetic material. From Earnshaw's theorem, this kind of configuration is basically unstable, i.e., a smaller clearance will increase the attractive force and make the clearance even smaller. Thus, a feedback control system is necessary. For the repulsive scheme, the force exerted on a magnetic field source moving over a conductor by the

field of the induced eddy current within the conductor is employed. Such a system is inherently stable.

Extensive studies of these suspension systems have been made[1,2]. Definitely, the details will depend on source and track geometry. Certain general results will be described below. And actually, up to today, there is still no clear evidence as to which one is the better one. Both are noiseless, not limited by speed, and can be operated in vacuum. In reality the suspension system is only part of a whole HSGT vehicle. Thus, whether a system is optimized or not can only be judged by analyzing the whole vehicle from the tradeoff among the performances, technical merits, economic conditions, etc.

Generally speaking, in order to have a sufficiently supporting force, the attractive scheme can only allow a small clearance of about 1 or 2 cm, but the repulsive scheme can have a clearance of 20 cm. This will also play an important role in deciding what kinds of propulsion systems to use. Also, as we know, ferromagnetic materials are generally conductors. Thus, when the magnetic field source is moving over it, there always are eddy currents induced. This will give an undesired repulsive force component. When the velocity becomes large enough, sometimes this will result in a net repulsive force. Of course, we cannot allow this to happen. Thus, tracks and sources must be suitably designed to prevent this phenomenon from happening within the operating speed range. For the repulsive scheme, since it mainly depends on the eddy currents induced, eddy current losses are inevitable. These will give an additional drag force. An increased

propulsive force is necessary to overcome it. According to former analyses, it is found that at high speed this drag force will decay to a very small value. However, a very large drag force will exist at a very small speed. Certain methods[3] have been suggested to bypass this low speed drag.

Since the proposed suspension system is a non-contact one, the conventional method of using the direct reaction with the ground is not available. Thus, a new propulsion system is needed. In the early period, jets, propellers and rockets have been suggested. However, pollution and noise problems eventually led to the use of linear machines.

The idea of linear machines is not new. Back in the 19th century and the early 20th century, people have tried to apply it in train transportation, luggage handling, etc.[4,5]. However, due to economic and practical reasons, the interest in linear machines declined. Recently as Laithwaite[6,7,8] and Poloujadoff[4,5] put it, "engineering fashions" have been changing. Due to Laithwaite's continuous efforts in promoting them, linear machines are being reevaluated and they begin to be extensively used in HSGT, impact extrusion, E.M. pumps, actuators, etc.

Now, if the repulsive suspension scheme is used in HSGT, because of its high clearance perhaps the linear synchronous[9] motor is preferable. Also, power-pickup and weight problems are more easily handled by the linear synchronous motor. However, in the following discussions we will mainly consider linear induction motors. Linear synchronous motors will not be included.

The principle of the linear induction motor can be easily understood from the conventional rotating induction motor. Actually, the simplest form of LIM is just an unrolled rotating induction motor. A number of alternativeforms of LIMs serving different purposes can be constructed by just adding or changing the primary or the secondary structures. Laithwaite and Nasar[6] have given a complete classification in terms of the different possible topological configurations. Also, a "machine's good factor"[10] and a consideration of the economic problems were introduced to decide which kind of LIM is preferable. Among them, the "double-sided short primary sheet rotor motor" (DSLIM)[8,11,15,16] seems to be the best candidate for HSGT. Actually, the DSLIM had already been used in prototype HSGT vehicles built in Germany, the U.S., etc. But those vertically built DSLIMs suffered from several severe problems, such as lateral instability in curves, high cross sections of the vehicles, etc. Hence, an alternative, the single-sided LIM (SLIM)[12,13,14] was introduced. Although the analyses of these conventional rotating motors are well known and are not too difficult, the analysis of LIMs is much more complicated, due to the inevitable end effect and the dissymmetry of primary currents. Those extra effects will introduce undesirable phenomena. Today, research in LIMs concentrates on explaining these effects and looking for methods to compensate them. Yamamura and Ito[16], Wang[11], and Dukowicz[15] considered DSLIM with non-ferromagnetic sheet rotors. Nasar and Del Cid, Jr.[14] and Wang[13] discussed SLIMs with non-ferromagnetic sheet rotors backed by steel.

However, no matter which LIM was considered, up to now all of the analyses were made under the assumption of separated suspension and propulsion systems. Although an experimental vehicle has already been constructed by Rohr Inc.[17], no serious analysis has been made to consider a vehicle with a LIM used for both suspension and propulsion purposes. Of course, this would introduce extra control problems, but it also offers advantages such as less weight.

The SLIM analyzed by Nasar and Del Cid, Jr.[14], Wang[13], etc. will give either an attractive or a repulsive force, depending on the velocity of the vehicle. However, if we want the LIM to be used for both levitation and propulsion, a deeper analysis must be made as to which geometry and which material to select so that only either an attractive or a repulsive force is observed within the operating speed range.

The ferromagnetic track was ruled out as unsuitable for DSLIM by Laithwaite and Barwell[8] because of skin and nonlinear effects. These authors, however, were only concerned about the thrust force. As we want to include a levitating force, the inherent force between the magnetic field source and ferromagnetic material has to be reconsidered seriously. Furthermore, the undesired skin effect which gives rise to nonlinear effects can also be partly taken care of by suitably laminating the ferromagnetic material or composing the track both from ferromagnetic and non-ferromagnetic material.

The following discussion will begin with an investigation of the possibility of using a linear induction motor as a combined propulsion

and supporting system in a HSGT vehicle. Linear machines of four layers will be used as the starting point of the analysis. Most of the proposed configurations can be described by suitably specifying those parameters as conductivity, permeability, layer thickness, etc. for different regions. The analysis of machine performance will exclude unsuitable geometries and give possible methods to reduce the undesired end effects. Expressions for machine performances will then be evaluated for those promising geometries.

A possible way of computing the effective conductivity and permeability for a composite track will be sketched. Up to now these parameters were determined experimentally, and no theoretical analysis has ever been attempted. Definitely, it is difficult. An extremely simplified geometry will be considered to check the validity of this effective conductivity and permeability concept. Possible necessary conditions for the validity will then be given. Starting from this point, another possible configuration will be suggested and analyzed. The transfer matrix method is employed to solve the 2-dimensional problem. At the end of this discussion, a 3-dimensional correction will be introduced. Of course, the previously nonexistent lateral force will now appear. A corresponding quantitative approximation will then be given.

CHAPTER II

GENERAL FORMULATION

The linear induction motors which will be considered consist of four layers as shown in Fig. 2.1. The source with a given current or B-field distribution (depending on how the source is connected) is located at the interface of regions 3 and 4. Region 3 is the free space. Regions 1 and 4 are any zero conductivity material, such as the infinitely laminated iron or free space. Regions 1 and 2 which make up the track are moving at a constant velocity $\underline{v}$ relative to the source. The material properties of region 2 in its rest frame are arbitrarily specified by constant conductivity and constant permeability uniaxial tensors $\underset{\sim}{\sigma} = \sigma_j \delta_{ij} \hat{e}_i \hat{e}_j$, $\underset{\sim}{\mu} = \mu_j \delta_{ij} \hat{e}_i \hat{e}_j$ $(i,j = x,y,z)$ respectively. These constants can generally describe the material used in LIMs satisfactorily.

Maxwell's equations involving moving magnetic material are complicated. However, in this case, neglecting the displacement current and relativistic effects is always a good approximation. In the rest frame of the source, Maxwell's equations can then be simplified to give us (see Appendix A):

$$\nabla \times \underline{E} = - \frac{\partial \underline{B}}{\partial t} \tag{2.1a}$$

$$\nabla \times \underline{H} = \underline{J} \tag{2.1b}$$

$$\underline{J} = \underset{\sim}{\sigma} \cdot (\underline{E} + \underline{v} \times \underline{B}) \tag{2.1c}$$

$$\underline{B} = \underset{\sim}{\mu} \cdot \underline{H} \tag{2.1d}$$

or, for a nonsingular $\underset{\sim}{\sigma}$ (i.e., region 2)

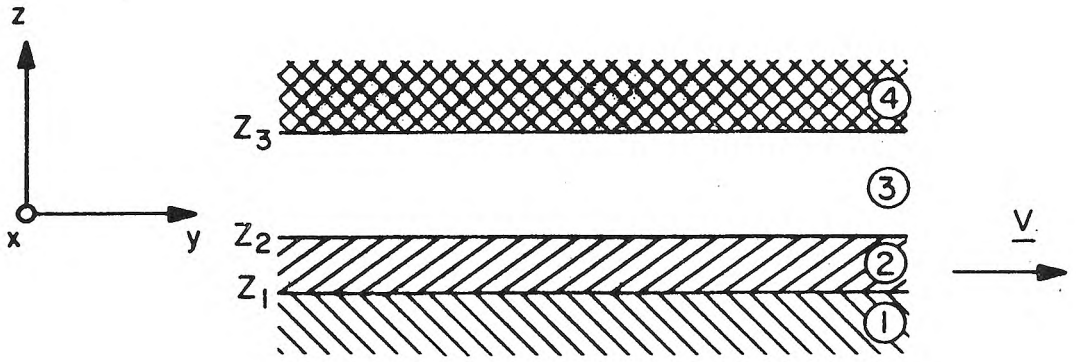

Fig. 2.1

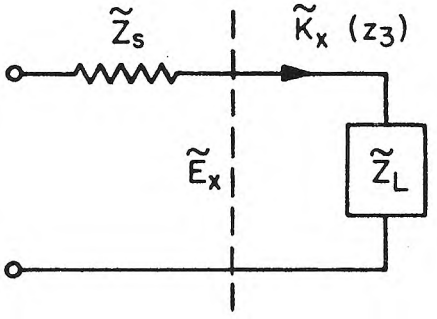

Fig. 2.2

$$\nabla \times [\underset{\sim}{\sigma}^{-1} \cdot (\nabla \times \underline{H})] = -\frac{\partial}{\partial t}(\underset{\sim}{\mu} \cdot \underline{H}) - (\underline{v} \cdot \nabla)(\underset{\sim}{\mu} \cdot \underline{H}) \tag{2.2a}$$

$$\nabla \times [\underset{\sim}{\mu}^{-1} \cdot (\nabla \times \underline{E})] = -\frac{\partial}{\partial t}(\underset{\sim}{\sigma} \cdot \underline{E}) + \underset{\sim}{\sigma} \cdot (\underline{v} \times \nabla \times \underline{E}) \tag{2.2b}$$

$$\underline{J} = \underset{\sim}{\sigma} \cdot [\underline{E} + \underline{v} \times (\underset{\sim}{\mu} \cdot \underline{H})] \tag{2.2c}$$

$$\underline{B} = \underset{\sim}{\mu} \cdot \underline{H} \tag{2.2d}$$

and, for $\underset{\sim}{\sigma} = 0$ (i.e., regions 1,3,4)

$$\nabla \times [\underset{\sim}{\mu}^{-1} \cdot (\nabla \times \underline{E}] = 0 \tag{2.3a}$$

$$\nabla \times \underline{H} = \underline{J} = 0 \tag{2.3b}$$

$$\nabla \cdot (\underset{\sim}{\mu} \cdot \underline{H}) = 0 \tag{2.3c}$$

$$\underline{B} = \underset{\sim}{\mu} \cdot \underline{H} \tag{2.3d}$$

With a $e^{-i\omega t}$ time dependence, a Fourier transform pair, given in (2.4a) and (2.4b), can be introduced to solve the differential equations:

$$\tilde{\underline{A}}(k_x,k_y,z) = \frac{1}{2\pi} \int_{-\infty}^{\infty} \int_{-\infty}^{\infty} \underline{A}(x,y,z)\, e^{-ik_x x - ik_y y}\, dxdy \tag{2.4a}$$

$$\underline{A}(x,y,z) = \frac{1}{2\pi} \int_{-\infty}^{\infty} \int_{-\infty}^{\infty} \underline{A}(k_x,k_y,z)\, e^{ik_x x + ik_y y}\, dk_x dk_y \tag{2.4b}$$

Then, by applying suitable boundary conditions, in principle, the problem has a unique solution.

However, generally this is tedious. To make the problem easier, we assume at first that the source is infinitely extended along the x-axis. Thus, x-dependence can be suppressed. The 3-dimensional correction for some simple geometries will be made later in Chapter V.

For this 2-dimensional problem with the coordinate system as shown, the only non-zero components of $\underline{\tilde{E}}$, $\underline{\tilde{H}}$, $\underline{\tilde{J}}$ are $\tilde{E}_x$, $\tilde{H}_y$, $\tilde{H}_z$, $\tilde{J}_x$. As suggested by Freeman[18], Cullen and Barton[19], etc., the transfer matrix method can be used to find the field. Actually we have:

Region 1:

$$\begin{bmatrix} \tilde{B}_z(z_1) \\ \tilde{H}_y(z_1) \end{bmatrix} = e^{-\gamma_1(z_1-z)} \begin{bmatrix} \tilde{B}_z(z) \\ \tilde{H}_y(z) \end{bmatrix} \tag{2.5}$$

with $\tilde{H}_y(z) = \beta_1 \tilde{B}_z(z)$ (2.6)

Regions 2,3:

$$\begin{bmatrix} \tilde{B}_z(z) \\ \tilde{H}_y(z) \end{bmatrix} = T_k(z) \begin{bmatrix} \tilde{B}_z(z_{k-1}) \\ \tilde{H}_y(z_{k-1}) \end{bmatrix} \tag{2.7}$$

with $z_{k-1} < z < z_k$, k=2,3.

$$T_k(z) = \begin{bmatrix} \cosh \gamma_k(z-z_{k-1}) & \frac{1}{\beta_k} \sinh \gamma_k(z-z_{k-1}) \\ \beta_k \sinh \gamma_k(z-z_{k-1}) & \cosh \gamma_k(z-z_{k-1}) \end{bmatrix} \tag{2.8}$$

Region 4:

$$\begin{bmatrix} \tilde{B}_z(z) \\ \tilde{H}_y(z) \end{bmatrix} = e^{-\gamma_4(z-z_3)} \begin{bmatrix} \tilde{B}_z(z_3) \\ \tilde{H}_y(z_3) \end{bmatrix} \tag{2.9}$$

with $\tilde{H}_y(z) = -\beta_4 \tilde{B}_z(z)$ (2.10)

Also, in the above

$$\gamma_k = \left[\frac{\mu_{ky}}{\mu_{kz}} k_y^2 - i(\omega - k_y v)\, \mu_{ky}\sigma_{kx}\right]^{1/2} \tag{2.11}$$

$$\beta_k = \frac{\gamma_k}{-i\, \mu_{ky}\, k_y} \tag{2.12}$$

γ_k are suitably chosen such that they contain only positive real parts.

In these formulas the boundary conditions can then be introduced. The field distribution in the whole space can be obtained. Now the case with a specified current source will be considered (i.e., series connected source):

The continuity conditions of $\tilde{B}_z$, $\tilde{H}_y$ at z_1, z_2 give

$$\begin{bmatrix} \tilde{B}_z(z_3-\varepsilon) \\ \tilde{H}_y(z_3-\varepsilon) \end{bmatrix} = T_3(z_3)\, T_2(z_2) \begin{bmatrix} \tilde{B}_z(z_1) \\ \tilde{H}_y(z_1) \end{bmatrix} \tag{2.13a}$$

$$= \begin{bmatrix} t_{11} & t_{12} \\ t_{21} & t_{22} \end{bmatrix} \begin{bmatrix} \tilde{B}_z(z_1) \\ \beta_1 \tilde{B}_z(z_1) \end{bmatrix} \tag{2.13b}$$

Here ε is positive but small. $t_{ij} = [T_3(z_3)\, T_2(z_2)]_{ij}$ are the elements of $T_3(z_3)\, T_2(z_2)$.

The boundary conditions at z_3 give

$$\tilde{H}_y(z_3+\varepsilon) = \tilde{H}_y(z_3-\varepsilon) - \tilde{K}_x \tag{2.14a}$$

$$= -\beta_4 \tilde{B}_z(z_3+\varepsilon) \tag{2.14b}$$

$$= -\beta_4 \tilde{B}_z(z_3-\varepsilon) \tag{2.14c}$$

$\tilde{K}_x$ is the Fourier component of the specified current distribution. Combine (2.13), (2.14) to get:

$$\tilde{B}_z(z_1) = \frac{1}{(t_{21}+\beta_1 t_{22}) + \beta_4(t_{11}+\beta_1 t_{12})}\,\tilde{K}_x \tag{2.15a}$$

$$\tilde{B}_z(z_3-\varepsilon) = \frac{t_{11}+\beta_1 t_{12}}{(t_{21}+\beta_1 t_{22}) + \beta_4(t_{11}+\beta_1 t_{12})}\,\tilde{K}_x \tag{2.15b}$$

The Fourier components of the field distribution can be obtained from equations (2.5) to (2.12). The field distribution in real space can then be obtained by using the Fourier inverse transform (2.4b).

From the above derivation, it is obvious that the problem can also be solved by applying transmission line theory. With the field components $\tilde{E}_x = -\frac{\omega}{k_y}\tilde{B}_z$ and $\tilde{H}_y$ serving as the voltage and the current respectively, the characteristic impedance can easily be defined. Afterward the field distribution can be obtained by suitably matching the input impedance or by using the Smith chart. Once we know the field distribution, we can evaluate the machine performances. Among them, the forces, efficiency, power input, power factor are the most important.

As described by Fano, Chu, Adler[20] in calculating forces involving magnetic material, the Minkowski formulation which we have used so far cannot give satisfactory results. Thus, an alternative called Chu's formulation is introduced. By using this new formulation, the forces within the magnetic material can be clearly explained. Details concerning the forces existing in the given LIM systems are included in Appendix A. In our problem, the force which has to be calculated is just the total force exerted on the source, which by the principle of reaction, is just the total force acting on the combined regions 1 and 2. According to Chu's formulation, this force can be obtained simply

by integrating the Maxwell's stress energy tensor over the surface in the free space just outside of region 2, i.e.,

$$F_i = \int_S T_{ij}^{(c)} \, ds_j \qquad (i,j = x,y,z) \tag{2.16a}$$

with

$$T_{ij}^{(c)} = \varepsilon_o[E_i^{(c)} E_j^{(c)} - \frac{1}{2}\delta_{ij}|\underline{E}^{(c)}|^2 + \mu_o[H_i^{(c)}H_j^{(c)} - \frac{1}{2}\delta_{ij}|\underline{H}^{(c)}|^2] \tag{2.16b}$$

Fortunately, in the free space, the Maxwell's stress energy tensors for Chu's and Minkowski's formulations happen to be the same. Furthermore, in the free space, the electric part of the stress energy tensor is always small compared to the magnetic part. Definitely, it can be neglected, and actually this is equivalent to neglecting the displacement current which was done at the very beginning. Thus, the calculation of forces can be simplified. Finally, the time averaged total forces are given by:

$$\overline{F}_i = \frac{1}{2}\,\mathrm{Re}\int_S \overline{T_{ij}} \, ds_j \tag{2.17}$$

with

$$\overline{T}_{ij} = \mu_o[H_i H_j^* - \frac{1}{2}\delta_{ij}|\underline{H}|^2] \tag{2.18}$$

Thus, for the 2-dimensional case:

$$\overline{F}_x = 0 \tag{2.19}$$

$$\overline{F}_y = \frac{1}{2}\,\mathrm{Re}\int_{-\infty}^{\infty} H_y(z_2)B_z^*(z_2)\, dy \tag{2.20a}$$

$$= \frac{1}{2}\,\mathrm{Re}\int_{-\infty}^{\infty} \tilde{H}_y(z_2)\tilde{B}_z^*(z_2)\, dk_y \tag{2.20b}$$

$$\bar{F}_z = \frac{\mu_o}{4} \mathrm{Re} \int_{-\infty}^{\infty} \left[\frac{B_z(z_2)B_z^*(z_2)}{\mu_o^2} - H_y(z_2)H_y^*(z_2)\right] dy \qquad (2.21a)$$

$$= \frac{\mu_o}{4} \mathrm{Re} \int_{-\infty}^{\infty} \left[\frac{|\tilde{B}_z(z_2)|^2}{\mu_o^2} - |\tilde{H}_y(z_2)|^2\right] dky \qquad (2.21b)$$

where the $\bar{F}_i$ represent the forces acting on a unit length of source in the x direction. Combine (2.20), (2.21), (2.15) and (2.7) to get the forces for the case of a specified current source:

$$\bar{F}_y = \frac{1}{2} \mathrm{Re} \int_{-\infty}^{\infty} \frac{[t_{21}^{(2)}(z_2) + \beta_1 t_{22}^{(2)}(z_2)][t_{11}^{(2)}(z_2) + \beta_1 t_{12}^{(2)}(z_2)]^*}{|(t_{21} + \beta_1 t_{22}) + \beta_4(t_{11} + \beta_1 t_{12})|^2} \times |\tilde{K}_x|^2 \, dky \qquad (2.22)$$

$$\bar{F}_z = \frac{\mu_o}{4} \mathrm{Re} \int_{-\infty}^{\infty} \frac{\frac{1}{2}|t_{11}^{(2)}(z_2) + \beta_1 t_{12}^{(2)}(z_2)|^2 - |t_{21}^{(2)}(z_2) + \beta_1 t_{22}^{(2)}(z_2)|^2}{|(t_{21} + \beta_1 t_{22}) + \beta_4(t_{11} + \beta_1 t_{12})|^2} \times |\tilde{K}_x|^2 \, dky \qquad (2.23)$$

where $t_{ij}^{(2)}(z_2)$ are the elements of matrix $T_2(z_2)$.

Sometimes it is easier to evaluate the stress energy tensor integral at the surface $z_3-\varepsilon$. Then we get:

$$\bar{F}_y = \frac{1}{2} \mathrm{Re} \int_{-\infty}^{\infty} \frac{(t_{21} + \beta_1 t_{22})(t_{11} + \beta_1 t_{12})^*}{|(t_{21} + \beta_1 t_{22}) + \beta_4(t_{11} + \beta_1 t_{12})|^2} |\tilde{K}_x|^2 \, dky \qquad (2.24)$$

$$\bar{F}_z = \frac{\mu_o}{4} \mathrm{Re} \int_{-\infty}^{\infty} \frac{\frac{1}{2}|t_{11} + \beta_1 t_{12}|^2 - |t_{21} + \beta_1 t_{22}|^2}{|(t_{21} + \beta_1 t_{22}) + \beta_4(t_{11} + \beta_1 t_{12})|^2} |\tilde{K}_x|^2 \, dky \qquad (2.25)$$

The average mechanical power input is:

$$\overline{P}_{mech} = \underline{\overline{F}} \cdot \underline{v} = \overline{F}_y \, v \tag{2.26}$$

The average power input is:

$$\overline{P} = \frac{1}{2} \int_{-\infty}^{\infty} E_x(z_3) \, K_x^*(z_3) \, dy \tag{2.27a}$$

$$= \frac{1}{2} \int_{-\infty}^{\infty} \tilde{E}_x(z_3) \tilde{K}_x^*(z_3) \, dk_y \tag{2.27b}$$

$$= \frac{1}{2} \int_{-\infty}^{\infty} \frac{\omega}{k_y} \tilde{B}_z(z_3) \, \tilde{K}_x^*(z_3) \, dk_y \tag{2.27c}$$

$$= \frac{1}{2} \int_{-\infty}^{\infty} \frac{\omega}{k_y} \frac{t_{11} + \beta_1 t_{12}}{(t_{21} + \beta_1 t_{22}) + \beta_4 (t_{11} + \beta_1 t_{12})} |\tilde{K}_x|^2 \, dk_y \tag{2.27d}$$

Power factor is given by:

$$PF = \frac{\text{Re } \overline{P}}{|\overline{P}|} \tag{2.28}$$

Efficiency is defined as:

$$\eta = \frac{\overline{P}_{mech}}{\text{Re } \overline{P}} \tag{2.29}$$

Finally, the induced eddy current loss is found from:

$$\overline{P}_{loss} = \text{Re } \overline{P} - \overline{P}_{mech} \tag{2.30a}$$

or

$$\overline{P}_{loss} = -\frac{1}{2} \text{Re} \int_{-\infty}^{\infty} \left(\frac{\omega}{k_y} - v\right) \frac{t_{11} + \beta_1 t_{12}}{(t_{21} + \beta_1 t_{22}) + \beta_4 (t_{11} + \beta_1 t_{12})} |\tilde{K}_x|^2 dk_y \tag{2.30b}$$

By inspection of the above formulas, an equivalent circuit can be constructed as shown in Fig. 2.2, with

$$\tilde{Z}_L = \frac{\omega}{k_y}(t_{21} + \beta_1 t_{22}) + \beta_4(t_{11} + \beta_1 t_{12})$$

and thus $\overline{P}$ can be rewritten as:

$$\overline{P} = \frac{1}{2}\int_{-\infty}^{\infty} \tilde{Z}_L \, |\tilde{K}_x|^2 \, dk_y$$

Now $\tilde{Z}_L$ can be decomposed into three parts:

$$\tilde{Z}_L = +i \, \mathrm{Im}(\tilde{Z}_L) + \frac{k_y v}{\omega} \, \mathrm{Re}(\tilde{Z}_L) + (1 - \frac{k_y v}{\omega}) \, \mathrm{Re}(\tilde{Z}_L)$$

The term $\frac{k_y v}{\omega} \, \mathrm{Re}\, \tilde{Z}_L$ contributes to the mechanical power, while $(1 - \frac{k_y v}{\omega})\mathrm{Re}\, \tilde{Z}_L$ gives the induced eddy current loss. Thus, in order to have a high efficiency or a low energy loss, $|\tilde{K}_x|^2$ is required to be concentrated around k_{yo} such that $1 - \frac{k_{yo} v}{\omega}$ is small. The imaginary part $\mathrm{Im}\, \tilde{Z}_L$ represents the difference between the average stored electric energy and magnetic energy. However, as we understand it, in this case the stored electric energy is relatively small compared to the stored magnetic energy. So the term $\mathrm{Im}\, \tilde{Z}_L$ will mainly take care of the average stored magnetic energy of the system.

In the above, the problem of a source with specific current distribution at z_3 is analyzed. Basically, this is the case of the so-called series-connected source. The case of a parallel-connected source with a specified $\underline{B}$ field distribution at z_3 can be analyzed in the same way. Definitely, if the source is infinitely extended such that it can be described as a travelling wave, it does not make any difference whether the source is series or parallel connected. However, their behavior is quite different for a more realistic source. We do not intend to

consider the parallel-connected case here.

This completes the general analysis. In the next chapter we shall start from this general formulation and consider several examples.

CHAPTER III

SEVERAL EXAMPLES

Up to now, the source circuit has been neglected in all of the analyses. But, in the machine design, there is always a source winding resistance $\tilde{Z}_s$. And no matter what kind of source connection is used, it is quite clear that $|\tilde{Z}_L| >> \tilde{Z}_s$ around k_{yo} is necessary to make the source winding loss small. Surely, under certain circumstances, the value of $\beta_4 \cong 0$ (i.e., using infinitely laminated iron in region 4 as assumed in nearly all of the LIMs considered in previously published papers) will achieve this. But this also means additional weight to the vehicles. Thus, other lighter material with a different $\underset{\sim}{\mu}$ can also be used. As pointed out previously, the LIMs are supposed to be used for both suspension and propulsion. Thus, if $\frac{1}{\mu_o^2} \frac{|t_{11}+ \beta_1 t_{12}|^2}{|t_{21}+ \beta_1 t_{22}|^2} >> 1$ around k_{yo} is required in (2.25) to give a sufficient attractive supporting force, $\beta_4 \cong 0$ is suggested. On the other hand, if $\frac{1}{\mu_o^2} \frac{|t_{11}+ \beta_1 t_{12}|^2}{|t_{21}+ \beta_1 t_{22}|^2} << 1$ around k_{yo} is required in (2.25) to give a sufficient repulsive supporting force, then the effect of β_4 can be neglected. Definitely, for the general case, the trade-off among the weight, cost of material in regions 3, 4, and the source winding loss, will determine what value of β_4 is superior in the machine design. But, unfortunately, the arbitrariness of β_4 will make the Fourier inverse integrals much more complicated to evaluate. Thus, in the following, only two extreme cases of $\beta_4 \cong 0$ for the infinitely laminated iron and $\beta_4 = i/\mu_o$ for the free space will be discussed; and other values of β_4 lying between them will be guessed

to give intermediate results.

The same assumptions can be made for β_1 . However, because region 1 is not on the vehicle, weight is not a serious problem. In reality, the earth (which can be considered as a free space) with $\beta_1 = i/\mu_o$, and infinitely laminated back iron with $\beta_1 \cong 0$, are most practical and will be considered in the following as the only possibilities.

Analytically evaluating the integrals (2.24) to (2.30) is very difficult, if not impossible. Only two extreme approximations, namely, thin and thick reaction rails, will be considered. That a reaction rail is thin or thick is defined by $|\gamma_2 h_2| << 1$ or $|\gamma_2 h_2| >> 1$ around k_{yo} where $|\tilde{K}_x|^2$ is large. The details about when those approximations are reasonable in describing the LIMs are given in Appendix B.

Under these assumptions, simplifications can definitely be made in (2.24) to (2.30) to evaluate the performance of the LIMs. However, instead of doing this immediately, we will first try to analyze the integrands. It will be found that this is a convenient way of looking into the system-optimizing problem and the compensation for end effects. First, let us consider the case with $\beta_1 \cong 0$.

(A) $\beta_1 \cong 0$: (region 1 is infinitely laminated iron)

From (2.8), (2.13), (2.31):

$$\tilde{Z}_L = \frac{-i\omega\mu_o}{k_z} \frac{1 + \frac{\mu_o \gamma_2}{\mu_{2y} k_z} \tanh \gamma_2 h_2 \tanh k_z h_3}{(\tanh k_z h_3 + \frac{\mu_o \gamma_2}{\mu_{2y} k_z} \tanh \gamma_2 h_2) + \alpha(1 + \frac{\mu_o \gamma_2}{\mu_{2y} k_z} \tanh \gamma_2 h_2 \tanh k_z h_3)} \tag{3.1}$$

$$\tilde{F}_y = \mathrm{Re}\,\frac{-i\mu_o}{2}\,\mathrm{Sgn}(k_y) \times \frac{1 + \frac{\mu_o\gamma_2}{\mu_{2y}k_z}\tanh\gamma_2h_2\,\tanh k_zh_3}{(\tanh k_yh_3 + \frac{\mu_o\gamma_2}{\mu_{2y}k_z}\tanh\gamma_2h_2) + \alpha(1 + \frac{\mu_o\gamma_2}{\mu_{2y}k_z}\tanh\gamma_2h_2\,\tanh k_zh_3)}\,|\tilde{K}_x|^2 \tag{3.2}$$

$$\tilde{F}_z = \frac{\mu_o}{4}\,\mathrm{Re} \times \frac{(1 - \frac{\mu_o^2|\gamma_2|^2}{\mu_{2y}\,k_y^2}\,|\tanh\gamma_2h_2|^2)\mathrm{sech}^2k_zh_3}{|(\tanh k_yh_3 + \frac{\mu_o\gamma_2}{\mu_{2y}k_z}\tanh\gamma_2h_2) + \alpha(1 + \frac{\mu_o\gamma_2}{\mu_{2y}k_z}\tanh\gamma_2h_2\,\tanh k_zh_3|^2}\,|\tilde{K}_x|^2 \tag{3.3}$$

Here $\alpha = \frac{\mu_o}{\sqrt{\mu_{4y}\mu_{4z}}}$, $k_z = |k_y|$. And $\tilde{F}_y$, $\tilde{F}_z$ are the integrands for the force integrals $\bar{F}_y, \bar{F}_z$ respectively. h_2, h_3 are respectively the thickness of regions 2 and 3.

It is not difficult to show that for a real k_y both $P_1 = (1 + \frac{\mu_o\gamma_2}{\mu_{2y}k_z}\tanh\gamma_2h_2\,\tanh k_zh_3)$ and $P_2 = (\tanh k_zh_3 + \frac{\mu_o\gamma_2}{\mu_{2y}k_z}\cdot\tanh\gamma_2h_2)$ have positive real parts. And, their imaginary parts will have the same signs as those of γ_2.

Thus, for a given source current distribution, a nonzero value of α will result in smaller total power input and forces, and thus degrade machine performance. Of course, as pointed out before, the effect of this term α will strongly depend on the relative magnitude of P_1 and P_2. Now, the thin and thick reaction rail assumption will be used to simplify the problem.

(i) Thin reaction rails:

Since $|\gamma_2 h_2|$ is small, the approximation that $\tanh \gamma_2 h_2 \cong \gamma_2 h_2$ can be made. Also, for LIMs used in HSGT, h_3 has to be small, i.e., $\tanh k_z h_3 \cong k_z h_3$ is also a reasonable approximation. We can now begin to consider different kinds of LIMs.

(i-1) $\alpha \cong 0$: (region 4 is infinitely laminated iron)

This is the most popular SLIM considered by Nasar, Del Cid, Jr.[14], Wang[13], etc. The result can also be directly applied to obtain the performance of DSLIM analyzed by Yamamura and Ito[16], Wang[11], and Dukowicz[15].

From (3.1), (3.2), (3.3), we get:

$$\tilde{Z}_L \cong \frac{-i\omega\mu_o}{k_y} \frac{\mu_{2y} k_y}{\mu_{2y} k_y^2 h_3 + \mu_o \gamma_2^2 h_2} \tag{3.4a}$$

$$= -i\omega\mu_o \frac{1}{k_y^2 - i(\omega - k_y v)K_1} \frac{\mu_{2z}}{\mu_{2z} h_3 + \mu_o h_2} \tag{3.4b}$$

$$= -i\omega\mu_o \frac{k_y^2 + i(\omega - k_y v)K_1}{k_y^4 + (\omega - k_y v)^2 K_1^2} \frac{\mu_{2z}}{\mu_{2z} h_3 + \mu_o h_2} \tag{3.4c}$$

$$\tilde{F}_y \cong \mathrm{Re} \frac{-i\mu_o}{2} \frac{\mu_{2y} k_y}{\mu_{2y} k_y^2 h_3 + \mu_o \gamma_2^2 h_2} |\tilde{K}_x|^2 \tag{3.5a}$$

$$= \mathrm{Re} \frac{-i\mu_o}{2} \frac{k_y}{k_y^2 - i(\omega - k_y v)K_1} \frac{\mu_{2z}}{\mu_{2z} h_3 + \mu_o h_2} |\tilde{K}_x|^2 \tag{3.5b}$$

$$= \frac{K_1^2}{2\sigma_x h_2} \frac{k_y(\omega - k_y v)}{k_y^4 + (\omega - k_{yv})^2 K_1^2} |\tilde{K}_x|^2 \tag{3.5c}$$

$$\tilde{F}_z \cong \frac{\mu_o}{4} \frac{\mu_{2y}^2 k_y^2 - \mu_o^2 |\gamma_2|^4 h_2^2}{|\mu_{2y} k_y^2 h_3 + \mu_o \gamma_2^2 h_2|^2} |\tilde{K}_x|^2 \tag{3.6a}$$

$$\cong \frac{\mu_o}{4} \frac{k_y^2 - (\omega - k_y v)^2 \mu_o^2 \sigma_x^2 h_2^2}{k_y^4 + (\omega - k_y v)^2 K_1^2} \frac{\mu_{2z}^2}{(\mu_{2z} h_3 + \mu_o h_2)^2} |\tilde{K}_x|^2 \tag{3.6b}$$

Here $K_1 = \dfrac{\mu_\sigma \sigma_x \mu_{2z} h_2}{\mu_{2z} h_3 + \mu_o h_2}$. It should be noticed that μ_2 always appears in the form of $\mu_{2z}/(\mu_{2z} h_3 + \mu_o h_2)$. Thus, except in the case that $h_2 >> h_3$, which is generally not true in this thin reaction rail geometry, the effect of the permeability is small.

After some tedious algebraic manipulations, $\dfrac{\tilde{F}_y}{|\tilde{K}_x|^2}$, $\dfrac{\tilde{F}_z}{|\tilde{K}_x|^2}$, $\tilde{Z}_L$ are plotted as functions of k_y in Fig. 3.1. With "a" defined as $k_y v/\omega$, it is found that $\tilde{F}_z/|\tilde{K}_x|^2 = 0$ at $a = a_z \cong \dfrac{1}{1 + \dfrac{1}{\mu_o \sigma_x h_2 v}}$. Also, $\tilde{F}_y/|\tilde{K}_x|^2$, Re $\tilde{Z}_L$, Im $\tilde{Z}_L$ have extrema at "a" equal to a_y, a_r, a_i satisfying equations given below, respectively:

$$2a_y^5 - 3a_y^4 + (1 - a_y)^2 \frac{K_1^2 v^4}{\omega^2} = 0 \tag{3.7a}$$

$$3a_r^4 - 4a_r^3 + (1 - a_r)^2 \frac{K_1^2 v^4}{\omega^2} = 0 \tag{3.7b}$$

$$-a_i^2 + (1 - a_i) \frac{K_1^2 v^4}{\omega^2} = 0 \tag{3.7c}$$

From these plots, it is quite obvious that different arrangements of $|\tilde{K}_x|^2$ can give machines which can be used for different purposes, (e.g., braking or propulsion in HSGT, or even other than HSGT systems). However, LIMs used for both propulsion and levitation are our only concern now.

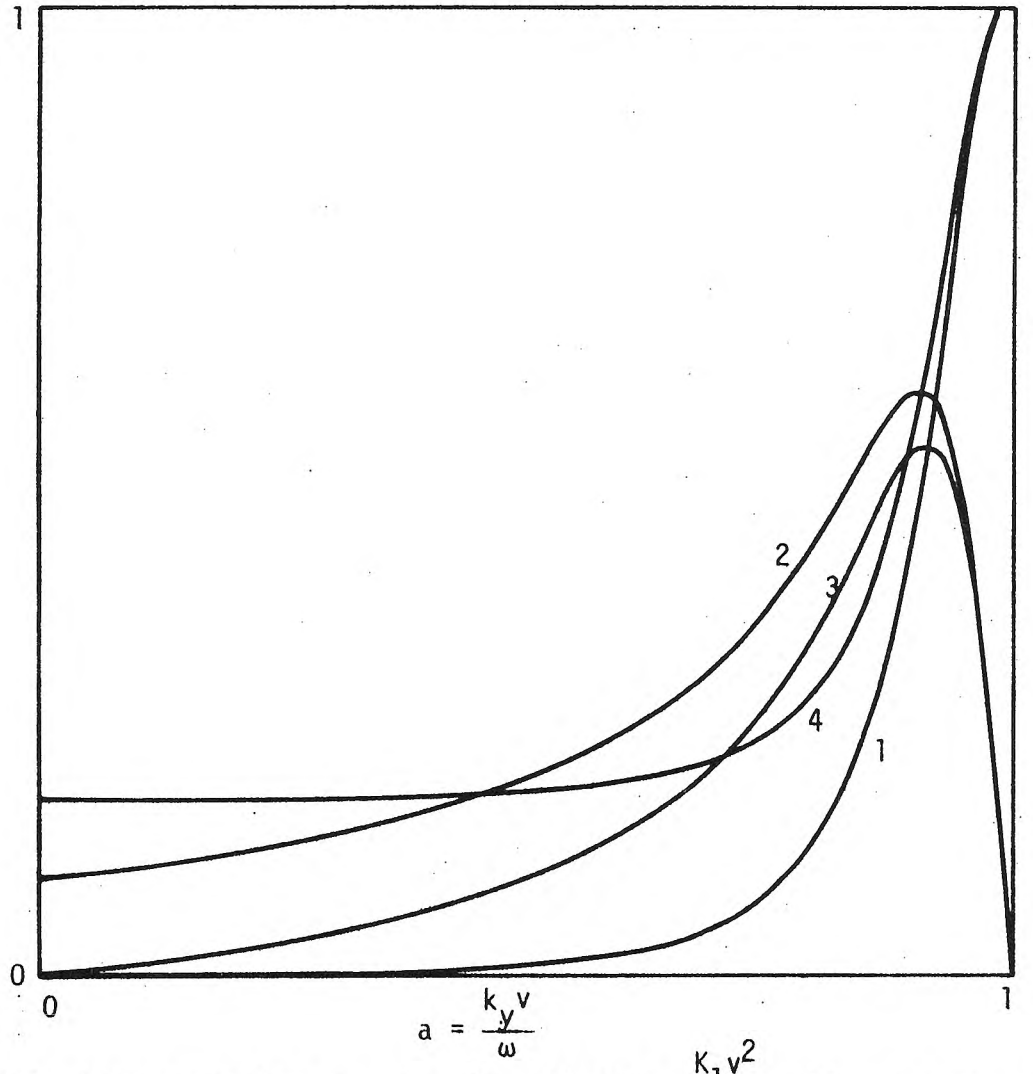

Fig. 3.1 Integrands for geometry (A-i-1) with $\frac{K_1 v^2}{\omega} = 10$, $\mu_o \sigma_x v h_2 = 2.$

(1) Re $\{\frac{\tilde{Z}_L}{-i\mu_o} \frac{\omega}{v^2} \frac{\mu_{2z} h_3 + \mu_o h_2}{\mu_{2z}}\}$, (2) Im $\{\frac{\tilde{Z}_L}{-i\mu_o} \frac{\omega}{v^2} \frac{\mu_{2z} h_3 + \mu_o h_2}{\mu_{2z}}\}$,

(3) $\frac{\tilde{F}_y}{|\tilde{K}_x|^2} \frac{20 \sigma_x h_2 \omega^2}{K_1^2 v^3}$, (4) $\frac{\tilde{F}_z}{|\tilde{K}_x|^2} \frac{3.2\omega^2 (\mu_{2z} h_3 + \mu_o h_2)^2}{\mu_o v^2 \mu_{2z}^2} + 0.2$

In order to get a net propulsion force, $k_{yo} = a_o \frac{\omega}{v}$ is generally required to satisfy $1 > a_o > 0$. Thus, in the following, only this region will be considered. Now, we will look more carefully into equations (3.4), (3.5), (3.6), especially (3.5).

It can be shown that there will only be one value of "a" satisfying each of the equations (3.7) for $1 \geq a \geq 0$. And, for those roots, $a_i > a_y > a_r$ are always true. Also, $a_y > a_z$ can be obtained for this thin reaction rail case. From (3.7a), a_y is found to be a monotonically increasing function of $K_1 v^2 / \omega$.

Whether the machine has a repulsive or an attractive levitation force depends mainly on whether a_o is smaller or larger than a_z. Nevertheless, a small $a_o < a_z$ generally means a larger energy loss and thus a smaller efficiency. Since $a_y > a_z$ is always true, a small $a_o < a_z$ also means a small thrust force. Furthermore, it is noticed that the maximum value of positive $\tilde{F}_z / |\tilde{K}_x|^2$ is always much larger than that of repulsive $\tilde{F}_y / |\tilde{K}_x|$, (actually the ratio is about $1 : \frac{\omega^2}{v^2} h^2$). So, this kind of LIM configuration is not good for use as a repulsive levitation system. Thus, it is preferable to use a source with $1 > a_o > a_z$ such that a net attractive and a large propulsive force can be obtained.

Two methods are suggested to operate the LIMs such that the above requirements of $1 > a_o > a_z$ can be met:

(1) Fixing k_{yo}, then trying to use different ω for different speed ranges. This is the method most people suggest. And, thus, a frequency converter is needed.

(2) Fixing ω, then trying to vary k_{yo} as v changes. This is similar to an antenna array to change the directivity by suitably arranging the current in each element.

In the ideal case where the source is a travelling wave with $\tilde{K}_x = \sqrt{2\pi}\,\delta(k_y - k_{yo})e^{-i\omega t}\,K_o$, the integrals for performance are easy to evaluate. (Of course, we cannot consider the infinite total forces and power any longer. But quantities per unit length in the y-direction are not difficult to derive). The following results can be obtained:

$$\frac{\overline{P}}{\text{unit length}} \cong \frac{-i\omega\mu_o}{2}\,\frac{k_{yo}^2 + i(\omega - k_{yo}v)\,K_1}{k_{yo}^4 + (\omega - k_{yo}v)^2\,K_1^2}\,\frac{\mu_{2z}}{\mu_{2z}h_3 + \mu_o h_2}\,K_o^2 \tag{3.8a}$$

$$\frac{\tilde{F}_y}{\text{unit length}} \cong \frac{K_1^2\,K_o^2}{2\sigma_x h_2}\,\frac{k_{yo}(\omega - k_{yo}v)}{k_{yo}^4 + (\omega - k_{yo}v)^2\,K_1^2} \tag{3.8b}$$

$$\frac{\tilde{F}_z}{\text{unit length}} \cong \frac{\mu_o K_o^2}{4}\,\frac{k_{yo}^2 - \mu_o^2\,\sigma_x^2\,h_2^2(\omega - k_{yo}v)^2}{k_{yo}^4 + (\omega - k_{yo}v)^2\,K_1^2}\,\frac{\mu_{2z}^2}{(\mu_{2z}h_3 + \mu_o h_2)^2} \tag{3.8c}$$

$$\eta = \frac{k_{yo}v}{\omega} \tag{3.8d}$$

$$PF = \frac{(\omega - k_{yo}v)K_1}{[k_{yo}^4 + (\omega - k_{yo}v)^2K_1^2]^{1/2}} \tag{3.8e}$$

Equations (3.8) are plotted in Fig. 3.2 as functions of v. The maximum thrust force will occur at $v_m = \omega/k_{yo} - \frac{k_{yo}}{K_1}$ with a corresponding maximum value of $1/4k_{yo} \cdot \mu_o\mu_{2z}/(\mu_{2z}h_3 + \mu_o h_2)$. Both the

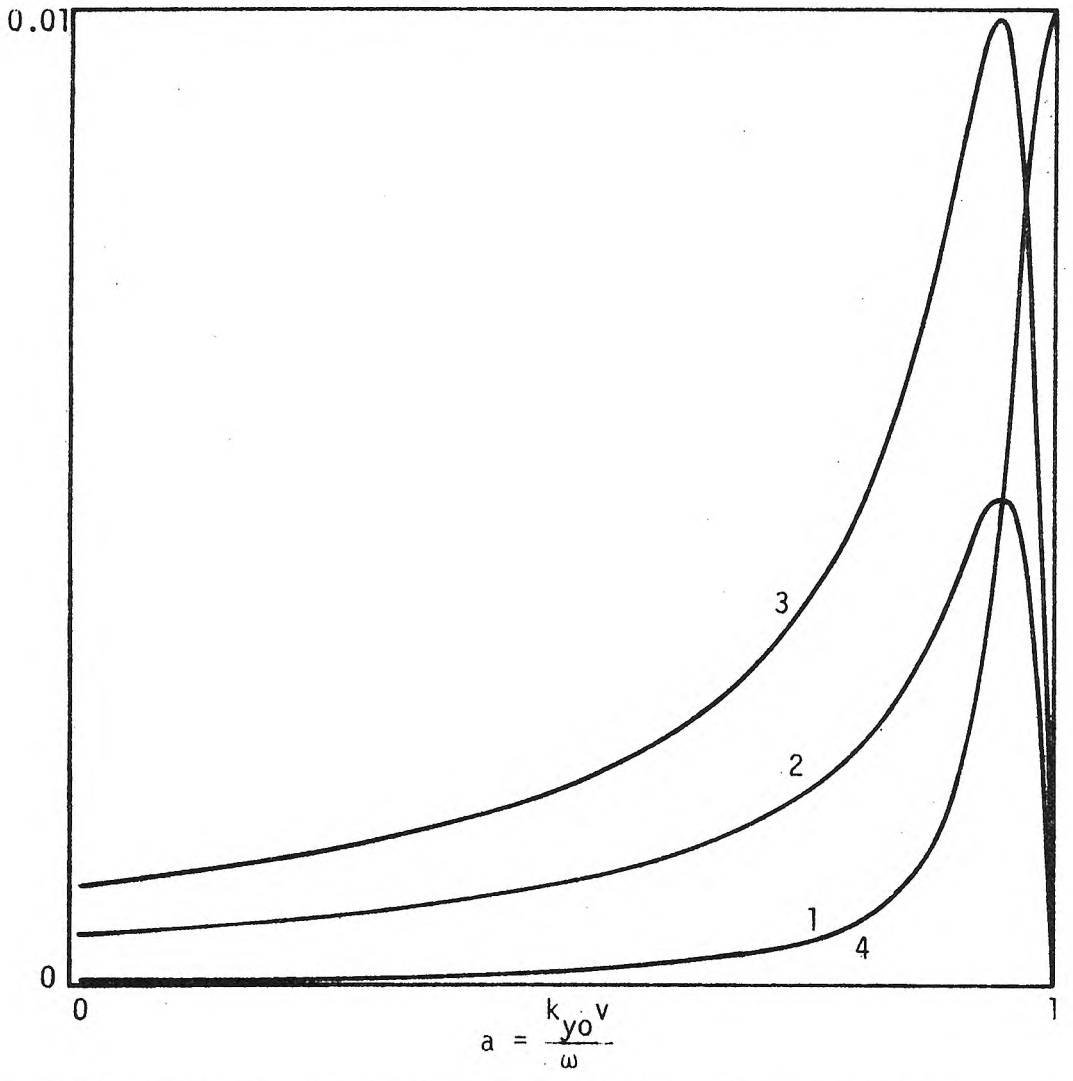

Fig. 3.2 Power and forces for geometry (A-i-1) with ideal source and $\omega K_1 = 2000$, $\omega\mu_o\sigma_x h_2 = 5$, $k_{yo} = 10$.

(1) $\mathrm{Re}\{\overline{P}\Big/(\frac{-i\omega\mu_o}{2}\ \frac{\mu_{2z} K_o^2}{\mu_{2z} h_3 + \mu_o h_2})\}$,

(2) $\mathrm{Im}\{\overline{P}\Big/(\frac{-i\omega\mu_o}{2}\ \frac{\mu_{2z} K_o^2}{\mu_{2z} h_3 + \mu_o h_2})\}$,

(3) $\overline{F}_y\Big/(\frac{5K_1 K_o^2}{2\sigma_x h_2})$, (4) $\overline{F}_z\Big/[\frac{\mu_o}{4}\ \frac{\mu_{2z}^2 K_o^2}{(\mu_{2z} h_3 + \mu_o h_2)^2}]$

supporting force and the efficiency are monotonically increasing functions of v. Thus, in order to have a high efficiency, it is suggested that the machine be operated in the attractive supporting force region. At v_m, a larger efficiency can be obtained by making $k_{yo}^2/\omega K_1$ smaller.

Unfortunately, a purely traveling wave source does not exist in nature. Generally, we can only have a finite source with a $|\tilde{K}_x|^2$ which is an oscillating function with a fast decaying envelop and a maximum value at k_{yo}. With the given information about the integrands, it is not difficult to understand how this so-called end effect comes into play. We will explain this by assuming the source has

$$|\tilde{K}_x|^2 = K_o^2 \frac{2}{\pi} \frac{\sin^2(k_y - k_{yo})L}{(k_y - k_{yo})^2}$$

(i.e., a source with $K_x = K_o e^{-i\omega t + ik_{yo}y}$ for $|y| \leq L$, and $K_x = 0$ otherwise. This is the most popular uncompensated source used by nearly all of the researchers.)

Now, let us go back to Fig. 3.1, where a typical plot for $\tilde{F}_y/|\tilde{K}_x|^2$ is shown. When L becomes infinitely large, $|\tilde{K}_x|^2$ becomes proportional to $\delta(k_y - k_{yo})$. The integral for $\bar{F}_y$ will just pick up the value of $\tilde{F}_y$ at k_{yo}, and the ideal source result is obtained. However, for the more realistic case where L is finite, the situation is different. It is obvious that $|\tilde{K}_x|^2$ will now have non-zero values at $k_y \neq k_{yo}$. Thus, the integrals will also receive a contribution from this region. And this explains how this so-called end effect comes into play. Definitely, the overall result depends

drastically on how functions $\tilde{F}_y/|\tilde{K}_x|^2$, $|\tilde{K}_x|^2$ vary.

By observing the $\tilde{F}_y/|\tilde{K}_x|^2$ curve more carefully, it can be seen that there is only one local maximum located at $k_y = a_y \frac{\omega}{v}$. Thus, if those points k_{yo}, $k_{yo} \pm \frac{\pi}{L}$, are not too close to $a_y \frac{\omega}{v}$, then although part of $|\tilde{K}_x|^2$ will spread into the region where $\tilde{F}_y/|\tilde{K}_x|^2$ is smaller than that at k_{yo}, there is always another part which will go into the larger $\tilde{F}_y/|\tilde{K}_x|^2$ region. So the overall effect will be small, i.e., the end effect causes little influence. On the contrary, if k_{yo} happens to be equal to $a_y \frac{\omega}{v}$, those non-zero $|\tilde{K}_x|^2$ at $k_y \neq k_{yo}$ will always pick up smaller $\tilde{F}_y/|\tilde{K}_x|^2$. Thus, the resultant force will decrease enormously, especially when L is small such that the spread is wide. And this is just the situation in which the end effect degrades the machine performances most. This also explains why a large L is suggested to reduce the undesired end effect. As for the case where k_{yo} is near $a_y \frac{\omega}{v}$, although there is a possibility that $|\tilde{K}_x|^2$ will go to the region where $\tilde{F}_y/|\tilde{K}_x|^2$ is larger, the increase is always small compared to the decrease coming from the spreading of $|\tilde{K}_x|^2$ into the opposite direction. Thus, although the detail will depend on how $\tilde{F}_y/|\tilde{K}_x|^2$ varies, a decrease in the resultant force can generally be observed.

In the above we have mainly talked about the influence of the source function. Now we will also say something about the other parameters.

It is known that a smaller $K_1 v^2/\omega$ will give a smaller a_y . Now, if there are two cases with the same ω/v but different a_y , then roughly speaking, the slope to the right of a_y will be steeper

for the case with larger a_y . Thus, if we have two systems with different K_1 operating at the same ω,v , then we are going to get a more serious end effect for the case with larger K_1 when k_{yo}'s are set to their corresponding values of $a_y \frac{\omega}{v}$. (Remember, a larger a_o is suggested to give a higher efficiency. And the above argument is only applied to the case where $a_y = a_o > \frac{1}{2}$). So generally, we are expecting a smaller end effect for a system which uses a track with a small $\sigma_x h_2$. Also, as we suggested before, the machine can also be used for supporting purposes. In this case, it is preferable to operate in the attractive region. Thus, it is more desirable to make $\sigma_x h_2$ small. This happens to be consistent with the small end effect requirement. So, it seems that composite tracks which will give a relatively smaller σ_x are promising.

Note, for practical material suggested in MAGLEV systems, nonferromagnetic material generally has a higher conductivity. Thus, although material with high $\underset{\sim}{\mu}$ does not offer too many advantages; composite tracks with ferromagnetic material contained are still recommended for use in this special case. We will postpone our discussion about how to construct the composite tracks until Chapter IV. However, it should also be remembered that K_1 cannot be made too low, otherwise $\tilde{F}_y/|\tilde{K}_x|^2$ will become too small in the low slip region. This will eventually decrease the force and degrade the machine performance. A suitable compromise is thus necessary.

For the geometry we are considering, one thing seems worthwhile mentioning. With all of the specified source and track configurations, we know that the maximum force is going to occur at $v_m = \frac{\omega}{k_{yo}} - \frac{k_{yo}}{K_1}$

for the ideal source. However, we also know that for this v_m the maximum value of $\tilde{F}_y/|\tilde{K}_x|^2$ is going to appear at $a_y \frac{\omega}{v_m}$ which is less than k_{yo}. Thus, the maximum thrust force point is not the point where the end effect is most serious. Later, this can be shown to be different from some of the other configurations.

In the above, we considered mainly the end effect on the force in the y-direction. Similar arguments can also be applied to F_z, η, PF. Since, for a given v, the integrand for the loss integral is monotonically decreasing for $0 \leq k_y \leq \frac{\omega}{v}$, so the end effect will not introduce too much influence to the loss. Thus, as for the efficiency, the end effect will have similar influence to that of F_y, i.e., it will generally degrade the efficiency. For most of k_y, $\tilde{F}_z/|\tilde{K}_x|^2$ is also monotonically increasing, so that the end effect is not serious for the supporting force either.

(i-2) $\alpha = 1$: (i.e., source without back iron)

Similar to the case $\alpha \cong 0$, we can get from (3.1), (3.2), (3.3) and the thin reaction rail assumption:

$$\tilde{Z}_L \cong -i\omega\mu_o \frac{\mu_{2y}}{\mu_{2y}k_z + \mu_{2y}k_y^2 h_3 + \mu_o\gamma_2^2 h_2} \tag{3.9a}$$

$$\cong -i\omega\mu_o \frac{k_z + i(\omega - k_y v)\mu_o\sigma_x h_2}{k_y^2 + (\omega - k_y v)^2\mu_o^2\sigma_x^2 h_2^2} \tag{3.9b}$$

$$\tilde{F}_y \cong \mathrm{Re}\, \frac{-i\mu_o}{2} \frac{\mu_{2y}k_y}{\mu_{2y}k_z + \mu_{2y}k_y^2 h_3 + \mu_o\sigma_2^2 h_2} |\tilde{K}_x|^2 \tag{3.10a}$$

$$\simeq \frac{\mu_o}{2} \frac{k_y(\omega-k_y v)\mu_o\sigma_x h_2}{k_y^2 + (\omega-k_y v)^2 \mu_o^2 \sigma_{2x}^2 h_2^2} |\tilde{K}_x|^2 \qquad (3.10b)$$

$$\tilde{F}_z \simeq \frac{\mu_o}{4} \mathrm{Re} \frac{\mu_{2y}k_y^2 - \mu_o|\gamma_2|^4 h_2^2}{|\mu_{2y}k_z + \mu_{2y}k_y^2 h_3 + \mu_o\sigma_2^2 h_2|^2} |\tilde{K}_x|^2 \qquad (3.11a)$$

$$\simeq \frac{\mu_o}{4} \frac{k_y^2 - (\omega-k_y)^2 \sigma_x^2 \mu_o^2 h_2^2}{k_y^2 + (\omega-k_y v)^2 \mu_o^2 \sigma_x^2 h_2^2} |\tilde{K}_x|^2 \qquad (3.11b)$$

All of the approximations (3.9b), (3.10b), (3.11b) are introduced for the convenience of integrand analyses with $0 < k_y < \frac{\omega}{v}$ where $k_y h_2 << 1$, $k_y h_3 << 1$ are very accurate. However, as far as the realistic performance integrals are concerned, (3.9a), (3.10a), (3.11a) will be more accurate.

Formulas (3.9a), (3.10a), (3.11a) are plotted in Fig. 3.3. For those "a" parameters as defined in (i-1), if only the region $0 \leq a \leq 1$ is considered, we will get:

$$a_y \simeq a_z \simeq \frac{1}{1 + \frac{1}{\mu_o\sigma_x h_2 v}} \qquad (3.12a)$$

$$a_r \simeq 1 - \frac{1}{\sqrt{1 + \mu_o^2\sigma_x^2 h_2^2 v^2}} \qquad (3.12b)$$

$$a_i \simeq \frac{1}{\sqrt{1 + \frac{1}{\mu_o^2\sigma_x^2 h_2^2 v^2}}} \qquad (3.12c)$$

In this case $a_i > a_y > a_r$ is always true, And all of them are monotonically increasing functions of $\gamma = \mu_o\sigma_x h_2 v$. In order to have

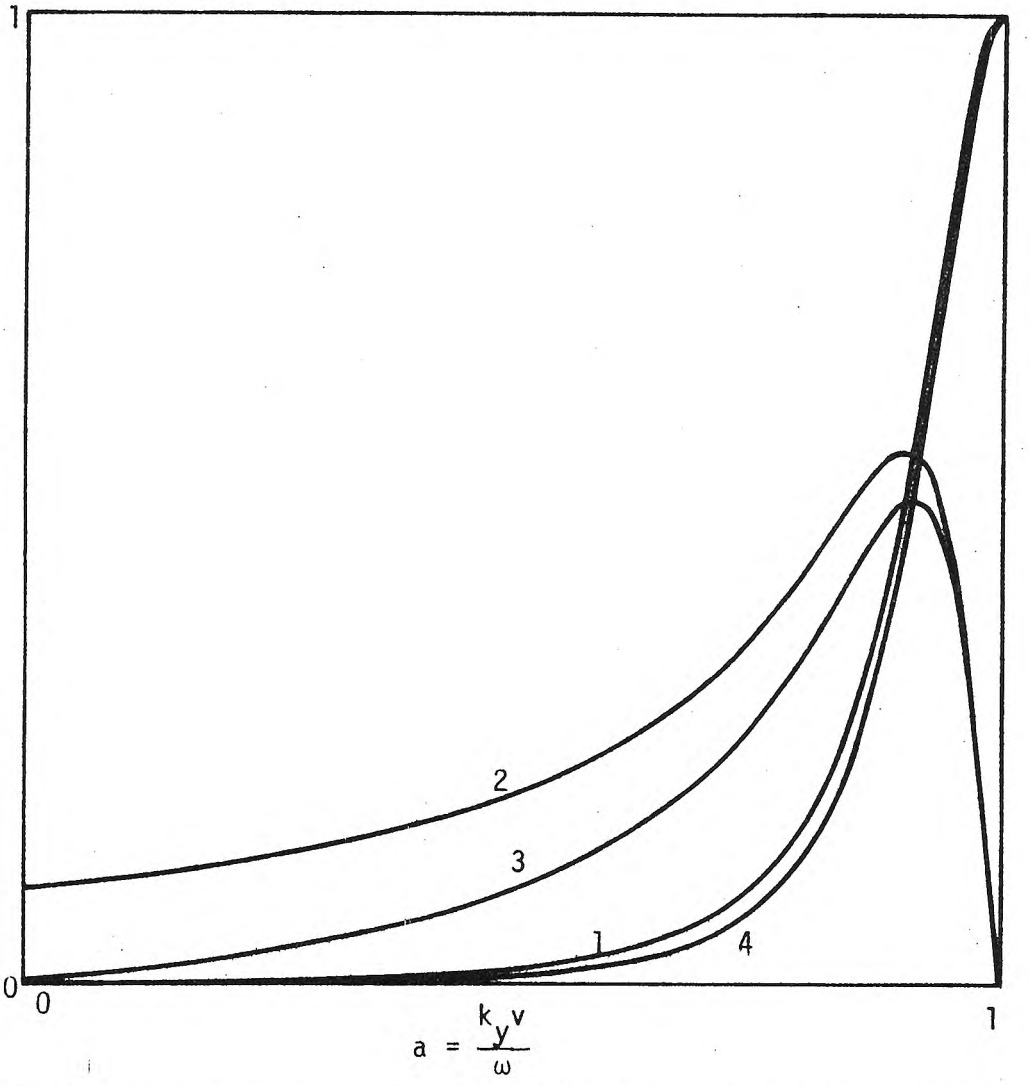

Fig. 3.3 Integrands for geometry (A-i-2) with $\gamma = \mu_o \sigma_x h_2 v = 10$.

(1) $\mathrm{Re}\{\tilde{Z}_L/(-i\mu_o v)\}$, (2) $\mathrm{Im}\{\tilde{Z}_L/(-i\mu_o v)\}$,

(3) $\dfrac{\tilde{F}_y}{|\tilde{K}_x|^2}\dfrac{2}{\mu_o}$, (4) $\dfrac{\tilde{F}_z}{|\tilde{K}_x|^2}\dfrac{2}{\mu_o} + \dfrac{1}{2}$

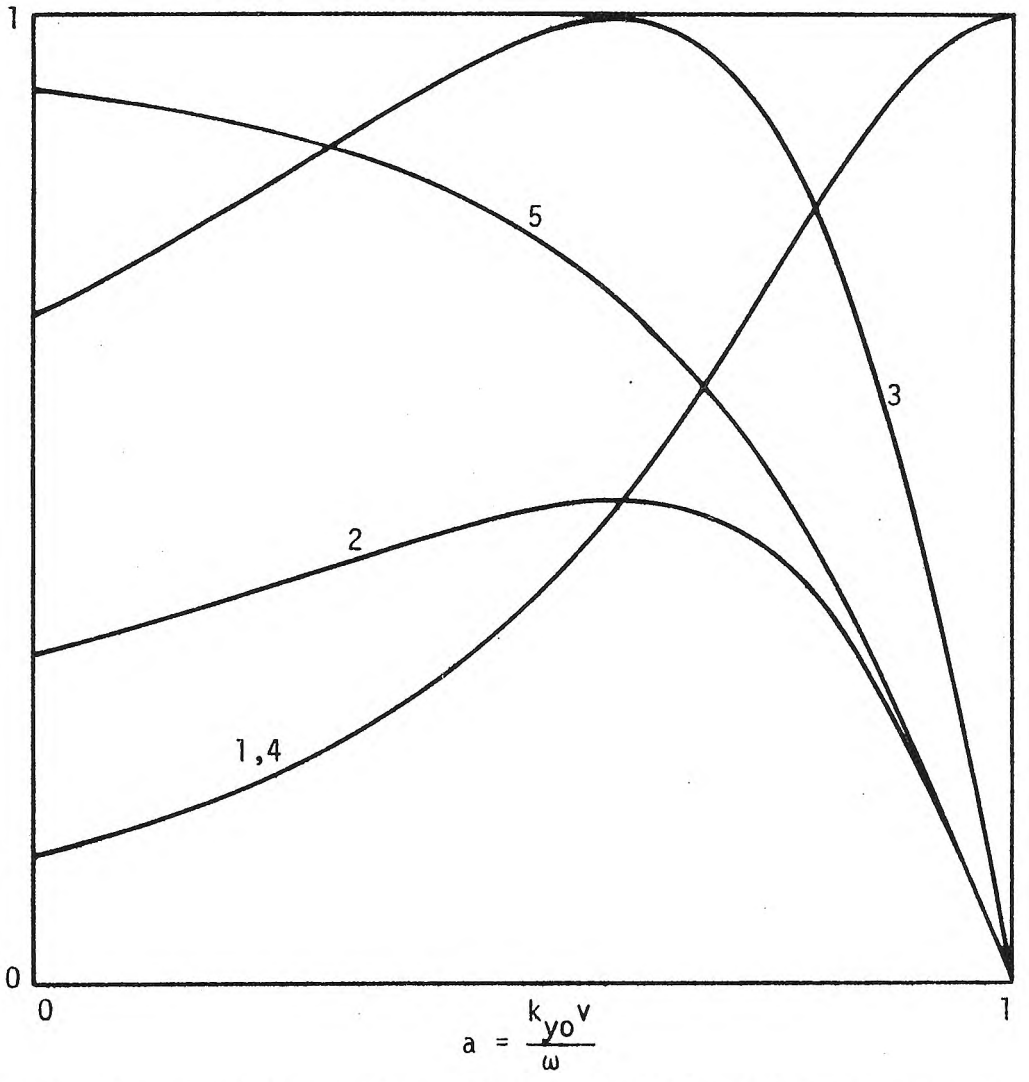

Fig. 3.4 Power and forces for geometry (A-i-2) with ideal source and $\omega\mu_o\sigma_x h_2 = 25$, $k_{yo} = 10$.

(1) $-\frac{20\ \mathrm{Im}\ \bar{P}}{\omega\mu_o K_o^2}$, (2) $\frac{20\ \mathrm{Re}\ \bar{P}}{\omega\mu_o K_o^2}$, (3) $\frac{\bar{F}_y}{\mu_o K_o^2}$

(4) $\frac{2\bar{F}_z}{\mu_o K_o^2} + \frac{1}{2}$, (5) PF

higher efficiency and enough supporting force, we suggest operating this machine with $a_o > a_y$, i.e., an attractive scheme is preferable. Now, since $a_y \cong a_z$, we cannot draw the largest possible propulsion force for this kind of geometry operating in the attractive supporting force region. Furthermore, for the same track configurations, ω, v, and k_y, geometry (i-1) always gives larger values of $\tilde{F}_y/|\tilde{K}_x|^2$, $\tilde{F}_z/|\tilde{K}_x|^2$, $|\tilde{Z}_L|$ than those of (i-2). So, if the same amounts of forces and power are required, larger $|\tilde{K}_x|^2$ is always necessary for geometry (i-2). Source windings of higher conductivities must be used to prevent intolerable ohmic losses. Thus, this geometry perhaps is not preferred in HSGT vehicles where large power and forces are always necessary. However, if the cost for a high conductivity source winding is manageable or high power is not a requirement, this LIM will still be applicable. Thus, we will still present some analysis for this geometry.

For the ideal source with $\tilde{K}_x = \sqrt{2\pi}\,\delta(k_y-k_{yo})e^{-i\omega t}\,K_o$, the machine performance is easy to get:

$$\frac{\overline{P}}{\text{unit length}} \cong \frac{-i\omega\mu_o}{2}\,\frac{k_{yo}+i(\omega-k_{yo}v)\,\mu_o\sigma_x h_2}{k_{yo}^2+(\omega-k_{yo}v)^2\,\mu_o^2\,\sigma_x^2\,h_2^2}\,K_o^2 \tag{3.13a}$$

$$\frac{\overline{F}_y}{\text{unit length}} \cong \frac{\mu_o K_o^2}{2}\,\frac{k_{yo}(\omega-k_{yo}v)\mu_o\sigma_x h_2}{k_{yo}^2+(\omega-k_{yo}v)^2\mu_o^2\,\sigma_x^2\,h_2^2} \tag{3.13b}$$

$$\frac{\overline{F}_z}{\text{unit length}} \cong \frac{\mu_o K_o^2}{4}\,\frac{k_{yo}^2-(\omega-k_{yo}v)^2\mu_o^2\,\sigma_x^2\,h_2^2}{k_{yo}^2+(\omega-k_{yo}v)^2\mu_o^2\,\sigma_x^2\,h_2^2} \tag{3.13c}$$

$$\eta \cong \frac{k_{yo}v}{\omega} \tag{3.13d}$$

$$PF \cong \frac{(\omega-k_{yo}v)\,\mu_o\sigma_x h_2}{[k_{yo}^2+(\omega-k_{yo}v)^2\,\mu_o^2\,\sigma_x^2\,h_2^2]^{1/2}} \tag{3.13e}$$

Here, of course, $k_{yo}h_2 << 1$ and $k_{yo}h_3 >> 1$ have been assumed such that (3.9b), (3.10b), (3.11b) can be used.

It should be noticed that $\underset{\sim}{\mu}$ does not have any effect on the machine performance. In (3.13a), for a given k_{yo}, the maximum thrust force occurs at $v_m = \frac{\omega}{k_{yo}} - \frac{1}{\mu_o\sigma_x h_2}$ with a corresponding value of $\frac{\mu_o}{4}K_o^2$ which is just proportional to K_o^2 and is independent of everything else. At v_m, $a_y\frac{\omega}{v_m}$ happens to be equal to k_{yo} and thus the corresponding $\bar{F}_z$ will be 0. Thus, if an attractive force is also desired, we cannot draw the possible maximum propulsion force for this given geometry. This is quite different from the previous case where $k_{yo} > a_y\frac{\omega}{v_m} > a_z\frac{\omega}{v_m}$, and thus at the maximum propulsion force point a reasonably large attractive force can also be obtained. This gives further evidence that geometry (i-1) is superior. Similar to (i-1), for a given k_{yo}, η is a monotonically increasing function of v. At v_m, a larger efficiency can be obtained by making $k_{yo}/(\omega\mu_o\sigma_x h_2)$ smaller.

For the more realistic case of $|\tilde{K}_x|^2 = K_o^2\frac{2}{\pi}\frac{\sin^2(k_y-k_{yo})L}{(k_y-k_{yo})^2}$, the end effect also plays an important role in degrading machine performance. The reason is definitely the same as before, i.e., $|\tilde{K}_x|^2$ will spread into the region where the integrand is smaller than that at k_{yo}.

Now, as we mentioned, for an ideal source with $\tilde{K}_x \propto \delta(k_y-k_{yo})$, $a_y(v_m)$ happens to be equal to $(k_{yo}v_m)/\omega$. Thus, the most serious end

effect is observed. Generally, it can be argued that the end effect can possibly be reduced by making $\sigma_x h_2$ smaller, which is also the same conclusion as that of (i-1). Of course, a suitable lower $\sigma_x h_2$ must be chosen to prevent the machine from going into the low efficiency region.

(ii) Thick reaction rails:

For $|\gamma_2| h_2 >> 1$, $\tanh \gamma_2 h_2 \tilde{=} 1$ is approximately true. In addition to this, $\tanh k_z h_3 = k_z h_3$ will further simplify the original formulas. However, in this case, the algebraic analysis is found to be much more complicated for problems with $\alpha \tilde{=} 0$. Thus, instead of considering $\alpha \tilde{=} 0$, we will take care of the problem with $\alpha = 1$ first. Then several results for $\alpha \tilde{=} 0$ can be obtained by comparing with those of $\alpha = 1$.

(ii-1) $\alpha = 1$: (region 4 is free space)

From (3.1), (3.2), (3.3) and the given assumptions:

$$\tilde{Z}_L \tilde{=} -i\omega\mu_o \frac{\mu_{2y}}{\mu_{2y} k_z + \mu_o \gamma_2} \tag{3.14}$$

$$= \frac{-i\omega\mu_o}{k_z} \frac{1 + \frac{\mu_o}{\sqrt{2}\mu_{2y}\mu_{2z}} \left[1 + \sqrt{1 + \frac{(\omega - k_y v)^2}{k_y^4} \sigma_x^2 \mu_{2z}^2} \right]^{1/2} + \frac{i\mu_o}{\sqrt{\mu_{2y}\mu_{2z}^2}} \operatorname{sgn}(\omega - k_y v) \left[-1 + \sqrt{1 + \frac{(\omega - k_y v)^2}{k_y^4} \sigma_x^2 \mu_{2z}^2} \right]^{1/2}}{1 + \frac{\mu_o^2}{\mu_{2y}\mu_{2z}} \sqrt{1 + \frac{(\omega - k_y v)^2}{k_y^4} \sigma_x^2 \mu_{2z}^2} + \frac{\mu_o \sqrt{5}}{\sqrt{\mu_{2y}\mu_{2z}}} \left[1 + \sqrt{1 + \frac{(\omega - k_y v)^2}{k_y^4} \sigma_x^2 \mu_{2z}^2} \right]^{1/2}} \tag{3.15}$$

$$\tilde{F}_y \cong \mathrm{Re}\ \frac{-j\mu_o}{2}\ \frac{\mu_{2y}k_y}{\mu_{2y}k_z + \mu_o\gamma_2}\ |\tilde{K}_x|^2 \tag{3.16}$$

$$= \frac{\mu_o}{2}\ \frac{\mu_o}{\sqrt{2\mu_{2y}\mu_{2z}}}\ \frac{\mathrm{sgn}(k_y)\ \mathrm{sgn}(\omega - k_y v)\left[-1 + \sqrt{1 + \frac{(\omega-k_y v)^2}{k_y^4}\sigma_x^2\mu_{2z}^2}\right]^{1/2}}{1 + \frac{\mu_o^2}{\mu_{2y}\mu_{2z}}\sqrt{1+\frac{(\omega-k_y v)^2}{k_y^4}\sigma_x^2\mu_{2z}^2} + \frac{\sqrt{2}\mu_o}{\sqrt{\mu_{2y}\mu_{2z}}}\left[1 + \sqrt{1+\frac{(\omega-k_y v)^2}{k_y^4}\sigma_x^2\mu_{2z}^2}\right]^{1/2}}\ |\tilde{K}_x|^2 \tag{3.17}$$

$$\tilde{F}_z \cong \frac{\mu_o}{4}\ \frac{\mu_{2y}^2 k_y^2 - \mu_o^2|\gamma_2|^2}{|(\mu_{2y}k_z + \mu_o\gamma_2)|^2} \tag{3.18}$$

$$= \frac{\mu_o}{4}\ \frac{1 - \frac{\mu_o^2}{\mu_{2y}\mu_{2z}}\sqrt{1 + \frac{(\omega-k_y v)^2}{k_y^4}\sigma_x^2\mu_{2z}^2}}{1 + \frac{\mu_o^2}{\mu_{2y}\mu_{2z}}\sqrt{1 + \frac{(\omega-k_y v)^2}{k_y^4}\sigma_x^2\mu_{2z}^2} + \frac{\sqrt{2}\mu_o}{\sqrt{\mu_{2y}\mu_{2z}}}\left[1 + \sqrt{1 + \frac{(\omega-k_y v)^2}{k_y^4}\sigma_x^2\mu_{2z}^2}\right]^{1/2}}\ |\tilde{K}_x|^2 \tag{3.19}$$

Algebraic analyses for $\tilde{F}_y/|\tilde{K}_x|^2$ and $\tilde{F}_z/|\tilde{K}_x|^2$ yield the results in Fig. 3.5. For the eddy current loss and real P, results can be obtained simply by multiplying $(\frac{\omega}{k_y} - v)$ and ω/k_y with $\tilde{F}_y/|\tilde{K}_x|^2$ respectively.

For $\underset{\sim}{\mu} = \mu_o \underset{\sim}{I}$, a maximum value for $\tilde{F}_y/|\tilde{K}_x|^2$ is found to be at $a_y = \dfrac{2}{1 + \sqrt{1 + \frac{4\omega}{K v^2}}}$ (here $K = \dfrac{\mu_o\sigma_x}{\sqrt{8 + 4\sqrt{5}}}$) with a corresponding value of

$\frac{\mu_o}{2\sqrt{2}} \frac{(\sqrt{5}+1)^{1/2}}{(4+2\sqrt{5})}$. If $\underset{\sim}{\mu} \neq \mu_o \underset{\sim}{I}$ and $\mu_o^2/\mu_{2y}\mu_{2z} << 1$ are true, $a_y \cong \frac{2}{1+\sqrt{4\omega/K_2 v^2+1}}$ with $K_2 = \frac{\mu_o^2 \sigma_x}{\mu_{2y}}$. And the corresponding maximum value is $\mu_o/(2\sqrt{2}(2+\sqrt{2}))$. Thus, if the peak propulsion force is of most concern, the bigger extreme value of $\tilde{F}_y/|\tilde{K}_x|^2$ for the ferromagnetic track will make the track a little bit more favorable than the nonferromagnetic one. $\tilde{F}_z/|\tilde{K}_x|^2$ is zero at $a_z = \frac{2}{1+\sqrt{1+\frac{4\omega}{K_3 v^2}}}$ with $K_3^{-1} = \sqrt{\frac{\mu_{2y}^2}{\mu_o^4 \sigma_x^2} - \frac{1}{\sigma_x^2 \mu_{2z}^2}}$. For the nonferromagnetic track, K_3^{-1} reduces to zero, i.e., the only zero point is at $a = 1$. And, no matter whether $\underset{\sim}{\mu} = \mu_o \underset{\sim}{I}$ or $\underset{\sim}{\mu} \neq \mu_o \underset{\sim}{I}$, $\tilde{F}_z/|\tilde{K}_x|^2$ has a maximum at $a = 1$. More information about these integrands can be obtained from Fig. 3.5.

It can easily be seen that for the thick reaction rail, the skin effect will prevent the medium in region 1 from influencing the machine performance. And the permeability $\underset{\sim}{\mu}$ begins to play a very important role. For the nonferromagnetic track, only the repulsive force can be observed. A larger repulsive force can be obtained only at a smaller "a". Thus, if high efficiency is desired, this geometry is not recommended to be used as a LIM both for propulsion and levitation. However, if it is mainly suggested for the propulsion purpose, there will always be an extra repulsive force to help in supporting the vehicles.

As for the ferromagnetic track, we will get a very similar result to that of the thin reaction rail (A-i-2). Both repulsive and

attractive forces can be obtained. Furthermore, $0 \leq a_z \tilde{=} a_y < 1$ is true for both cases. Thus, most of the arguments given there can be applied here. Depending on whether a_o is larger or smaller than a_z, the machine can have either an attractive or a repulsive force. But, if high efficiency is also required, the attractive one is preferable. Unfortunately, the largest propulsion force can only be obtained at $a_y = a_z$. It is also noticed that at a_y the peak integrand for $\bar{F}_y$ is a little bit smaller than that of (A-i-2) which is only of the order of $k_y h$ multiplied by that of (A-i-1). Thus, similar to (A-i-2), a high conductivity source winding is required to reduce the ohmic loss when similar forces as in (A-i-1) are desired. And, actually, this seems to be a common requirement for LIMs with $\alpha = 1$ when similar forces as LIMs with $\alpha_4 = 0$ are needed.

For the ideal source, the machine performance can easily be obtained by substituting k_y with k_{yo} in equations (3.15), (3.17) and (3.19). Plots of $\bar{F}_y$, $\bar{F}_z$, etc. are then shown in Fig. 3.6. Now, the maximum thrust force point will satisfy $\frac{k_{yo}v}{\omega} = \frac{2}{1+\sqrt{1+\frac{4\omega}{K_i v_m^2}}}$ with $K_i = K$ or K_2. The corresponding force will be on the order of $\frac{\mu_o k_o^2}{4}$. Actually, as derived from the integrand analyses, the ideal source results for $\underset{\sim}{\mu} \neq \mu_o \underset{\sim}{I}$ will be qualitatively similar to (A-i-2). Most of the other properties can also easily be observed from Fig. 3.6.

With the same argument as in (A-i), it is understood that the end effect can be reduced by making K_i smaller. Using a composite track generally can attain this objective. However, the decrease of K_i will also give a smaller a_y and thus a smaller efficiency. A suitable compromise should be made to determine which value of K_i to use.

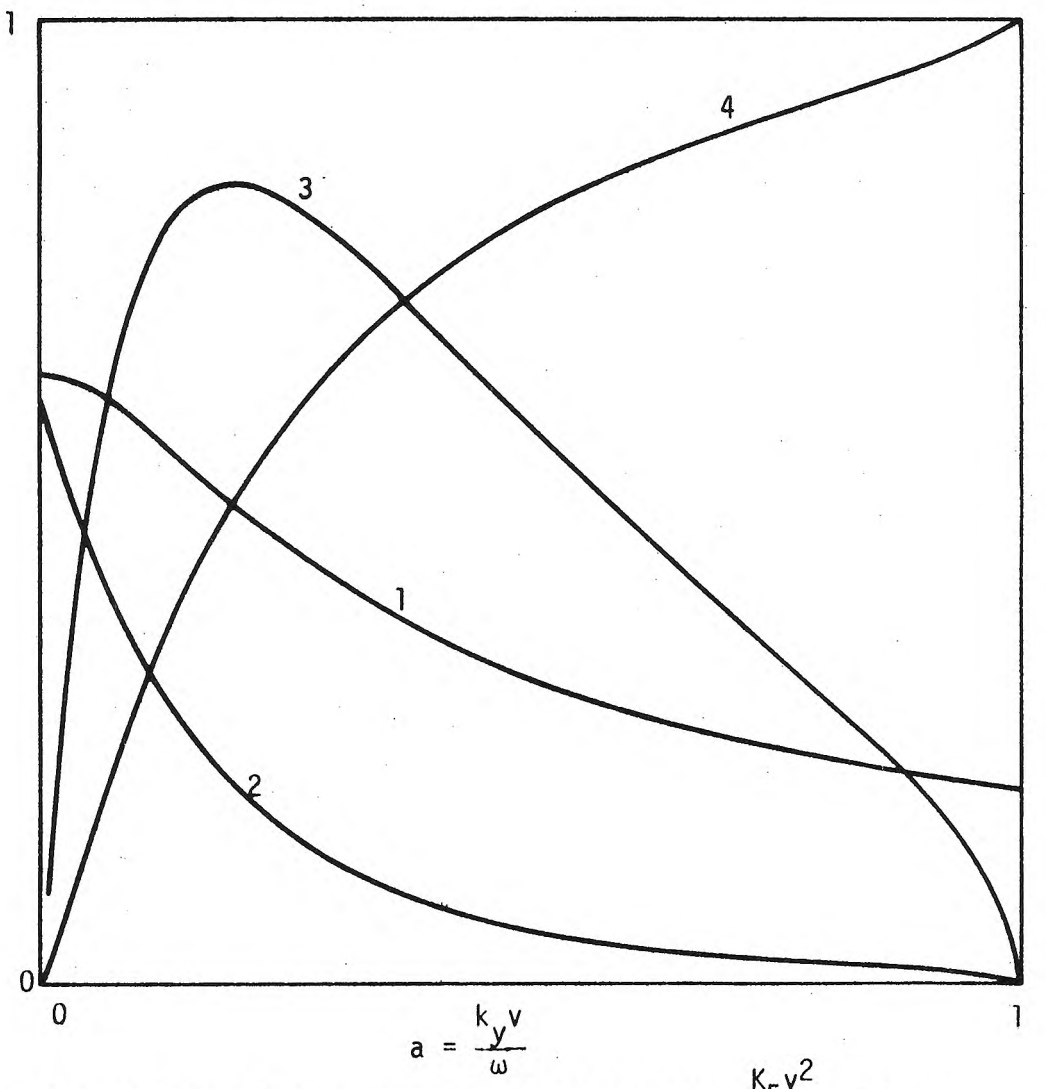

Fig. 3.5 Integrands for geometry (A-ii-1) with $\frac{K_5 v^2}{\omega} = 500$, $\frac{\mu_o}{\sqrt{\mu_{2y}\mu_{2z}}} = 0.01$.

(1) $\mathrm{Re}\{\frac{i\tilde{Z}_L}{5\mu_o v}\}$, (2) $\mathrm{Im}\{\frac{i\tilde{Z}_L}{5\mu_o v}\}$,

(3) $\frac{\tilde{F}_y}{|\tilde{K}_x|^2}\frac{8}{\mu_o}$, (4) $\frac{\tilde{F}_z}{|\tilde{K}_x|^2}\frac{2}{\mu_o} + \frac{1}{2}$

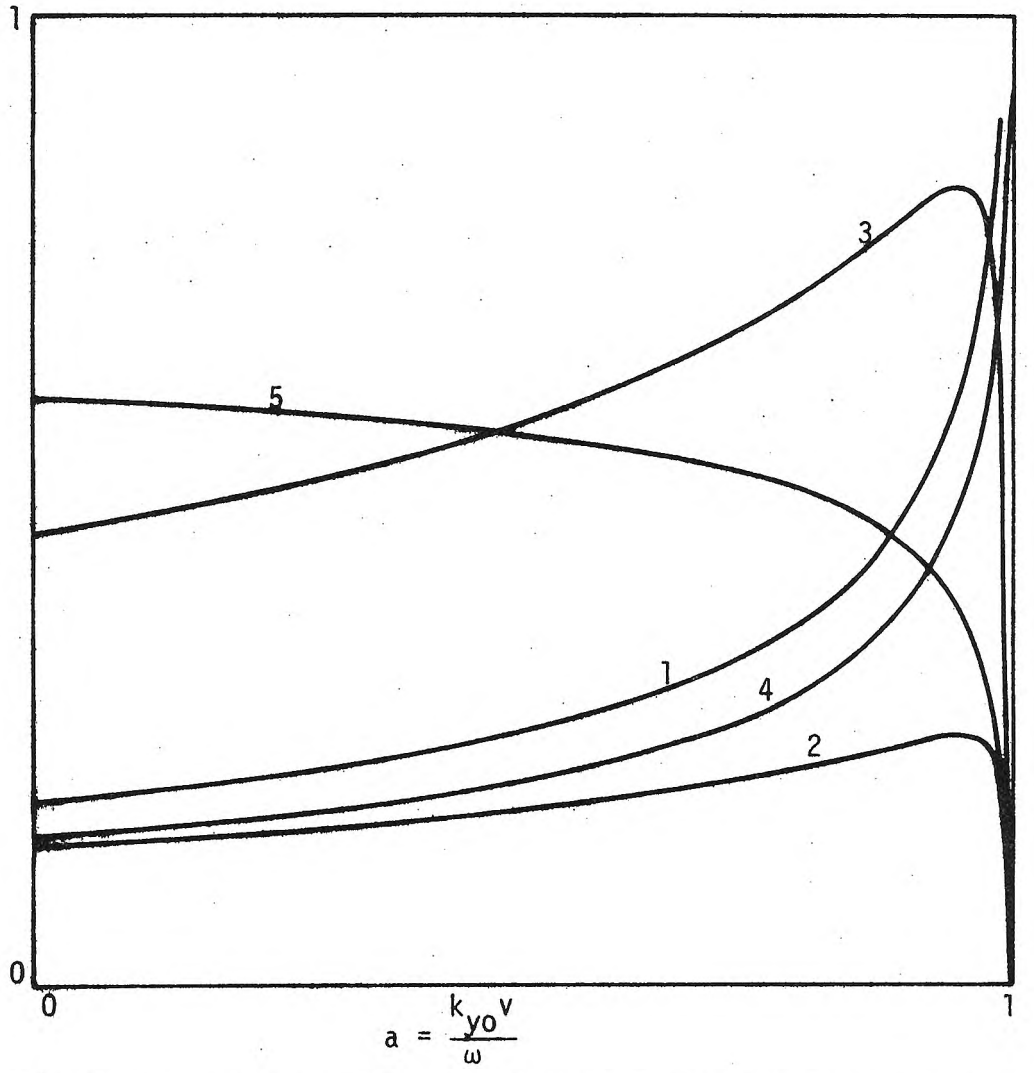

Fig. 3.6 Power and forces for geometry (A-ii-1) with ideal source and $\omega K_5 = 200{,}000$, $k_{yo} = 10$, $\frac{\mu_o}{\sqrt{\mu_{2y}\mu_{2z}}} = 0.1$.

(1) $-\frac{25\ \mathrm{Im}\ \overline{P}}{\omega\mu_o K_o^2}$, (2) $\frac{25\ \mathrm{Re}\ \overline{P}}{\omega\mu_o K_o^2}$

(3) $\frac{8\overline{F}_y}{\mu_o K_o^2}$, (4) $\frac{2\overline{F}_z}{\mu_o K_o^2} + \frac{1}{2}$

(5) Power factor

(ii-2) $\alpha \cong 0$: (region 4 is infinitely laminated iron)

From (3.1), (3.2), (3.3) and the given assumptions:

$$\tilde{Z}_L \cong -i\omega\mu_o \frac{\mu_{2y}}{\mu_{2y}k_y^2 h_3 + \mu_o\gamma_2} \tag{3.20a}$$

$$= \frac{-i\omega\mu_o}{k_y} \frac{k_y h_3 + \frac{\mu_o \mathrm{sgn}(k_y)}{\sqrt{2\mu_{2y}\mu_{2z}}}\left[1+\sqrt{1+\frac{(\omega-k_y v)^2}{k_y^4}\sigma_x^2\mu_{2z}^2}\right]^{1/2} + \frac{i\mu_o \mathrm{sgn}(k_y)}{\sqrt{2\mu_{2y}\mu_{2z}}}\mathrm{sgn}(\omega-k_y v)\left[-1+\sqrt{1+\frac{(\omega-k_y v)^2}{k_y^4}\sigma_x^2\mu_{2z}^2}\right]^{1/2}}{k_y^2 h_3^2 + \frac{\mu_o^2}{\mu_{2y}\mu_{2z}}\sqrt{1+\frac{(\omega-k_y v)^2}{k_y^4}\sigma_x^2\mu_{2z}^2} + \frac{\sqrt{2}\mu_o k_z h_3}{\sqrt{\mu_{2y}\mu_{2z}}}\left[1+\sqrt{1+\frac{(\omega-k_y v)^2}{k_y^4}\sigma_x^2\mu_{2z}^2}\right]^{1/2}} \tag{3.20b}$$

$$\tilde{F}_y \cong \mathrm{Re}\,\frac{-i\mu_o}{2} \frac{\mu_{2y}k_y}{\mu_{2y}k_y^2 h_3 + \mu_o\gamma_2} |\tilde{K}_x|^2 \tag{3.21a}$$

$$= \frac{\mu_o}{2}\mathrm{sgn}(k_y)\,\mathrm{sgn}(\omega-k_y v) \frac{\frac{\mu_o}{\sqrt{\mu_{2y}\mu_{2z}}}\left[-1+\sqrt{1+\frac{(\omega-k_y v)^2}{k_y^4}\sigma_x^2\mu_{2z}^2}\right]^{1/2}}{k_y^2 h_3^2 + \frac{\mu_o^2}{\mu_{2y}\mu_{2z}}\sqrt{1+\frac{(\omega-k_y v)^2}{\sqrt{\mu_{2y}\mu_{2z}}}\sigma_x^2\mu_{2z} + \frac{\sqrt{2}\mu_o k_z h_3}{\sqrt{\mu_{2y}\mu_{2z}}}\left[1+\sqrt{1+\frac{(\omega-k_y v)^2}{k_y^4}\sigma_x^2\mu_{2z}^2}\right]^{1/2}} |\tilde{K}_x|^2 \tag{3.21b}$$

$$\tilde{F}_z \cong \frac{\mu_o}{4} \frac{\mu_{2y}^2 k_y^2 - \mu_o^2|\gamma_2|^2}{|\mu_{2y}k_y^2 h_3 + \mu_o\gamma_2|^2} |\tilde{K}_x|^2 \tag{3.22a}$$

$$= \frac{\mu_o}{4} \frac{1 - \frac{\mu_o^2}{\mu_{2y}\mu_{2z}}\sqrt{1+\frac{(\omega-k_y v)^2}{k_y^4}\sigma_x^2\mu_{2z}^2}}{k_y^2 h_3^2 + \frac{\mu_o^2}{\mu_{2y}\mu_{2z}}\sqrt{1+\frac{(\omega-k_y v)^2}{k_y^4}\sigma_x^2\mu_{2z}^2} + \frac{\sqrt{2}\mu_o}{\sqrt{\mu_{2y}\mu_{2z}}}k_z h_3\left[1+\sqrt{1+\frac{(\omega-k_y v)^2}{k_y^4}\sigma_x^2\mu_{2z}^2}\right]^{1/2}} |\tilde{K}_x|^2 \tag{3.22b}$$

After comparing to the corresponding formulas in (A-ii-1), the different terms in (3.20b), (3.21b), (3.22b) are underlined and by changing these terms to "1", formulas for (A-ii-1) can be obtained. It is seen that $\underset{\sim}{\mu} = \mu_0 \underset{\sim}{I}$ and $\underset{\sim}{\mu} \neq \mu_0 \underset{\sim}{I}$ behave quite differently from each other. By observing this fact and the results from some rough algebraic calculation, the following remarks can be made.

Nonferromagnetic tracks:

- $\tilde{F}_z/|\tilde{K}_x|^2$ is always negative. And similar to that in (A-ii-1) $\tilde{F}_z/|\tilde{K}_x|^2$ is monotonically increasing for $0 \leq a \leq 1$ with a minimum value of $-\mu_0/4$ at $a = 0$ and a maximum value equal to 0 at $a = 1$.

- a_y is located at $\dfrac{2}{1+\sqrt{1+\dfrac{4\omega}{K_4 v^2}}}$ with K_4^{-1} lying between $\dfrac{\sqrt{3}}{\mu_0\sigma_x}$ and $\dfrac{\sqrt{8+4\sqrt{5}}}{\mu_0\sigma_x}$.

Ferromagnetic tracks:

- $a_z = \dfrac{2}{1+\sqrt{1+\dfrac{4\omega}{K_3 v^2}}}$ with $K_3^{-1} = \sqrt{\dfrac{\mu_{2y}^2}{\mu_0^4\sigma_x^2} - \dfrac{1}{\sigma_x^2\mu_{2z}^2}} \simeq \dfrac{\mu_{2y}}{\mu_0^2\sigma_x}$

- $\tilde{F}_z/|\tilde{K}_x|^2$ has a maximum lying between $a = 1$ and $a = a_z$.

- a_y is located at $\dfrac{2}{1+\sqrt{1+\dfrac{4\omega}{K_5 v^2}}}$ with K_5^{-1} lying between $\dfrac{\mu_{2y}}{\mu_0^2\sigma_x}$ and $\dfrac{\sqrt{3}}{\sigma_x\mu_{2z}}$. Thus, $a_y > a_z$ is generally true.

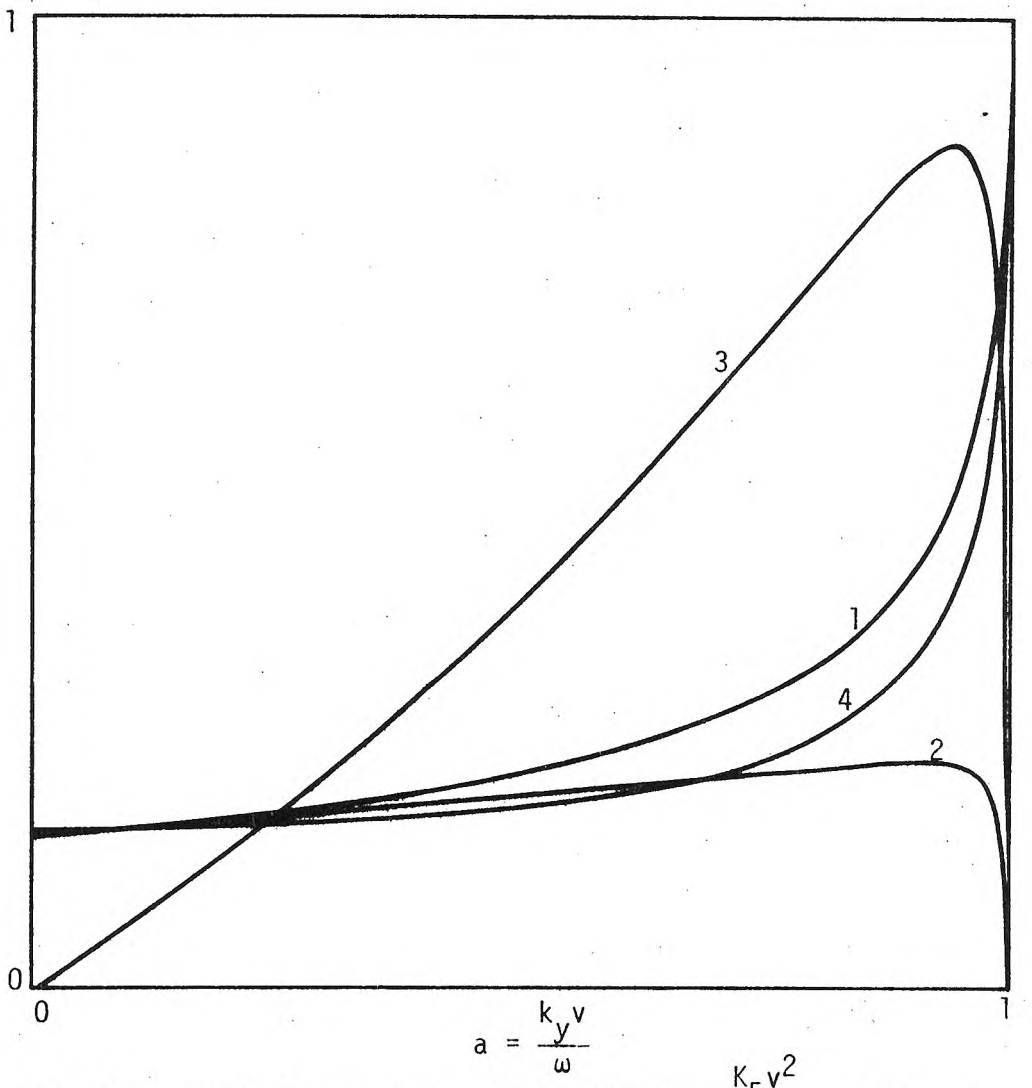

Fig. 3.7 Integrands for geometry (A-ii-2) with $\frac{K_5 v^2}{\omega} = 2000$,

$\frac{\mu_o}{\sqrt{\mu_{2y}\mu_{2z}}} = 0.02$, $\frac{v}{\omega}\frac{1}{h_3} = 5$

(1) Re $\{\frac{\omega h_3 \tilde{Z}_L}{-i\mu_o v^2}\}$, (2) Im $\{\frac{\omega h_3 \tilde{Z}_L}{-i\mu_o v^2}\}$

(3) $\frac{\tilde{F}_y}{|\tilde{K}_x|^2}\frac{8}{\mu_o}\frac{\omega}{v}h_3$, (4) $\frac{\tilde{F}_z}{|\tilde{K}_x|^2}\frac{3.2\omega^2 h_3^2}{\mu_o v^2} + 0.2$

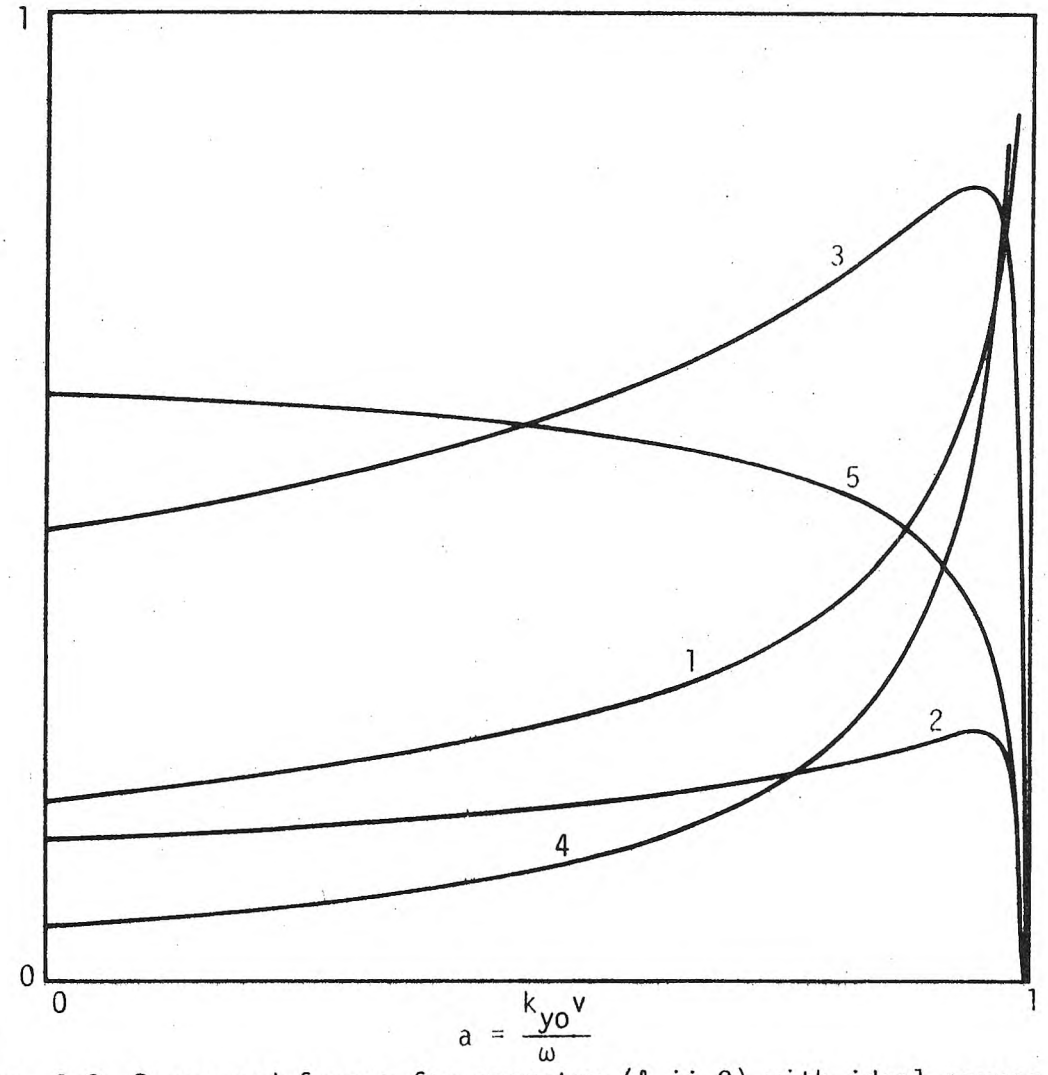

Fig. 3.8 Power and forces for geometry (A-ii-2) with ideal source and $\omega K_5 = 200{,}000$, $\frac{\mu_o}{\sqrt{\mu_{2y}\mu_{2z}}} = 0.01$, $h_3 = 0.01$, $k_{yo} = 10$.

(1) $-\frac{\text{Im } \bar{P}}{\omega\mu_o K_o^2} \frac{250h_3}{1}$, (2) $\frac{\text{Re } \bar{P}}{\omega\mu_o K_o^2} (250h_3)$,

(3) $\frac{80h_3\bar{F}_y}{\mu_o K_o^2}$, (4) $\frac{800h_3^2 \bar{F}_z}{\mu_o K_o^2}$,

(5) Power factor

Also, no matter which track is used, $|\tilde{F}_y|/|\tilde{K}_x|^2$ and $|\tilde{F}_z|/|\tilde{K}_x|^2$ will always be larger than those of the corresponding values of (A-ii-1). Most arguments given in (A-ii-1) can be applied here for the nonferromagnetic track except that, due to the relatively larger values of a_y, $|\tilde{F}_y|/|\tilde{K}_x|^2$ and $|\tilde{F}_z|/|\tilde{K}_x|^2$, this case will produce larger forces and efficiency. For the ferromagnetic track, the advantage over that of LIM with $\alpha = 1$ which was mentioned before is re-observed. Due to the fact that $a_y > a_z$, if the LIM is used for both propulsion and levitation purposes, the LIM is suggested to be operated in the attractive region. Then, a peak propulsion force can always be obtained while the attractive force is still relatively large. For the ideal source, the results can be obtained simply by substituting k_y with k_{yo}. Some plots with the machine performance as a function of v are given in Fig. 3.8. For ferromagnetic tracks, some results are qualitatively similar to those of (A-i-1). When $\tilde{K}_x$ is not a δ-function, the end effect will also appear. Decreasing σ_x is suggested to reduce it.

(B) $\beta_1 = \beta_3$: (region 1 is free space)

In (A), $\beta_1 \tilde{=} 0$. This means a lot of laminated ferromagnetic material must be used, and thus more cost. So, from the economic point of view, the free space, or just the earth for region 1 may be preferable.

From (2.8), (2.13), (2.31):

$$\tilde{Z}_L = \frac{-i\omega\mu_o}{k_z} \frac{Q_2}{Q_1 + \alpha Q_2} \qquad (3.23a)$$

$$\tilde{F}_y = \mathrm{Re}\,\frac{-i\mu_o}{2}\,\mathrm{sgn}(k_y)\,\frac{Q_2}{Q_1 + Q_2}\,|\tilde{K}_x|^2 \tag{3.23b}$$

$$\tilde{F}_z = \frac{\mu_o}{4}\,\frac{[|1+\frac{\mu_{2y}k_z}{\mu_o\gamma_2}\tanh\gamma_2h_2|^2 - |1+\frac{\mu_o\gamma_2}{\mu_{2y}k_z}\tanh\gamma_2h_2|^2]\,\mathrm{sech}^2k_zh_3}{|Q_1+\alpha Q_2|^2}\,|\tilde{K}_x|^2 \tag{3.23c}$$

Here

$$Q_1 = (\tanh k_zh_3 + \frac{\mu_o\gamma_2}{\mu_{2y}k_z}\tanh\gamma_2h_2) + (\frac{\mu_{2y}k_3}{\mu_o\gamma_2}\tanh\gamma_2h_2\tanh k_zh_3 + 1) \tag{3.23d}$$

$$Q_2 = (1+\frac{\mu_o\gamma_2}{\mu_{2y}k_z}\tanh\gamma_2h_2\tanh k_zh_3) + (\frac{\mu_{2y}k_z}{\mu_o\gamma_2}\tanh\gamma_2h_2 + \tanh k_zh_3) \tag{3.23e}$$

For thick reaction rails, there is no difference whether region 1 is the free space or a laminated iron, or any other material. Thus, in the following only the thin reaction rail is necessary to be considered.

(i-1) $\alpha \tilde{=} 0$: (region 4 is infihitely laminated iron)

Under the thin reaction rail assumption, (3.23) will give us:

$$\tilde{Z}_L \tilde{=} -i\omega\mu_o\,\frac{(1+\frac{\mu_{2y}h_2+\mu_oh_3}{\mu_o}k_z)}{k_y^2 - i(\omega-k_yv)K_1 + \frac{\mu_{2z}}{\mu_{2z}h_3+\mu_oh_2}k_z}\,\frac{\mu_{2z}}{\mu_{2z}h_3+\mu_oh_2} \tag{3.24a}$$

$$\tilde{=} -i\omega\mu_o\,\frac{(1+\frac{\mu_{2y}h_2+\mu_oh_3}{\mu_o}k_z)[k_z+i(\omega-k_yv)\mu_o\sigma_xh_2]}{k_y^2+(\omega-k_yv)^2\mu_o^2\sigma_x^2h_2^2} \tag{3.24b}$$

$$\tilde{F}_y \cong \mathrm{Re}\,\frac{-i\mu_o}{2}\,\frac{k_y\left(1+\dfrac{\mu_{2y}h_2+\mu_o h_3}{\mu_o}k_z\right)}{k_y^2-i(\omega-k_y v)K_1+\dfrac{\mu_{2z}}{\mu_{2z}h_3+\mu_o h_2}k_z}\,\frac{\mu_{2z}}{\mu_{2z}h_3+\mu_o h_2}\,|\tilde{K}_x|^2 \qquad (3.25a)$$

$$\cong \frac{\mu_o}{2}\,\frac{k_y\left(1+\dfrac{\mu_{2y}h_2+\mu_o h_3}{\mu_o}k_z\right)(\omega-k_y v)\mu_o\sigma_x h_2}{k_y^2+(\omega-k_y v)^2\mu_o^2\sigma_x^2 h_2^2}\,|\tilde{K}_x|^2 \qquad (3.25b)$$

$$\tilde{F}_z \cong \frac{\mu_o}{4}\,\frac{\mu_{2y}^2k_y^2\left[\left|1+\dfrac{\mu_{2y}k_z h_2}{\mu_o}\right|^2-\left|1+\dfrac{\mu_o\gamma_2^2 h_2}{\mu_{2y}k_z}\right|^2\right]}{\left|\mu_{2y}k_z+\mu_{2y}k_y^2 h_3+\mu_o\gamma_2^2 h_2\right|^2}\,|\tilde{K}_x| \qquad (3.26a)$$

$$\cong \frac{\mu_o}{4}\,\frac{k_z^3 h_2\left(2+\dfrac{\mu_{2y}\mu_{2z}+\mu_o^2}{\mu_o\mu_{2z}}k_z h_2\right)\dfrac{\mu_{2y}\mu_{2z}-\mu_o^2}{\mu_o\mu_{2z}}-(\omega-k_y v)^2\mu_o^2\sigma_x^2 h_2^2}{k_y^2+(\omega-k_y v)^2\sigma_x^2\mu_o^2 h_2^2}\,|\tilde{K}_x|^2 \qquad (3.26b)$$

Of course, (3.24b), (3.25b) and (3.26b) are introduced only for the purpose of simplifying the integrand analysis. Generally they cannot be used for the integral evaluation. (The ideal source with $k_{yo}h_3 \ll 1$ is one exception.)

Except for a factor, (3.24) is exactly the same as (3.9). However, this factor $\left(1+\dfrac{\mu_{2y}h_2+\mu_o h_3}{\mu_o}k_z\right)$ will make the algebraic analysis much more complicated.

Several remarks will be given:

Nonferromagnetic tracks:

- Since $[1 + k_z(h_2+h_3)] \sim 1$, except for the value $\tilde{F}_z/|\tilde{K}_x|^2$, the difference between this geometry and (A-i-2) is small. Thus we will get similar plots of $\tilde{F}_y/|\tilde{K}_x|^2$ and $\tilde{Z}_L$ for both cases. And $a_y \cong \frac{1}{1+\frac{1}{\gamma}}$, $a_r \cong 1 - \frac{1}{\sqrt{1+\gamma^2}}$, $a_i \cong \frac{1}{\sqrt{1+\frac{1}{\gamma^2}}}$ with $\gamma = \mu\sigma_x h_2 v$. Of course, the corresponding maximum values will be a little bit larger than those of (A-i-2).

- $\tilde{F}_z/|\tilde{K}_x|^2$ will be different from the corresponding (A-i-2) result. Actually, $\tilde{F}_z/|\tilde{K}_x|^2 = \frac{-(\omega-k_y v)^2 \mu_o^2 \sigma_x^2 h_2^2}{k_y^2 + (\omega-k_y v)^2 \mu_o^2 \sigma_x^2 h_2^2}$, i.e., it will always be repulsive. This is not surprising because now there is no back-iron to give the attractive force component any longer. Also, there is a minimum value of $-\mu_o/4$ at $k_y = 0$ and a maximum value of 0 at $a = 1$.

Ferromagnetic tracks: ($\frac{\mu_{2y} h_2 + \mu_o h_3}{\mu_o} k_z$ cannot be neglected)

- For $a > 0$ it can be shown that a_y lies to the right of $\frac{1}{1+\frac{1}{\mu_o \sigma_x h_2 v}}$. And for $0 < a < \frac{1}{1+\frac{1}{\gamma}}$, $\tilde{F}_y/|\tilde{K}_x|^2$ is monotonically increasing. At $a = \frac{1}{1+\frac{1}{\gamma}}$, $\tilde{F}_y/|\tilde{K}_x|^2 = (1 + \frac{\mu_{2y} h_2 + \mu_o h_3}{\mu_o} \times \frac{\omega}{v} \frac{1}{1+\frac{1}{\gamma}}) \frac{\tilde{F}_{ym(A\text{-}i\text{-}2)}}{|\tilde{K}_x|^2}$.

- For $a > 0$ it can be shown that if $\frac{\mu_{2y} h_2}{\mu_o} \frac{\omega}{v} \frac{1}{1+\frac{1}{\gamma}} \gtrless \sqrt{2} - 1$, a_z lies to the $\binom{\text{left}}{\text{right}}$ of $a = 1/(1+\frac{1}{\gamma})$. And, there is only

one value of a_z lying between 0 and 1. Also, at $k_y = \frac{\omega}{v}$, $\tilde{F}_z/|\tilde{K}_x|^2 = \frac{\mu_o}{4}(\frac{\omega}{v} h_2 \frac{\mu_{2y}}{\mu_o})$ which is the maximum value of $\tilde{F}_z/|\tilde{K}_x|^2$. Other properties of the integrands can roughly be obtained from the plots in Fig. 3.9.

For the same source distributions, it can be seen that for non-ferromagnetic tracks the machine performance in terms of F_y, η, and PF is roughly similar to that of (A-i-2). The main difference is that now we get only a purely repulsive force. And the small absolute value of the integrand for $\bar{F}_z$ at large "a" will exclude this geometry from being used as a LIM for both supporting and propulsion purposes. For ferromagnetic tracks, the situation is different. Of course, if $\frac{\mu_{2y}h_2 + \mu_o h_3}{\mu_o} k_{yo}$ is still small, the result definitely will be nearly the same as before. However, if μ_{2y} is large enough, then $\frac{\mu_{2y}h_2 + \mu_o h_3}{\mu_o} k_{yo}$ becomes important; especially when $\frac{\mu_{2y}h_2\omega}{\mu_o v} \frac{1}{1 + \frac{1}{\gamma}} > \sqrt{2} - 1$ such that $a_y > a_z$ is true. Then, we can try to design a LIM to support and simultaneously accelerate the vehicle. Thus, from this point of view, we can conclude that a larger value of $\frac{\mu_{2y}h_2\omega}{\mu_o v} \frac{1}{1 + \frac{1}{\gamma}}$ is more desirable. And making μ_{2y} and h_2 large is the easiest way to reach this objective. As for the factor $\frac{1}{1 + \frac{1}{\gamma}}$, we can also try to make σ_x larger to get a value approximately equal to 1 at the peak velocity. However, as far as the end effect is concerned, it is more desirable to keep it at a moderate value (say 0.8). Then it seems that a somewhat smaller σ_x is preferred over a higher σ_x. All of this will make the composite iron the most promising track material.

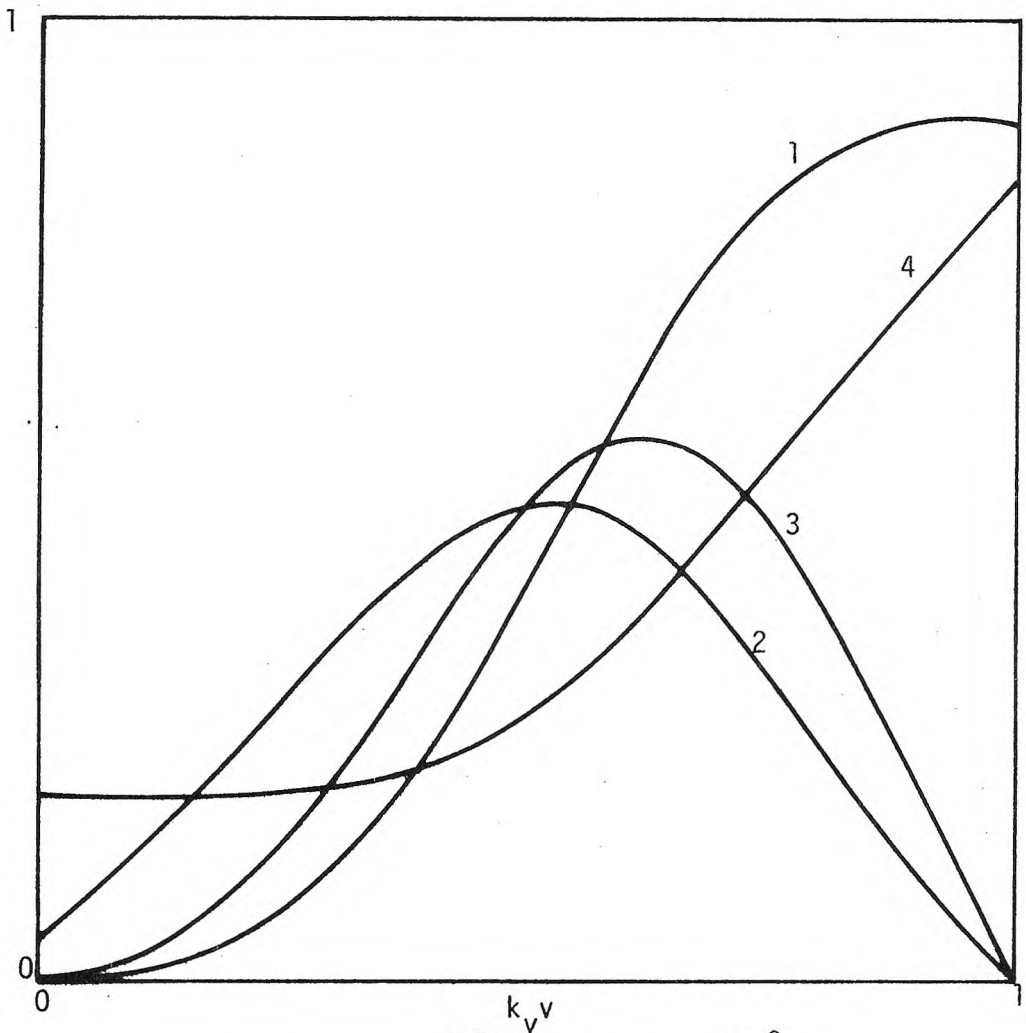

Fig. 3.9 Integrands for geometry (B-i-1) with $\frac{K_1 v^2}{\omega} = 10$,

$\frac{\mu_{2z}}{\mu_{2z}h_3 + \mu_o h_2} \frac{v}{\omega} = 8$, $\frac{\mu_{2y}h_2 + \mu_o h_3}{\mu_o} \frac{\omega}{v} = 15$, $\frac{\mu_{2y}h_2}{\mu_o} \frac{\omega}{v} = 14.9$,

$\frac{\mu_o}{\mu_{2z}} \frac{\omega}{v} h_2 = 0.0015$. (1) $\mathrm{Re}\{\frac{\tilde{Z}_L}{-i\mu_o v^2} \frac{\omega(\mu_{2z}h_3 + \mu_o h_2)}{2\mu_{2z}}\}$,

(2) $\mathrm{Im} \frac{\tilde{Z}_L}{-i\mu_o v^2} \frac{\omega(\mu_{2z}h_3 + \mu_o h_2)}{2\mu_{2z}}$, (3) $\frac{\tilde{F}_y}{|\tilde{K}_x|^2} \frac{2\omega(\mu_{2z}h_3 + \mu_o h_2)}{\mu_o \mu_{2z} v}$,

(4) $\frac{\tilde{F}_z}{|\tilde{K}_x|^2} \frac{0.8\omega^2(\mu_{2z}h_3 + \mu_o h_2)^2}{\mu_o v^2 \mu_{2z}^2} + 0.2$

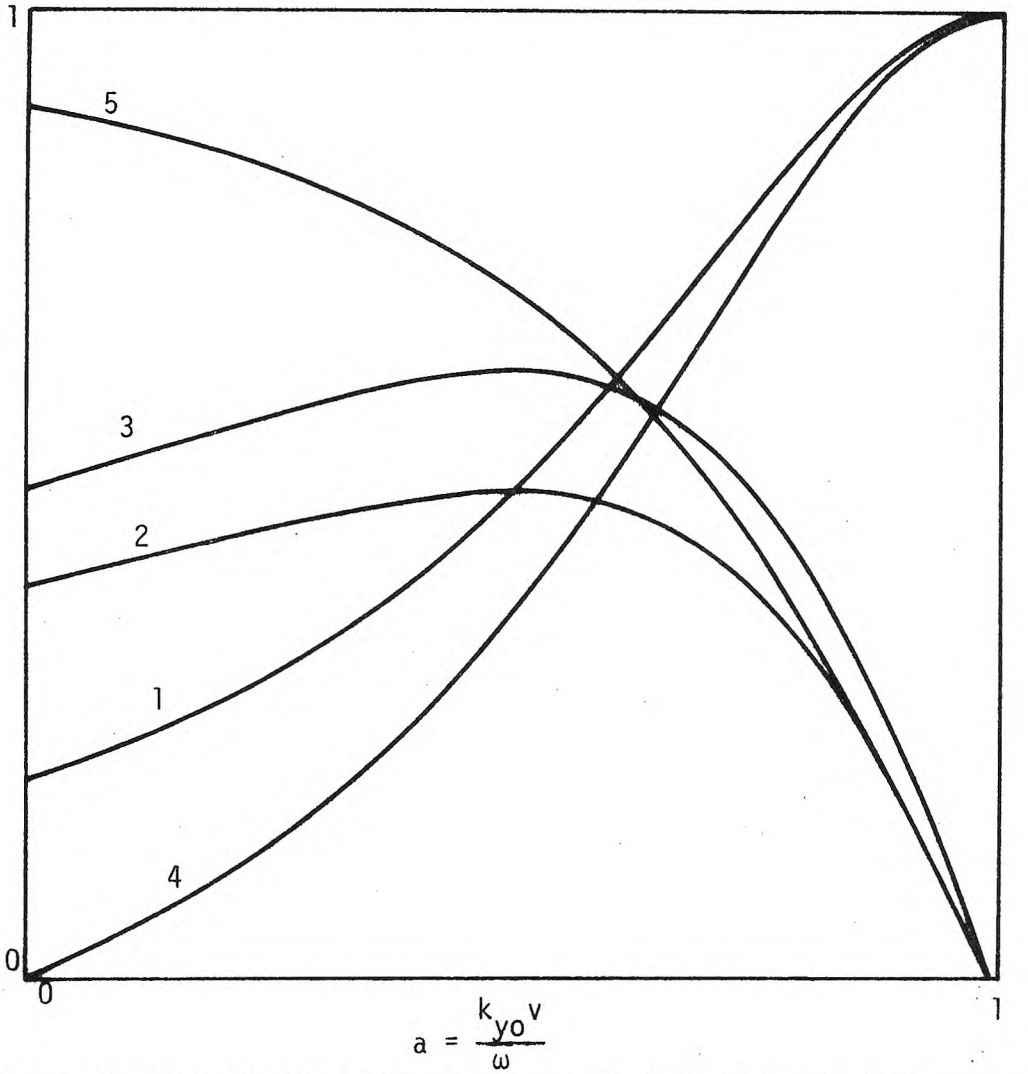

Fig. 3.10a Power and forces for geometry (B-i-1) with ideal source and $\omega K_1 = 1000$, $\frac{\mu_{2z}}{\mu_{2z}h_3 + \mu_o h_2} = 40$, $\frac{\mu_{2y}h_2 + \mu_o h_3}{\mu_o} = 0.025$,

$\frac{\mu_{2y}h_2}{\mu_o} = 0.01$, $\frac{\mu_o h_2}{\mu_{2z}} = 0.01$, $k_{yo} = 10$

(1) $\frac{-800(\mu_{2z}h_3 + \mu_o h_2)}{\omega\mu_o K_o^2 \mu_{2z}}$ Im $\bar{P}$, (2) $\frac{800(\mu_{2z}h_3 + \mu_o h_2)}{\omega\mu_o K_o^2 \mu_{2z}}$ Re $\bar{P}$,

(3) $\frac{100\sigma_x h_2 \bar{F}_y}{K_o^2 K_1}$, (4) $\frac{8000\bar{F}_z(\mu_{2z}h_3 + \mu_o h_2)^2}{\mu_o \mu_{2z}^2 K_o^2} + 1$,

(5) Power factor

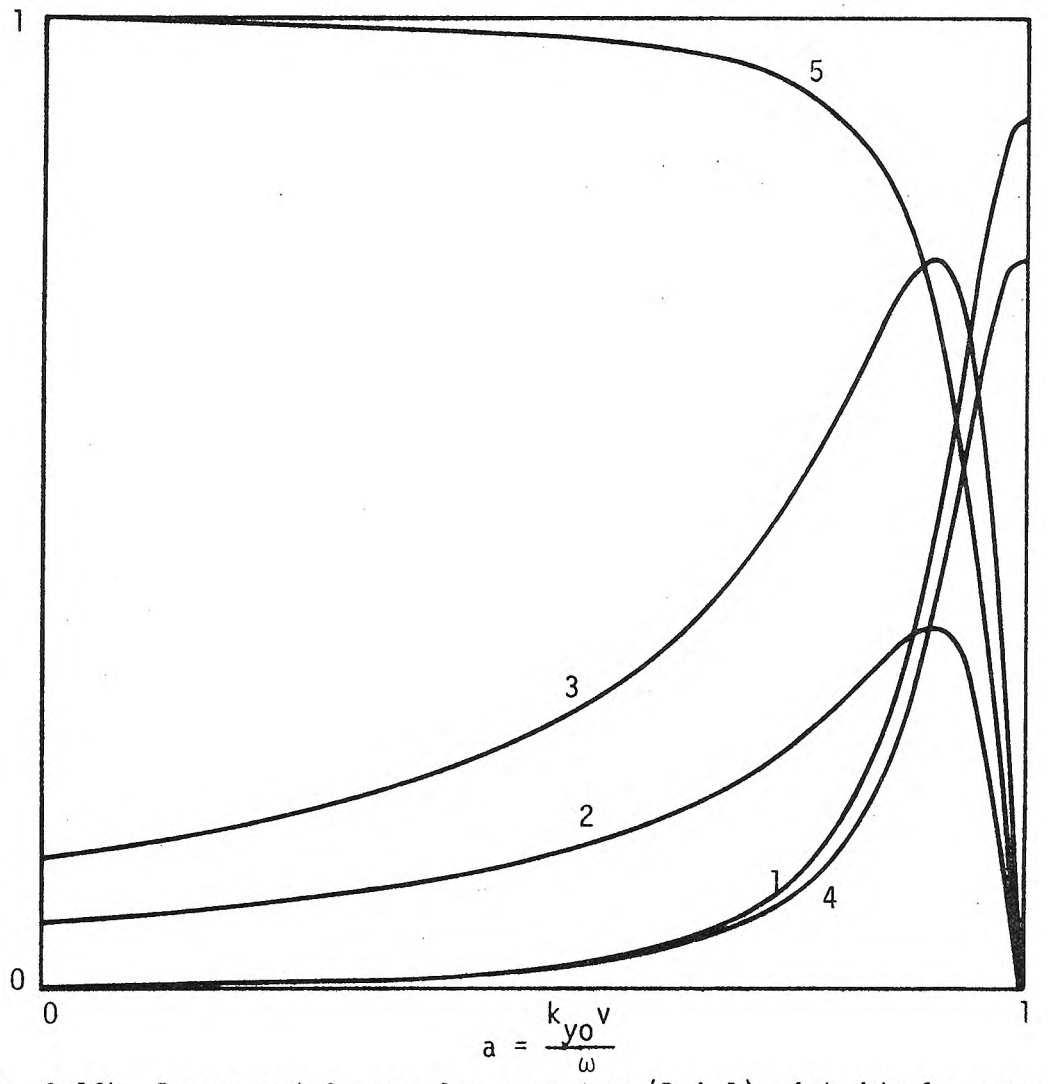

Fig. 3.10b Power and forces for geometry (B-i-1) with ideal source and

$$\omega K_1 = 10{,}000, \quad \frac{\mu_{2z}}{\mu_{2z} h_3 + \mu_o h_2} = 80 , \quad \frac{\mu_{2y} h_2 + \mu_o h_3}{\mu_o} = 1.25 ,$$

$$\frac{\mu_{2y} h_2}{\mu_o} = 1.25 , \quad \frac{\mu_o h_2}{\mu_{2z}} = 0.008 , \quad k_{yo} = 10$$

$$(1) \frac{-100(\mu_{2z} h_3 + \mu_o h_2)}{\omega \mu_o K_o^2 \mu_{2z}} \operatorname{Im} \bar{p} , \quad (2) \frac{100(\mu_{2z} h_3 + \mu_o h_2)}{\omega \mu_o K_o^2 \mu_{2z}} \operatorname{Re} \bar{p} ,$$

$$(3) \frac{20 \sigma_x h_2 \bar{F}_y}{K_1 K_o^2} , \quad (4) \frac{160(\mu_{2z} h_3 + \mu_o h_2)^2 \bar{F}_z}{\mu_o \mu_{2z}^2 K_o^2} , \text{ (5) Power factor}$$

(i-2) $\alpha = 1$: (region 4 is free space)

Under the thin reaction rail assumption, (3.23) will give us:

$$\tilde{Z}_L \cong \frac{-i\omega\mu_o}{k_z} \frac{1 + (\frac{\mu_{2y}h_2 + \mu_o h_3}{\mu_o})\, k_z}{2 + (\frac{\mu_o\gamma_2}{\mu_{2y}k_z} + \frac{\mu_{2y}k_z}{\mu_o\gamma_2})\, \gamma_2 h_2} \tag{3.27a}$$

$$\cong -i\omega\mu_o \frac{(1 + \frac{\mu_{2y}h_2 + \mu_o h_3}{\mu_o} k_z)[2k_z + \frac{\mu_{2y}\mu_{2z} + \mu_o^2}{\mu_o\mu_{2z}} k_y^2 h_2) + i(\omega - k_y v)\, \mu_o\sigma_x h_2]}{(2k_z + \frac{\mu_{2y}\mu_{2z} + \mu_o^2}{\mu_o\mu_{2z}} k_y^2 h_2)^2 + (\omega - k_y v)^2 \mu_o^2 \sigma_x^2 h_2^2} \tag{3.27b}$$

$$\tilde{F}_y \cong \mathrm{Re}\, \frac{-i\mu_o}{2} \mathrm{sgn}(k_y) \frac{1 + \frac{\mu_{2y}h_2 + \mu_o h_3}{\mu_o} k_z}{2 + (\frac{\mu_o\gamma_2}{\mu_{2y}k_z} + \frac{\mu_{2y}k_z}{\mu_o\gamma_2})\gamma_2 h_2} |\tilde{K}_x|^2 \tag{3.28a}$$

$$= \frac{\mu_o}{2} \frac{k_y(1 + \frac{\mu_{2y}h_2 + \mu_o h_3}{\mu_o} k_z)(\omega - k_y v)\mu_o\sigma_x h_2}{(2k_z + \frac{\mu_{2y}\mu_{2z} + \mu_o^2}{\mu_o\mu_{2z}} k_y^2 h_2)^2 + (\omega - k_y v)^2 \mu_o^2 \sigma_x^2 h_2^2} |\tilde{K}_x|^2 \tag{3.28b}$$

$$\tilde{F}_z \cong \frac{\mu_o}{4} \frac{\left|1 + \frac{\mu_{2y} h_2}{\mu_o} k_z\right|^2 - \left|1 + \frac{\mu_o \gamma_2^2 h_2}{\mu_{2y} k_z}\right|^2}{\left|2 + \left(\frac{\mu_o \gamma_2}{\mu_{2y} k_z} + \frac{\mu_{2y} k_z}{\mu_o \gamma_2}\right) \gamma_2 h_2\right|^2} |\tilde{K}_x|^2 \qquad (3.29a)$$

$$\cong \frac{\mu_o}{4} \frac{k_z^3 h_2 (2 + \frac{\mu_{2y}\mu_{2z} + \mu_o^2}{\mu_o \mu_{2z}} k_z h_2) \frac{\mu_{2y}\mu_{2z} - \mu_o^2}{\mu_o \mu_{2z}} - (\omega - k_y v)^2 \mu_o^2 \sigma_x^2 h_2^2}{(2k_z + \frac{\mu_{2y}\mu_{2z} + \mu_o^2}{\mu_o \mu_{2z}} k_y^2 h_2)^2 + (\omega - k_y v)^2 \mu_o^2 \sigma_x^2 h_2^2} |\tilde{K}_x|^2 \qquad (3.29b)$$

Some tedious algebraic analyses will give us the following results:

Nonferromagnetic tracks:

- $(2k_z + \frac{\mu_{2y}\mu_{2z} + \mu_o^2}{\mu_o \mu_{2z}} k_y^2 h_2)^2$ can be further approximated as $4k_y^2$. And $1 + \frac{\mu_{2y} h_2 + \mu_o h_3}{\mu_o} k_z \cong 1$. Then (3.24b) and (3.27b) look nearly the same; so do (3.25b) and (3.28b). By comparing the formulas with each other it follows that $a_y \cong \frac{1}{1 + \frac{2}{\gamma}}$, $a_r \cong 1 - \frac{1}{\sqrt{1 + \frac{2}{\gamma}}}$, and $a_i \cong \frac{1}{\sqrt{1 + \frac{4}{\gamma^2}}}$. Generally, the corresponding maximum values are smaller for geometry (B-i-2). Actually $\tilde{F}_y/|\tilde{K}_x|^2$ at $a_y \cong \frac{1}{1 + \frac{2}{\gamma}}$ for geometry (B-i-2) is only about one-half of the value of $\tilde{F}_y/|\tilde{K}_x|^2$ at $a_y = \frac{1}{1 + \frac{1}{\gamma}}$ for the case (B-i-1).

- $\tilde{F}_z/|\tilde{K}_x|^2 = \frac{-(\omega - k_y v)^2 \mu_o^2 \sigma_x^2 h_2^2}{4k_y^2 + (\omega - k_y v)^2 \mu_o^2 \sigma_x^2 h_2^2} \frac{\mu_o}{4}$. This is similar to the previous case (B-i-1) and will always be negative. Actually, a minimum value of $-\mu_o/4$ occurs at $k_y = 0$, and a maximum value

of "0" occurs at $k_y = \frac{\omega}{v}$. However, for the same "a" it will be a little bit smaller for geometry (B-i-2).

Ferromagnetic tracks:

- For $1 > a > 0$, if $\frac{\omega}{v}\frac{\mu_{2y}}{\mu_o} h_2$ is still small, then the same conclusion as for that of nonferromagnetic tracks can be used as an approximation.
- For $a > 0$, if $\frac{\omega}{v}\frac{\mu_{2y}}{\mu_o} h_2$ is not small, then, except in a very small region where k_z is small such that $\frac{\mu_{2y}}{\mu_o} k_z h_2 << 1$ is still true so as to make the integrands behave in the same manner as that of nonferromagnetic track, the situation is different for the remaining regions.
- In order to have a LIM with reasonable efficiency, it is suggested that k_{yo} be a little bit smaller than ω/v (say, $k_{yo} = 0.8\ \omega/v$). Now for $a > 0$, if $\frac{\omega}{v}\frac{\mu_{2y}}{\mu_o} h_2 >> 1$, then, in the region where $|\tilde{K}_x|^2$ is large (i.e., say around $k_{yo} \cong 0.8\ \omega/v$), the approximation $1 + \frac{\mu_{2y}\mu_{2z} + \mu_o^2}{\mu_o \mu_{2z}} k_z h_2 \cong \frac{\mu_{2y}}{\mu_o} k_z h_2$ can be made. Then, it can be shown that $a_y \cong \frac{2}{1 + \sqrt{1 + \frac{4}{Kv^2}}}$ and $\tilde{F}_{ym}/|\tilde{K}_x|^2 = \mu_o/4$. $\tilde{F}_z/|\tilde{K}_x|^2$ is found to be monotonically increasing with $a_z \cong a_y$. A maximum value of $\mu_o/4$ at $a = 1$ and a minimum value of $-\mu_o/4$ at $a = 0$ can also be observed.

For small $\frac{\mu_{2y}}{\mu_o}\frac{\omega}{v} h_2$, the terms $\tilde{F}_y/|\tilde{K}_x|^2$, $\tilde{F}_z/|\tilde{K}_x|^2$ and $\tilde{Z}_L$ are found to behave in a similar manner as in (B-i-1). The main difference is that the most important factor $\gamma = \mu_o h_2 \sigma_x v$ of the previous case

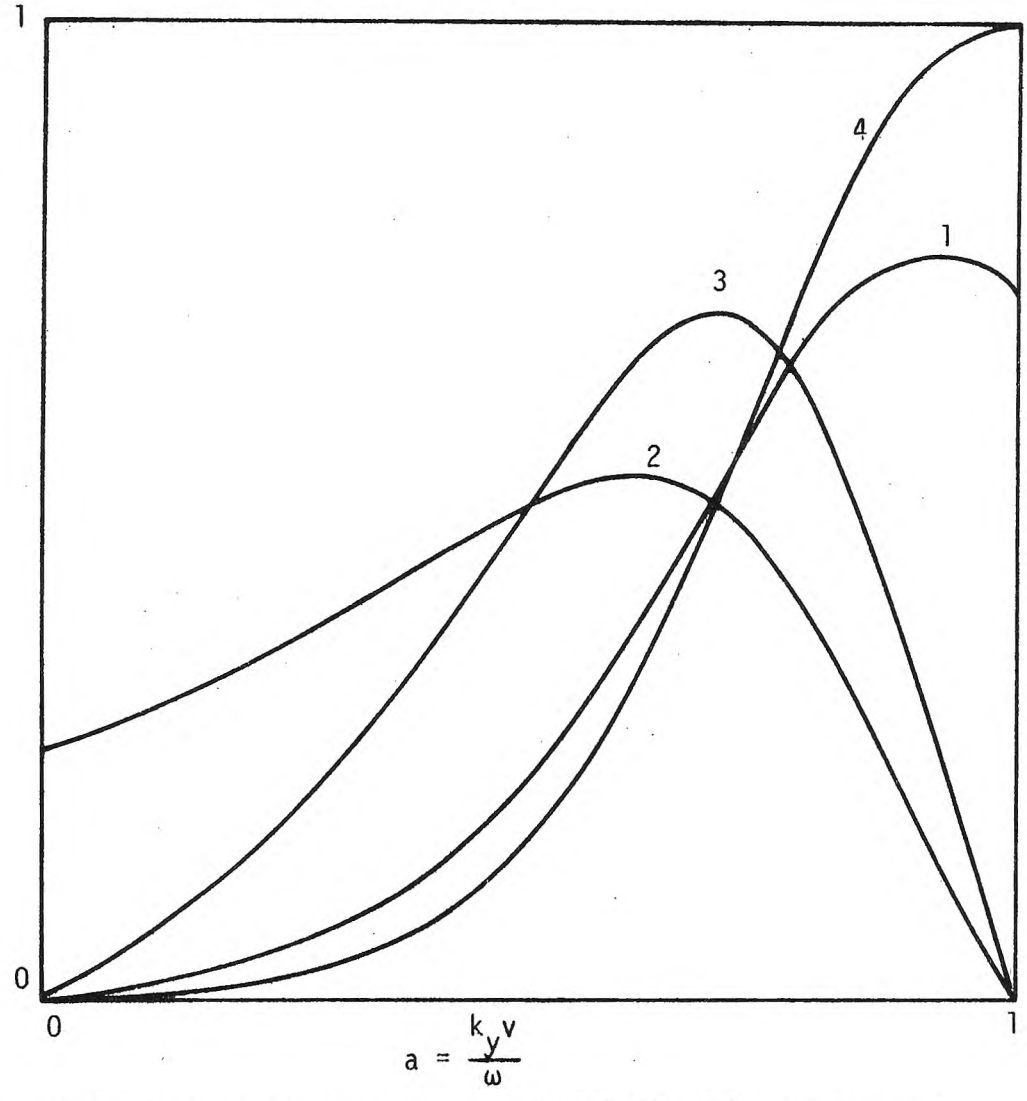

Fig. 3.11 Integrands for geometry (B-ii-2) with $\mu_o \sigma_x h_2 v = 5$,

$\frac{\mu_{2y}\mu_{2z} + \mu_o^2}{\mu_o \mu_{2z}} \frac{\omega}{v} h_2 = 0.4$, $\frac{\mu_{2y} h_2 + \mu_o h_3}{\mu_o} \frac{\omega}{v} = 0.4$,

$\frac{\mu_{2y} h_2}{\mu_o} \frac{\omega}{v} = 0.2 = \frac{\mu_o h_2}{\mu_{2z}} \frac{\omega}{v}$

(1) $\mathrm{Re}\{\frac{1.25\ \tilde{Z}_L}{-i\mu_o v}\}$, (2) $\mathrm{Im}\{\frac{1.25\ \tilde{Z}_L}{-i\mu_o v}\}$

(3) $\frac{5\tilde{F}_y}{\mu_o |\tilde{K}_x|^2}$, (4) $\frac{4\tilde{F}_z}{\mu_o |\tilde{K}_x|^2} + 1$

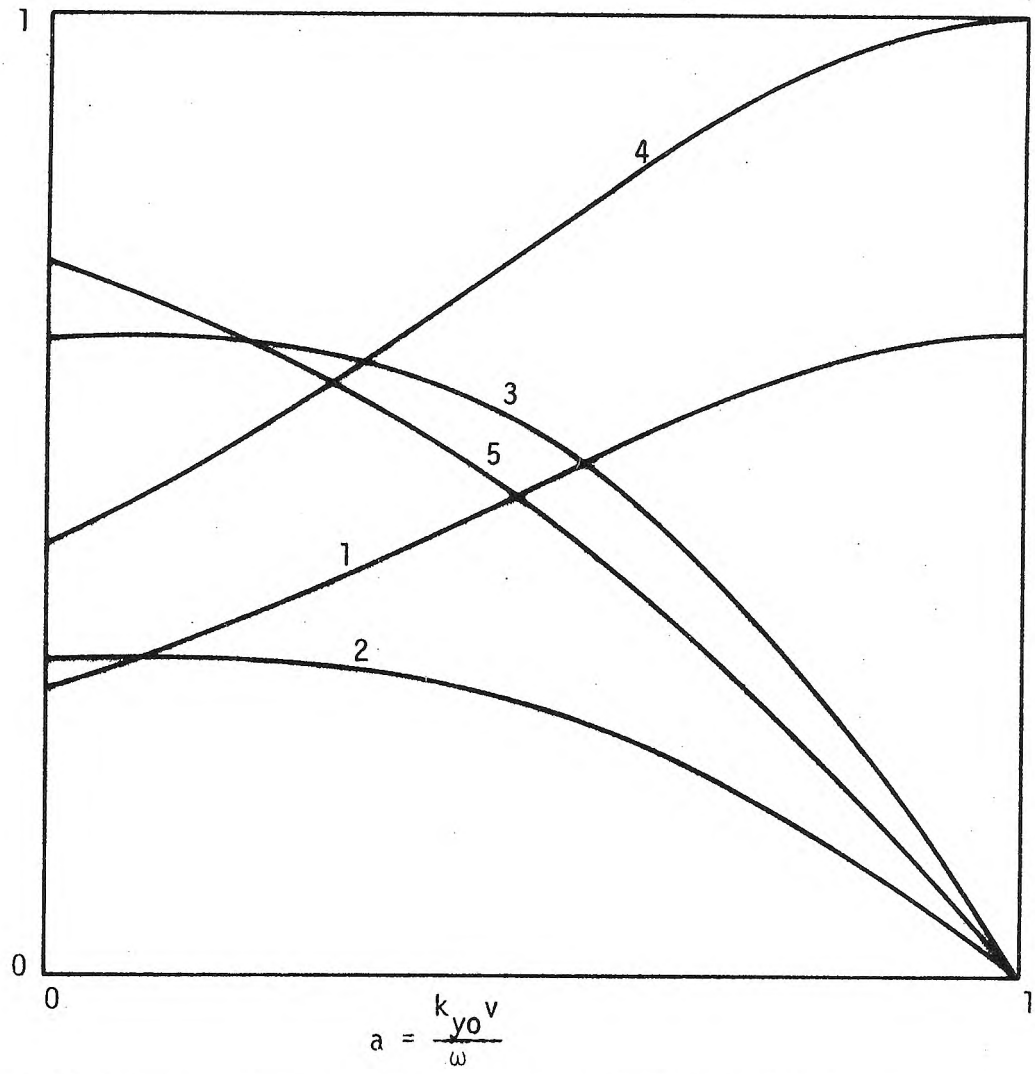

Fig. 3.12 Power and forces for geometry (B-ii-2) with ideal source and $\omega\mu_o\sigma_x h_2 = 25$

$\frac{\mu_{2y}\mu_{2z} + \mu_o^2}{\mu_o\mu_{2z}} h_2 = 0.025$, $\frac{\mu_{2y} h_2 + \mu_o h_3}{\mu_o} = 0.02$,

$\frac{\mu_{2y} h_2}{\mu_o} = 0.01$, $\frac{\mu_o h_2}{\mu_{2z}} = 0.01$, $k_{yo} = 10$

(1) $\frac{-25\ \mathrm{Im}\ \bar{p}}{\omega\mu_o K_o^2}$, (2) $\frac{25\ \mathrm{Re}\ \bar{p}}{\omega\mu_o K_o^2}$, (3) $\frac{5\ \bar{F}_y}{\mu_o K_o^2}$,

(4) $\frac{4\bar{F}_z}{\mu_o K_o^2} + 1$, (5) Power Factor

(B-i-1) is now changed to $\gamma/2$ and the corresponding maximum values of $\tilde{F}_y/|\tilde{K}_x|^2$, $\tilde{Z}_r$, $\tilde{Z}_i$ for this case are smaller. For a large $\frac{\mu_{2y}}{\mu_o}\frac{\omega}{v}h_2$, it is a different story. Actually, it looks more similar to (A-ii-1). In both geometries (B-i-2) and (A-ii-1), we have $a_y = a_z$, $\frac{\tilde{F}_y(a=a_y)}{|\tilde{K}_x|^2} = \frac{\tilde{F}_z(a=1)}{|\tilde{K}_x|^2} = \frac{\mu_o}{4}$ and $\frac{\tilde{F}_z(a=0)}{|\tilde{K}_x|^2} \cong -\frac{\mu_o}{4}$. Thus, most arguments given in (A-ii-1) can also be applied here.

After the above analysis, a general discussion will be given. Now that the LIMs are supposed to be used both for supporting and propulsion, large forces in both directions and high efficiency are all required. This will eventually eliminate the possibility of using LIMs which give repulsive supporting forces. So cases (A-ii) and (B) with nonferromagnetic tracks are not recommended. For the remaining geometries which can be operated to give attractive supporting forces, they can be divided into two categories, namely, $a_y > a_z$ and $a_y \cong a_z$. The property that a larger propulsion force can only be obtained in a region where $\tilde{F}_z/|\tilde{K}_x|^2$ is relatively small will further exclude the cases with $a_y = a_z$ which generally occur for $\alpha_4 = 1$. Thus, finally, the only remaining geometries are (A-ii-2) and (B-i-1) with $\mu \neq \mu_o I$ and (A-i-1). It should also be noticed that maximum values of $\tilde{F}_z/|\tilde{K}_x|^2$ are generally larger than those of $\tilde{F}_y/|\tilde{K}_x|^2$ for the remaining cases. And thus, for a suitable $|\tilde{K}_x|^2$, a larger $\bar{F}_z$ can always be obtained. This happens to be consistent with the requirement for vehicle design, since an acceleration of "1g" is always necessary to support the vehicle, while for comfort, human beings can only tolerate a horizontal acceleration of several tenths of "1g".

Of course, if $|\tilde{K}_x|^2$ is specified, the machine performance can be evaluated either numerically or analytically. Generally, numerical integrations are straightforward and analytical evaluations are difficult. However, for some of the simplified geometries with thin or thick reaction rails, analytical evaluations seem to be possible. Now, we will consider the most popular source distribution $|\tilde{K}_x|^2 = \frac{2K_o^2}{\pi} \frac{\sin^2(k_y-k_{yo})L}{(k_y-k_{yo})^2}$ and try to evaluate the machine performance integrals. Of course, it would be the best situation if we could analytically evaluate them for all of the recommended geometries. However, geometry (A-ii-2) is quite difficult. Thus, although geometry (A-ii-1) is not promising, it will be analytically examined as an alternative of the thick reaction rails. And we hope that it will give us some information about geometry (A-ii-2). (Results for geometry (A-ii-2) are also given in Appendix F.)

(a) Geometry (A-i-1):

In this case all of the integrands (with the source term excluded) can be easily factorized. The integrals can be rewritten as the summations of integrals similar to $S_1(\alpha,k_{yo},L)$. Appendix C can then be used to get:

$$\overline{P} \cong \frac{-i\omega\mu_o K_o^2}{\pi} \frac{\mu_{2z}}{\mu_{2z}h_3^+ \mu_o h_2} \sum_{\substack{m=1,2 \\ k\neq m}} \frac{1}{\alpha_m - \alpha_k} S_1(\alpha_m,k_{yo},L) \qquad (3.30a)$$

$$\tilde{F}_y \cong \mathrm{Re}\ \frac{-i\mu_o K_o^2}{\pi} \frac{\mu_{2z}}{\mu_{2z}h_3^+ \mu_o h_2} \sum_{\substack{m=1,2 \\ k\neq m}} \frac{\alpha_m}{\alpha_m-\alpha_k} S_1(\alpha_m,k_{yo},L) \qquad (3.30b)$$

$$\bar{F}_z \cong \frac{\mu_o K_o^2}{2\pi} \left(\frac{\mu_{2z}}{\mu_{2z} h_3 + \mu_o h_2}\right)^2 \sum_{i=1,2,3,4} \beta_m S_1(\alpha_m, k_{yo}, L) \tag{3.30c}$$

$$= \mathrm{Re} \frac{\mu_o K_o^2}{2\pi} \sum_{\substack{m=1,2 \\ k \neq m}} \frac{\left(\frac{K_1 v}{\gamma}\right)^2 + i(\omega - \alpha_m v) K_1}{(\alpha_m - \alpha_k)} S_1(\alpha_m, k_{yo}, L) \tag{3.30d}$$

where $\alpha_1 = \frac{K_1 v}{2} \left[\sqrt{\frac{b-1}{2}} + i\left(\sqrt{\frac{b+1}{2}} - 1\right)\right]$ (3.30e)

$$\alpha_2 = -\frac{K_1 v}{2} \left[\sqrt{\frac{b-1}{2}} + i\left(\sqrt{\frac{b+1}{2}} + 1\right)\right] \tag{3.30f}$$

$$\beta_m = \frac{\alpha_m^2 - (\omega - \alpha_m v)^2 \mu_o^2 \sigma_x^2 h_2^2}{\prod_{\substack{j=1,2,3,4 \\ j \neq m}} (\alpha_m - \alpha_j)}$$

with $b = \sqrt{1 + \left(\frac{4\omega}{K_1 v^2}\right)^2}$, $K_1 = \frac{\mu_o h_2 \sigma_x \mu_{2z}}{\mu_{2z} h_3 + \mu_o h_2}$, $\gamma = \mu_o \sigma_x h_2 v$

In the above derivation, the thin reaction rail approximation is used for the whole range of k_y extended from $-\infty$ to ∞. It is obviously not very accurate. Actually, this thin reaction rail assumption is only introduced to analyze the integrands within $0 \leq k_y \leq \frac{\omega}{v}$ or even only around k_{yo} where $|\tilde{K}_x|^2$ is large. In the region where k_z is large, generally $\gamma_2 h_2$ is also large, i.e., the thin reaction rail condition cannot be satisfied. However, if we go back to the original exact expressions for the integrands, we find that the contributions from the large k_z region are always very small. And, in the meanwhile, if we look into the thin reaction rail approximations,

then, in the same region we will also see very small integrands. Furthermore, the source function $|\tilde{K}_x|^2$ is only significant around k_{yo}. Thus, we can conclude that the use of the thin reaction rail approximation for the whole range of k_y does not introduce too much error for the machine performance integrals. This argument can also be applied to other geometries.

Numerical values can be used in (3.30) to evaluate the machine performance. However, before doing that, we will look into these formulas more carefully. For practical cases, $|\text{Im } 2\alpha_m L|$ is generally large (e.g., $> \pi$). Thus, $e^{2i(\alpha_m - k_{yo})L}$ can be neglected in $S_1(\alpha_m, k_{yo}, L)$. It is quite obvious that the term proportional to L in S_1 will give a result corresponding to the ideal source case (i.e., will give formulas (3.8)). The remaining term of $\frac{\pi i}{2}\frac{1}{(\alpha_m - k_{yo})^2}$ is essentially the reason for the end effect. Actually, we will have

$$\bar{P}_1 \cong \frac{-i\omega\mu_o K_o^2}{\pi}\,\frac{K_1 v}{\gamma}\,\frac{\pi i}{2(\alpha_1-\alpha_2)}\left[\frac{1}{(\alpha_1-k_{yo})^2}+\frac{1}{(\alpha_2-k_{yo})^2}\right] \tag{3.31a}$$

$$\bar{F}_{y_1} \cong \text{Re}\,\frac{-i\mu_o K_o^2}{\pi}\,\frac{K_1 v}{\gamma}\,\frac{\pi i}{2(\alpha_1-\alpha_2)}\left[\frac{\alpha_1}{(\alpha_1-k_{yo})^2}+\frac{\alpha_2}{(\alpha_2-k_{yo})^2}\right] \tag{3.31b}$$

$$\bar{F}_{z_1} \cong \frac{\mu_o}{4}\,\frac{K_o^2}{\pi}\,\text{Re}\,\frac{i\pi}{2(\alpha_1-\alpha_2)}\left[\frac{(\frac{K_1 v}{\gamma})^2+i(\omega-\alpha_1 v)K_1}{(\alpha_1-k_{yo})^2}+\frac{(\frac{K_1 v}{\gamma})^2+i(\omega-\alpha_2 v)K_1}{(\alpha_2-k_{yo})^2}\right] \tag{3.31c}$$

Here, the subscripts "1" are introduced to represent the contribution from the term $\frac{\pi i}{2}\frac{1}{(\alpha_m-k_{yo})^2}$ in $S_1(\alpha_m, k_{yo}, L)$. Also, (3.30d) is used

for $\bar{F}_z$ which will make the analysis simpler.

Now, two extreme cases with $4\omega/K_1v^2$ being either large or small will be considered in investigating the effects due to the term as shown above.

(α) $\frac{4\omega}{K_1v^2} << 1$:

From (3.30):

$$\alpha_1 \cong \frac{\omega}{v}\left(1 + i\,\frac{\omega}{K_1v^2}\right) \tag{3.32a}$$

$$\alpha_2 \cong -\frac{\omega}{v}\left(1 - i\,\frac{K_1v^2}{\omega}\right) \tag{3.32b}$$

It is noticed that $|\alpha_2 - k_{yo}|$ is much larger than $|\alpha_1 - k_{yo}|$; thus, the term $\frac{1}{|\alpha_2 - k_{yo}|^2}$ can be neglected in (3.31). By looking into (3.31), we see that the properties of the expressions (3.31) can be observed by considering:

$$(\alpha_1-\alpha_2)(\alpha_1-k_{yo})^2 \cong \frac{\omega^2 K_1}{v}\left\{-\frac{2}{K_1v^2}\left[a_o(1-a_o)+\frac{\omega^2}{K_1^2v^4}\right]\right.$$
$$\left. + i\left[(1-a_o)^2 + \frac{\omega^2}{K_1^2v^4}(3-4a_o)\right]\right\} \tag{3.33a}$$

$$\alpha_1^{-1}(\alpha_1-\alpha_2)(\alpha_1-ky_o)^2 \cong \omega K_1\left\{\frac{\omega}{K_1v^2}\left[(1-a_o)(1-3a_o)+\frac{\omega^2}{K_1^2v^4}(1-4a_o)\right]\right.$$
$$\left. + i\left[(1-a_o)^2+\frac{\omega^2}{K_1^2v^4}\left(3-2a_o-2a_o^2+\frac{2\omega^2}{K_1^2v^4}\right)\right]\right\} \tag{3.33b}$$

$$\alpha_1^{-2}(\alpha_1-\alpha_2)(\alpha_1-k_{yo})^2 \cong K_1 v \left\{\frac{\omega}{K_1 v^2}\left[(1-a_o)(2-4a_o)+\frac{2\omega^2}{K_1^2 v^4}(2-3a_o-a_o^2+\frac{\omega^2}{K_1^2 v^4}\right]\right.$$

$$\left. + i\left[(1-a_o)^2+\frac{\omega^2}{K_1^2 v^4}(2+2a_o-5a_o^2)+\frac{\omega^4}{K_1^4 v^8}(1+4a_o)\right]\right\} \quad (3.33c)$$

It should first be noted that these terms are small when $a_o \tilde{=} 1$.

Also, for the ideal source case we know that $\mathrm{Re}\,\overline{P} \geq 0$, $\overline{F}_y \geq 0$, and $\mathrm{Im}\,\overline{P} \leq 0$ within the operating range of $0 \leq a_o \leq 1$. Now, from (3.31) and (3.33), we realize that $\mathrm{Re}\,\overline{P}_1$ is generally negative; $-\mathrm{Im}\,\overline{P}_1$ and $\overline{F}_{z1}$ vary in a similar way and are negative only when $1-a_o < \frac{\omega}{K_1 v^2}$; $\overline{F}_{y1}$ is negative for $a_o > \frac{1}{3}$. And, roughly, it can be shown that the efficiency decreases for $1 > a_o > \frac{1}{2}$. The degrading of the machine performance is thus observed in the high a_o region.

(β) $\frac{\omega}{K_1 v^2} >> 1$:

We then have:

$$\alpha_1 \cong \frac{\sqrt{\omega K_1}}{2}(1+i) \cong -\alpha_2$$

Now, we need only consider the following terms:

$$\frac{1}{\alpha_1-\alpha_2}\left[\frac{1}{(\alpha_1-k_{yo})^2}+\frac{1}{(\alpha_2-k_{yo})^2}\right] \cong \frac{e^{-i45^o}}{\sqrt{\omega K_1}} \frac{a_o^2 + i\frac{K_1 v^2}{\omega}(1+a_o)}{\frac{\omega^2}{v^2}\left[a_o^2 - i\frac{K_1 v^2}{\omega}(1-a_o)\right]^2} \quad (3.34a)$$

$$\frac{1}{\alpha_1-\alpha_2}\left[\frac{1}{(\alpha_1-k_{yo})^2}+\frac{2}{(\alpha_2-k_{yo})^2}\right] \cong \frac{e^{-i45^o}}{2\sqrt{\omega K_1}} \frac{K_1 v\left[-\frac{K_1 v^2}{\omega} + i a_o(4-a_o)\right]}{\frac{\omega^2}{v^2}\left[a_o^2 - i\frac{K_1 v^2}{\omega}(1-a_o)\right]^2} \quad (3.34b)$$

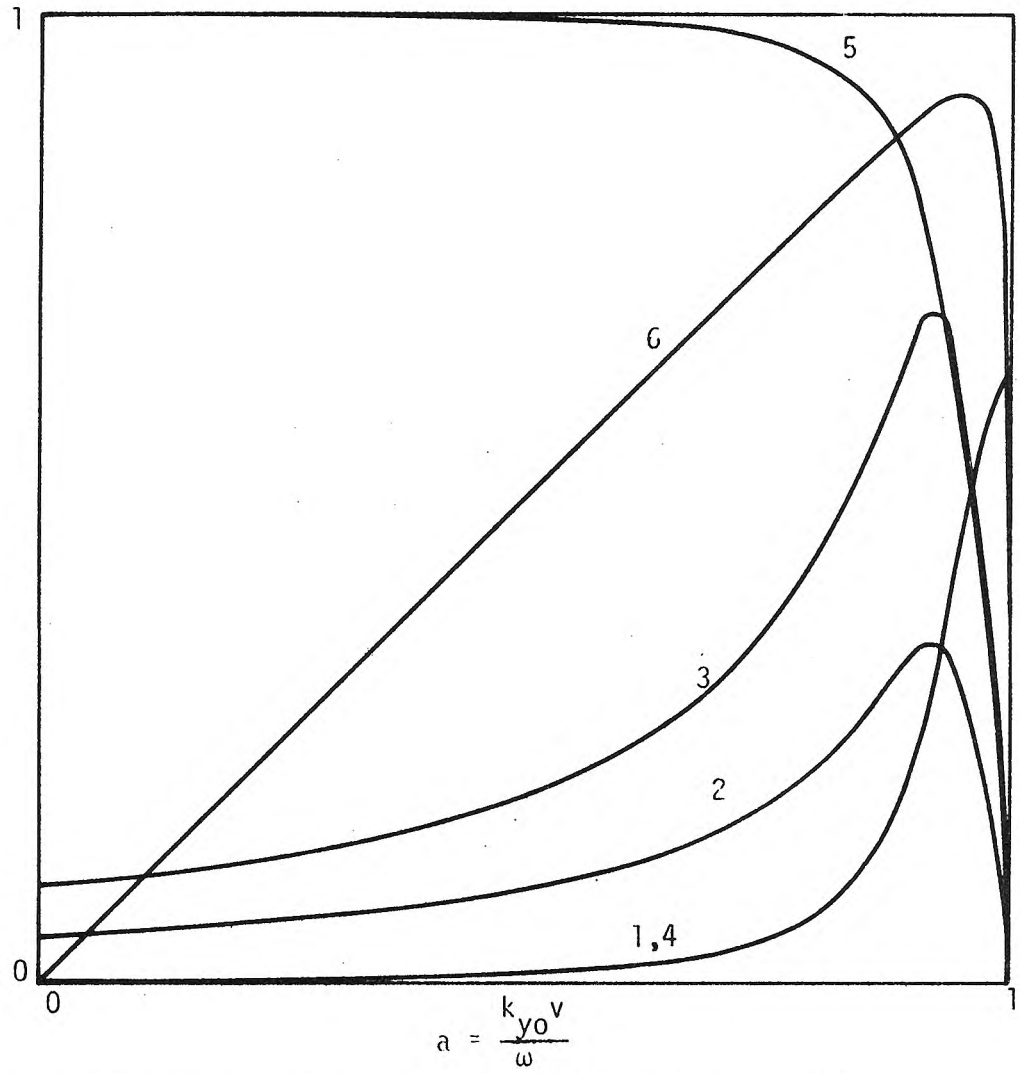

Fig. 3.13a Machine performance for geometry (A-i-1) with

$$|\tilde{K}_x|^2 = \frac{2K_o^2}{\pi} \frac{\sin^2(k_y - k_{yo})L}{(k_y - k_{yo})^2}$$

All parameters are the same as in Fig. 3.2. L = 2.512m. Curves (1), (2), (3) and (4) represent the same quantities as in Fig. 3.2. Curve (6) is the efficiency and Curve (5) is the power factor.

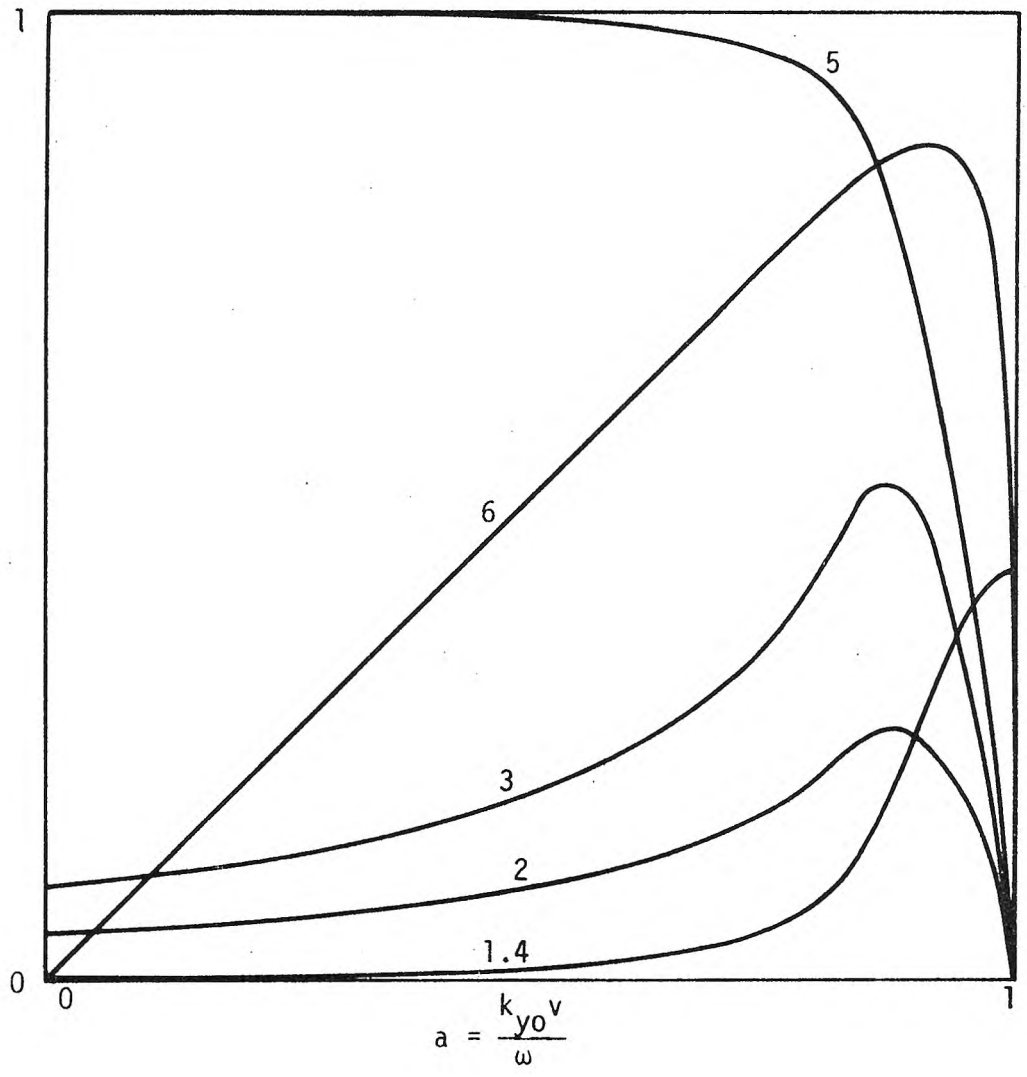

Fig. 3.13b All quantities are the same as in Fig. 3.13a, except L = 1.256m.

It can be shown that the phase angles of (3.34a) and (3.34b) are all monotonically decreasing functions of a_o for $0 \leq a_o \leq 1$. Actually, for (3.34a) (or, $\bar{P}_1$), the phase angle increases from $-\pi/4$ at $a_o = 1$ to $\pi/2$ at $a_o \cong \sqrt{(K_1 v^2)/\omega}$ to $5/4\pi$ at $a_o = 0$. And, for (3.34b), it will vary from $\pi/4$ at $a_o \cong 1$ to π at $a_o = \sqrt{(K_1 v^2)/\omega}$ and finally to $7/4\pi$ at $a_o = 0$. Thus, except in a very small region $a_o < \sqrt{(K_1 v^2)/\omega}$, increases in Re $\bar{P}$ and possible increases in PF are expected. For $a_o^2 \cong (K_1 v^2)/\omega$, both $\bar{F}_y$ and machine efficiency are observed to decrease. If $(K_1 v^2)/\omega >> \gamma^2$, $\bar{F}_{z1}$ behaves in the same way as -Im $\bar{P}_1$. On the contrary, if $(K_1 v^2)/\omega << \gamma^2$, $\bar{F}_{z1}$ behaves in a way similar to -Re $\bar{P}_1$.

From the above analysis, it is not surprising that most conclusions are basically similar to those obtained from the integrand analysis. Typical plots of machine performance for this realistic source are given in Fig. 3.13. The degrading in the machine performance can then be observed by comparing with the results shown in Fig. 3.2 for the ideal source.

(b) Geometry (A-ii-1):

Similar to (a), $\bar{F}_y$ and $\bar{P}$ can be evaluated by using suitable factorization in (3.14a) and (3.15a) to get:

$$\bar{P} \cong -\frac{i\omega\mu_o K_o^2}{\pi} \frac{\mu_{2y}\mu_{2z}}{\mu_{2z}\mu_{2y} - \mu_o^2} \sum_{\substack{m,k=3.4 \\ k\neq m}} \frac{1}{\alpha_m - \alpha_k} \left[S_2(\alpha_m, k_{yo}, L) - \frac{\mu_o}{\sqrt{\mu_{2y}\mu_{2z}}} S_3(\alpha_m, k_{yo}, L) \right] \qquad (3.35a)$$

$$\bar{F}_y \tilde{=} \mathrm{Re}\ \frac{-i\mu_o K_o^2}{\pi}\ \frac{\mu_{2y}\mu_{2z}}{\mu_{2y}\mu_{2z}-\mu_o^2}\ \sum_{\substack{m,k=3,4\\ k\neq m}}\ \frac{\alpha_m}{\alpha_m-\alpha_k}\ [S_2(\alpha_m,k_{yo},L) -$$

$$- \frac{\mu_o}{\sqrt{\mu_{2y}\mu_{2z}}}\ S_3(\alpha_m,k_{yo},L)] \qquad (3.35b)$$

where α_3 and α_4 are roots of $k_y^2 + i(\omega-k_y v)K_6 = 0$ with

$$K_6 = \frac{\mu_o^2\,\sigma_x}{\mu_{2y}}\ \frac{\mu_{2y}\mu_{2z}}{\mu_{2z}\mu_{2y}-\mu^2}\ \text{ or:}$$

$$\alpha_3 = \frac{K_6 v}{2}\left[-\sqrt{\frac{b_1-1}{2}} + i\left(\sqrt{\frac{b_1+1}{2}} + 1\right)\right] \qquad (3.36a)$$

$$\alpha_4 = \frac{K_6 v}{2}\left[\sqrt{\frac{b_1-1}{2}} - i\left(\sqrt{\frac{b_1+1}{2}} - 1\right)\right] \qquad (3.36b)$$

with $b_1 = \sqrt{1 + \left(\frac{4\omega}{K_6 v^2}\right)^2}$.

Definitions for $S_2(\alpha_m,k_{yo},L)$ and $S_3(\alpha_m,k_{yo},L)$ are given in Appendices D and E. However, it should be noted that the exact expression for $S_3(\alpha_m,k_{yo},L)$ is difficult to get. Thus, only an asymptotic formula is derived.

As for $\bar{F}_z$, the integral is much more complicated. However, as we mentioned, the end effect is generally small provided that $k_{yo}L$ is large. Thus, we can always use the formula for the ideal source as an approximation for the more realistic source we are now considering.

It is obvious that ideal results can be obtained by just considering the terms proportional to L in $S_2\ (\alpha_m,k_{yo},L)$ and $S_3\ (\alpha_m,k_{yo},L)$.

Here we will begin to consider effects due to the remaining terms. However, as we just mentioned, the end effects on the supporting force are relatively small, so we are not going to include any further analyses for the $\overline{F}_z$. Now, under the assumption of $k_{yo}L \gg 1$ and $|\mathrm{Im}(\alpha_m L)| \gg 1$, we can write:

$$\overline{P}_1 \cong \frac{-i\omega\mu_o K_o^2}{\pi} \cdot \frac{\mu_{2y}\mu_{2z}}{\mu_{2y}\mu_{2z} - \mu_o^2} \frac{1}{\alpha_3-\alpha_4} \left\{ \frac{\alpha_3}{(\alpha_3-k_{yo})^2} \left(i\frac{\pi}{2} - \ell n \frac{\alpha_3}{k_{yo}}\right) + \frac{\alpha_4}{(\alpha_4-k_{yo})^2} \left(i\frac{\pi}{2} + \ell n \frac{\alpha_4}{k_{yo}}\right) - \frac{\alpha_3-\alpha_4}{(\alpha_3-k_{yo})(\alpha_4-k_{yo})} \right\} \tag{3.37a}$$

$$\overline{F}_{y1} \cong \mathrm{Re}\, \frac{-i\mu_o K_o^2}{\pi} \frac{\mu_{2y}\mu_{2z}}{\mu_{2y}\mu_{2z} - \mu_o^2} \frac{1}{\alpha_3-\alpha_4} \left\{ \frac{\alpha_3^2}{(\alpha_3-k_{yo})^2} \left(i\frac{\pi}{2} - \ell n \frac{\alpha_3}{k_{yo}}\right) + \frac{\alpha_4^2}{(\alpha_4-k_{yo})^2} \left(i\frac{\pi}{2} + \ell n \frac{\alpha_4}{k_{yo}}\right) - \frac{(\alpha_3-\alpha_4)k_{yo}}{(\alpha_3-k_{yo})(\alpha_4-k_{yo})} \right\} \tag{3.37b}$$

Subscript "1" is introduced to point out that (3.37a) and (3.37b) correspond to the term $\frac{k_3}{(k_y-\alpha_3)(k_y-\alpha_4)}$ in (3.14) and (3.16). Now let us consider two extreme cases:

(α) $\frac{4\omega}{K_6 v^2} \ll 1$

From (3.36), we have

$$\alpha_3 \cong \frac{\omega}{v}\left(-1 + i\frac{K_6 v^2}{\omega}\right) \tag{3.38a}$$

$$\alpha_4 \cong \frac{\omega}{v}\left(1 - i\frac{\omega}{K_6 v^2}\right) \tag{3.38b}$$

$$\ell n \frac{\alpha_3}{k_{yo}} \cong \ell n\left(\frac{K_6 v}{k_{yo}}\right) + i\left(\frac{\pi}{2} + \frac{\omega}{K_6 v^2}\right) \tag{3.39a}$$

$$\ell n \frac{\alpha_4}{k_{yo}} \tilde{\cong} \ell n\left(\frac{\omega}{k_{yo} v}\right) - i \frac{\omega}{K_o v^2} \tag{3.39b}$$

When a_o is not close to "1", values for $\bar{P}_1$ and $\bar{F}_{y1}$ are generally small. However, when $1-a_o$ is small, (e.g., $1-a_o \cong \frac{\omega}{K_6 v^2}$) a very large influence is observed. The underlined terms in (3.37a) and (3.37b) dominate and produce a phase angle of about 0^o in $\bar{P}_1$. There is also an increase in the propulsion force. Roughly speaking, expressions (3.37) will help to ease the degrading of the machine performance.

(β) $\frac{\omega}{K_6 v^2} >> 1$:

From (3.36), we have:

$$\alpha_3 \cong \sqrt{\frac{\omega K_6}{2}}\,(-1+i) \tilde{=} -\alpha_4 \tag{3.40a}$$

$$\ell n \frac{\alpha_3}{k_{yo}} \cong \ell n \sqrt{\frac{K_6 v^2}{\omega a_o^2}} + i \frac{3\pi}{4} \tag{3.40b}$$

$$\ell n \frac{\alpha_2}{k_{yo}} = \ell n \sqrt{\frac{K_6 v^2}{\omega a_o^2}} - i \frac{\pi}{4} \tag{3.40c}$$

(3.37a) and (3.37b) can then be rewritten as:

$$\bar{P}_1 \cong -\frac{i\omega\mu_o K_o^2}{\pi}\frac{\mu_{2y}\mu_{2z}}{\mu_{2y}\mu_{2z}-\mu_o^2}\left\{-\left(\frac{i\pi}{4}+\ell n\ \frac{K v^2}{\omega a_o^2}\right)\frac{(\alpha_4^2+k_{yo}^2)}{[k_{yo}^2+i(\omega-k_{yo}v)K_6]^2}\right.$$

$$\left.-\frac{1}{k_{yo}^2+i(\omega-k_{yo}v)K_6}\right\} \qquad (3.41a)$$

$$\bar{F}_{y1} \cong \mathrm{Re}\ \frac{-i\mu_o K_o^2}{\pi}\frac{\mu_{2y}\mu_{2z}}{\mu_{2y}\mu_{2z}-\mu_o^2}\left\{\left(\frac{i\pi}{4}+\ell n\ \frac{K_6 v^3}{\omega a_o^2}\right)\frac{2ia_o\frac{K_6 v^2}{\omega^2}}{[a_o^2+i(1-a_o)\frac{K_6 v^2}{\omega}]^2}\right.$$

$$\left.-\frac{a_o\frac{v}{\omega}}{[a_o^2+i(1-a_o)\frac{K_o v^2}{\omega}]}\right\} \qquad (3.41b)$$

When a_o is close to 1, (3.41a) and (3.41b) are relatively small. However, when a_o is small (e.g., $a_o^2 \sim (K_6 v^2)/\omega$) the situation is different. Re $\bar{P}_1$, Im $\bar{P}_1$ and $\bar{F}_{y1}$ are all positive and somewhat larger.

As for the contribution due to the term $\frac{\mu_o}{\mu_{2y}}\frac{\gamma_2}{(k_y-\alpha_3)(k_y-\alpha_4)}$, the results in Appendix E are used. As we can see, $S_3(\alpha_m, k_{yo}, L)$ is decomposed into two parts. One is due to the residues of all the poles, while the other is due to the integrations along the branch cuts. However, if $\frac{4\omega}{K_5 v^2} \ll 1$ is true (Note that $K_5 = \sigma_x \mu_{2z} \gg K_6$ is large, thus $4\omega/(K_5 v^2) \ll 1$ covers most operating regions. The only exception occurs in the very low speed region.) $|\beta_2|$ is much larger than $|\beta_1|$. Most terms in the branch cut parts are then shown to be much smaller than the corresponding terms in the residue parts. Further conditions of $|\mathrm{Im}(\alpha_m L)| > \pi$ will make it possible for us to write down the final approximate results as:

$$\overline{P}_2 \cong \frac{-i\omega\mu_o K_o^2}{\pi} \frac{\mu_o}{\sqrt{\mu_{2y}\mu_{2z}}} \frac{-\mu_{2y}\mu_{2z}}{\mu_{2y}\mu_{2z} - \mu_o^2} \frac{1}{\alpha_3 - \alpha_4} \left\{ \left[\frac{i\pi}{(\alpha_3 - k_{yo})^2} - \frac{i\pi}{(\alpha_4 - k_{yo})^2} \right] \right.$$

$$\times \frac{\sqrt{k_{yo}^2 - i(\omega - k_{yo}v)K_5}}{2} - \left(\frac{i\pi}{\alpha_3 - k_{yo}} - \frac{i\pi}{\alpha_4 - k_{yo}} \right) \frac{\beta_1 + \beta_2 - 2k_{yo}}{4\sqrt{k_{yo}^2 - i(\omega - k_{yo}v)K_5}}$$

$$\left. + \frac{i\pi}{(\alpha_4 - k_{yo})^2} \sqrt{\alpha_4^2 - i(\omega - \alpha_4 v)K_5} \right\} \qquad (3.42a)$$

$$\overline{F}_{y2} \cong \mathrm{Re} \frac{-i\mu_o K_o^2}{\pi} \frac{\mu_o}{\sqrt{\mu_{2y}\mu_{2z}}} \frac{-\mu_{2y}\mu_{2z}}{\mu_{2y}\mu_{2z} - \mu_o^2} \frac{1}{\alpha_3 - \alpha_4} \left\{ \left[\frac{i\pi\alpha_3}{(\alpha_3 - k_{yo})^2} - \frac{i\pi\alpha_4}{(\alpha_4 - k_{yo})^2} \right] \right.$$

$$\times \frac{\sqrt{k_{yo}^2 - i(\omega - k_{yo}v)K_5}}{2} - \left(\frac{i\pi\alpha_3}{\alpha_3 - k_{yo}} - \frac{i\pi\alpha_4}{\alpha_4 - k_{yo}} \right) \frac{\beta_1 + \beta_2 - 2k_{yo}}{4\sqrt{k_{yo}^2 - i(\omega - k_{yo}v)K_5}}$$

$$\left. + \frac{i\pi\alpha_4}{(\alpha_4 - k_{yo})^2} \sqrt{\alpha_4^2 - i(\omega - \alpha_4 v)K_5} \right\} \qquad (3.42b)$$

Here α_3 and α_4 are defined in (3.36) while β_1 and β_2 are roots of $\gamma_2^2 = 0$, i.e.,

$$\beta_1 = \frac{K_5 v}{2} \left[\sqrt{\frac{b_2 - 1}{2}} + i\left(\sqrt{\frac{b_2 + 1}{2}} - 1 \right) \right] \qquad (3.43a)$$

$$\beta_2 = -\frac{K_5 v}{2} \left[\sqrt{\frac{b_2 - 1}{2}} + i\left(\sqrt{\frac{b_2 + 1}{2}} + 1 \right) \right] \qquad (3.43b)$$

with $K_5 = \sigma_x \mu_{2z}$ and $b_2 = \sqrt{1 + \left(\frac{4\omega}{K_5 v^2} \right)^2}$

Now, under the condition $\frac{4\omega}{K_5 v^2} << 1$, we have:

$$\beta_1 \cong \frac{\omega}{v}\left(1 + i\,\frac{\omega}{K_5 v^2}\right) \tag{3.43c}$$

$$\beta_2 \cong -\frac{\omega}{v}\left(1 + i\,\frac{K_5 v^2}{\omega}\right) \tag{3.43d}$$

We will begin to consider two extreme cases:

(α) $\frac{4\omega}{K_6 v^2} << 1$

It is obvious that the values for $\overline{P}_2$ and $\overline{F}_{y2}$ are small when a_o is not close to 1. We are most concerned with the case when $a_o \sim 1$ where the values are large. Now, under the assumption $\frac{4\omega}{K_6 v^2} << 1$, those terms with α_3 involved can be neglected. For $1 - a_o \cong \omega/(K_6 v^2)$, the contributions due to the underlined terms approximately give us $\text{Re}\,\overline{P}_2 \cong 0$, $F_{y2} \cong 0$ and a positive $\text{Im}\,\overline{P}_2$. For the remaining terms, it can be shown that $\text{Re}\,\overline{P}_2$, $\text{Im}\,\overline{P}_2$ and $\overline{F}_{y2}$ are all negative. And the magnitudes are so large that they will not only cancel the positive values in $\overline{P}_1$ and $\overline{F}_{y1}$, but will also eventually give us large negative values of $\text{Re}\,\overline{P}$, $\text{Im}\,\overline{P}$ and $\overline{F}_y$. Thus, we can conclude that large decreases in the propulsion force, the power factor and the efficiency will be observed for $1 - a_o \cong \frac{\omega}{K_6 v^2}$. This conclusion is basically similar to that described in the earlier integrand analyses.

(β) $\frac{\omega}{K_6 v^2} >> 1$ and $\frac{4\omega}{K_5 v^2} << 1$:

In this case, the values are relatively small for an "a_o" which

is not too small. Thus, we are most concerned with the region where $a_o^2 \sim (K_6 v^2)/\omega$. Of course, the terms corresponding to α_3 cannot be neglected any longer. After some rough algebraic manipulations, it can be shown that the underlined terms will give us a positive value for $\text{Im}\,\overline{P}_2$ and nearly zero values for $\text{Re}\,\overline{P}_2$ and $\overline{F}_{y2}$. However, the most important contribution comes from the remaining terms. Generally, $\overline{F}_{y2} < 0$, $\text{Re}\,\overline{P}_2 < 0$ and $\text{Im}\,\overline{P}_2 < 0$ are obtained. And the values are so large that overall decreases in the propulsion force, efficiency and power factor will be observed. Thus, the most serious degrading in machine performance is seen around $a_o^2 \sim (K_y v^2)/\omega$. This is also the same conclusion as that obtained from the integrand analysis. A typical plot of the machine performances for this more realistic source is then given in Fig. 3.14. And, by comparing with Fig. 3.6, the degrading of the machine performances is observed.

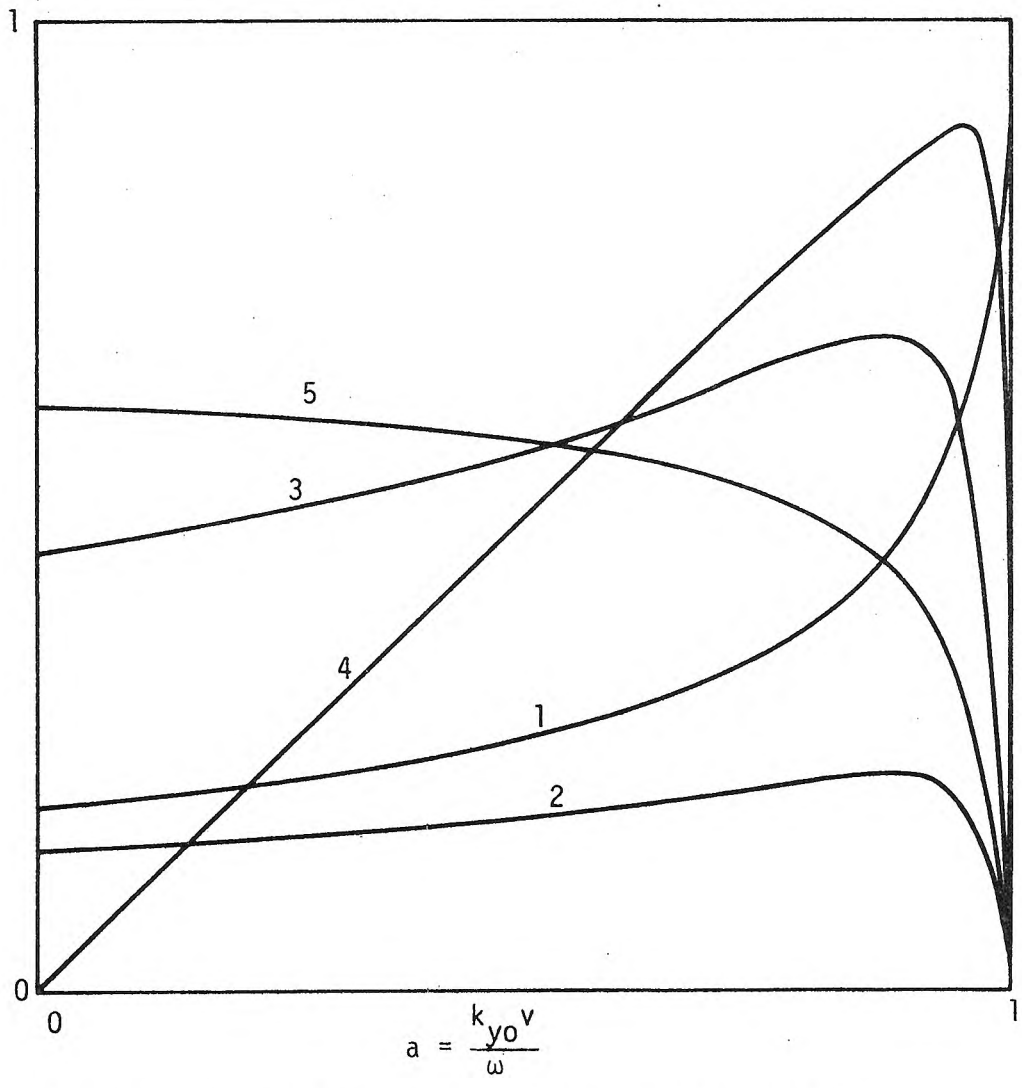

Fig. 3.14a Machine performance for geometry (A-ii-1) with

$$|\tilde{K}_x|^2 = \frac{2K_o^2}{\pi} \frac{\sin^2(k_y-k_{yo})L}{(k_y-k_{yo})^2}$$

All parameters are the same as in Fig. 3.6. L = 2.512m. Curves (1), (2), (3) and (5) represent the same quantities as in Fig. 3.6. Curve (4) is the machine efficiency.

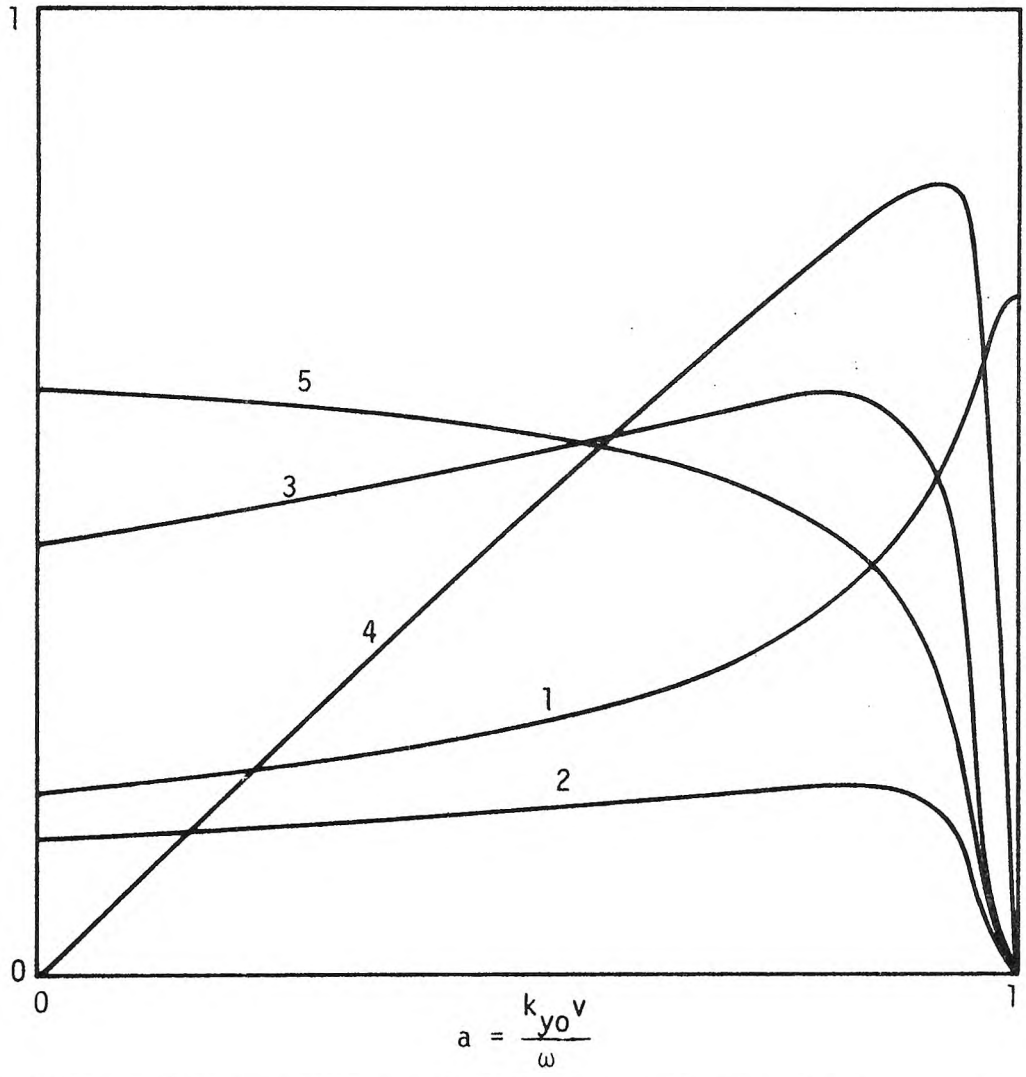

Fig. 3.14b All quantities are the same as in Fig. 3.14a except L = 1.256m.

(c) Geometry (B-i-1):

We can now apply Appendices C and D to (3.24a) and (3.25a) to get:

$$\bar{p} \cong \frac{-i\omega\mu_o K_o^2}{\pi} \frac{\mu_{2z}}{\mu_{2z}h_3 + \mu_o h_2} \sum_{m=1,2,3,4} [\psi_m s_1(\delta_m, k_{yo}, L) + \eta_m s_2(\delta_m, k_{yo}, L)] \tag{3.44a}$$

$$\bar{F}_y \cong \text{Re} \frac{-i\mu_o K_o^2}{\pi} \frac{\mu_{2z}}{\mu_{2z}h_3 + \mu_o h_2} \sum_{m=1,2,3,4} [\psi_m \delta_m s_1(\delta_m, k_{yo}, L) + \eta_m \delta_m s_2(\delta_m k_{yo}, L)] \tag{3.44b}$$

$$\bar{F}_z \cong \frac{\mu_o K_o^2}{2\pi} \frac{\mu_{2z}^2}{(\mu_{2z}h_3 + \mu_o h_2)^2} \sum_{m=1,\ldots,8} [\xi_m s_1(\delta_m, k_{yo}, L) + \zeta_m s_2(\delta_m, k_{yo}, L)] \tag{3.44c}$$

Here δ_m are roots of $k_y^2 - i(\omega - k_y v)K_1 \pm \frac{\mu_{2z} k_y}{\mu_{2z}h_3 + \mu_o h_2} = 0$ for $m = 1,2,3,4$. Also, $\delta_{m+4} = \delta_m^*$. And

$$\psi_m = \frac{g_1(\delta_m)}{\prod_{\substack{k=1,2,3,4 \\ k\neq m}} (\delta_m - \delta_k)}$$

$$\eta_m = \frac{g_2(\delta_m)}{\prod_{\substack{k=1,2,3,4 \\ k\neq m}} (\delta_m - \delta_k)}$$

$$\xi_m = \frac{\delta_m^2[g_1(\delta_m)g_1^*(\delta_m) + \delta_m^2 g_2(\delta_m)\, g_2^*(\delta_m)]}{\prod_{\substack{k=1,\ldots,8 \\ k\neq m}} (\delta_m - \delta_k)}$$

$$\zeta_m = \frac{\delta_m^2[g_1(\delta_m)g_2^*(\delta_m) + g_1^*(\delta_m)g_2(\delta_m)]}{\prod_{\substack{k=1,\cdots,8 \\ m\neq k}} (\delta_m-\delta_k)}$$

with $$g_1(\delta_m) = \delta_m^2 \frac{(\mu_o^2 - \mu_{2y}\mu_{2z})h_2}{\mu_o(\mu_{2z}h_3 + \mu_o h_2)} - i(\omega-\delta_m v)K_1$$

$$g_2(\delta_m) = \frac{\mu_{2y}h_2 + \mu_o h_3}{\mu_o}[\delta_m^2 - i(\omega-\delta_m v)K_1 - \frac{\mu_o\mu_{2z}}{(\mu_{2y}h_2 + \mu_o h_3)(\mu_{2z}h_3+\mu_o h_2)}]$$

$\overline{F}_z$ is very complicated and we will not analyze it any further. But, similar to the previous case (b), the result for the ideal source can be used as a good approximation provided that $k_{yo}L \gg 1$.

The formulas given in (3.44) are complicated. By looking into Appendix D we know that integral $S_2(\delta_i,k_{yo},L)$ can be decomposed into two parts, namely, I_1 and $2I_2$. Now we will consider the contribution from I_1. It is obvious that the ideal source result can be obtained by just considering the terms proportional to L in S_1 and S_2, and, similar to geometry (A-i-1), $|\text{Im } 2\delta_i L|$ can be considered as large (e.g., $\gtrsim \pi$) for most practical cases. Thus, in S_1 and S_2 the terms involving $e^{\pm 2(\delta_i - k_{yo})L}$ can be neglected. Under the above assumption, we can then write down the following expressions:

$$\overline{p}_1 \cong \frac{-i\omega\mu_o K_o^2}{\pi} \frac{\mu_{2z}}{\mu_{2z}h_3 + \mu_o h_2} \frac{i\pi}{2(\delta_1-\delta_2)} \{\frac{1}{(\delta_1-k_{yo})^2} + \frac{1}{(\delta_2-k_{yo})^2}$$

$$+ \frac{\mu_{2y}h_2 + \mu_o h_3}{\mu_o}[\frac{\delta_1}{(\delta_1-k_{yo})^2} + \frac{\delta_2}{(\delta_2-k_{yo})^2}]\} \qquad (3.45a)$$

$$\bar{F}_{y_1} \cong \mathrm{Re}\ \frac{-i\mu_o K_o^2}{\pi}\ \frac{\mu_{2z}}{\mu_{2z}h_3^+ + \mu_o h_2}\ \frac{i\pi}{2(\delta_1-\delta_2)}\Big\{\frac{\delta_1}{(\delta_1-k_{yo})^2} + \frac{\delta_2}{(\delta_2-k_{yo})^2}$$

$$+ \frac{\mu_{2y}h_2^+ + \mu_o h_3}{\mu_o}\Big[\frac{\delta_1^2}{(\delta_1-k_{yo})^2} + \frac{\delta_2^2}{(\delta_2-k_{yo})^2}\Big]\Big\} \qquad (3.45b)$$

here δ_1 and δ_2 are roots of $k_y^2 - i(\omega-k_y v)K_1 + \frac{\mu_{2z}}{\mu_{2z}h_3^+ + \mu_o h_2}k_y = 0$. And the subscripts "1" are introduced to distinguish (3.45) from the other terms where the contributions are due to integrals similar to I_2.

Now, we will begin to consider two extreme cases:

(α) $\gamma = \mu_o h_2 \sigma_x v >> 1$:

In this case, the equation for δ_i is approximated as $k_y^2 - i(\omega-k_y v)K_1 = 0$. Also, $\gamma >> 1$ ensures that $K_1 v >> 1$, $\omega/Kv^2 << 1$. Thus, similar to (A-i-1), most terms involving $i/[(\delta_2-k_{yo})^2]$ (Note: $\delta_1 \cong \alpha_1$, $\delta_2 \cong \alpha_2$) can be neglected. (Perhaps the only exception is the last term in $\bar{F}_{y_1}$; it can be rewritten as $1 + \frac{2\delta_2 k_{yo} - k_{yo}^2}{(\alpha_2-k_{yo})^2}$. For the "1" part, a very small additional propulsion force is added. For the remaining part, the neglect is reasonable. Actually, the whole thing can be shown to be cancelled by another term due to an integral similar to I_2).

By applying (3.33), roughly speaking, the power factor, efficiency and the propulsion force decrease for a larger a_o (e.g., $a_o > 2/3$), i.e., a degrading of the machine performance will be observed. And the maximum decreases generally occur at a value of a_o where $1 - a_o \gtrsim \frac{\omega}{K_1 v^2}$ is true.

(β) $\gamma << 1$:

In this case, the equation for δ_i can be approximated as $k_y^2 + \frac{\mu_{2z}}{\mu_{2z}h_3 + \mu_o h_2} k_y - i\omega K_1 = 0$, and the roots are found to be:

$$\delta_1 \cong \frac{K_1 v}{2\gamma} \{[\sqrt{\frac{1+b_3}{2}} - 1] + i\sqrt{\frac{b_3-1}{2}}\}$$

$$\delta_2 \cong \frac{K_1 v}{2\gamma} -[\sqrt{\frac{1+b_3}{2}} + 1] - i\sqrt{\frac{b_3-1}{2}}$$

with $b_3 = \sqrt{1 + (\frac{4\omega\gamma^2}{K_1 v^2})^2}$

When γ is small, $\frac{4\omega\gamma^2}{K_1 v^2}$ is small too. However, $K_1 v/\gamma$ is large. Thus δ_1 and δ_2 can be further simplified as:

$$\delta_1 \cong \frac{\omega\gamma}{v} (\frac{\omega\gamma^2}{K_1 v^2} + i) = \frac{K_1 v}{\gamma} (\frac{\omega^2\gamma^4}{K_1^2 v^4} + i \frac{\omega\gamma^2}{K_1 v^2})$$

$$\delta_2 \cong - \frac{K_1 v}{\gamma} (1 + i \frac{\omega\gamma^2}{K_1 v^2})$$

Since $|\delta_2 - k_{yo}| >> |\delta_1 - k_{yo}|$, so, similar to the previous $\gamma >> 1$ case in (3.45), most terms involving $1/[(\delta_2 - k_{yo})^2]$ can be neglected. (The same argument as the previous $\gamma >> 1$ case can also be applied to the last term in $\bar{F}_{y_1}$. From a later consideration, it can be shown that this term will be cancelled by another term due to I_2.) Also, we have:

$$\frac{1}{(\delta_1 - \delta_2)} \frac{1}{(\delta_1 - k_{yo})^2} \cong \frac{\gamma v}{\omega^2 K_1} \frac{1}{(a_o^2 - \gamma^2) - 2ia_o\gamma} \qquad (3.46a)$$

$$\frac{1}{(\delta_1 - \delta_2)} \frac{\delta_1}{(\delta_1 - k_{yo})^2} \cong \frac{\gamma^2}{\omega K_1} \frac{1}{-2a_o\gamma - i(a_o^2 - \gamma^2)} \qquad (3.46b)$$

$$\frac{1}{(\delta_1-\delta_2)}\,\frac{\delta_1^2}{(\delta_1-k_{yo})^2} \cong \frac{\gamma^3}{K_1 v}\,\frac{1}{-(a_o^2-\gamma^2)+2ia_o\gamma} \tag{3.46c}$$

From (3.45) and (3.46) we know that $\mathrm{Re}\ \bar{P}_1$ is positive when $A_2 = (a_o^2 - \gamma^2) - \frac{\omega}{v}\gamma\,\frac{\mu_{2y}h_2+\mu_o h_3}{\mu_o}(2a_o)$ is positive and $\mathrm{Re}\ \bar{P}_1$ is negative when A_2 is negative. A similar argument can be applied to $\mathrm{Im}\ \bar{P}_1$ by changing A_2 to $A_3 = 2a_o\gamma + \frac{\omega}{v}\gamma(a_o^2-\gamma^2)\,\frac{\mu_{2y}h_2+\mu_o h_3}{\mu_o}$. Thus the influence of (3.45a) on the overall power factor largely depends on a_o. However, an increase in the power factor is expected when $a_o >> \gamma$ and $\frac{\omega}{v}\,\frac{\mu_{2y}h_2+\mu_o h_3}{\mu_o} \simeq 1$. Unfortunately, a decrease in the propulsion force is always observed when $a_o \gtrsim \gamma$. And, the most serious decrease will occur for a value of $a_o \sim \gamma$

Now, we begin to consider the contribution due to the term I_2 in S_2. However, instead of using (3.44) directly, we go back to the original force and integrand formulas to get:

$$\bar{P}_2 \cong \frac{-i\omega\mu_o K_o^2}{\pi}\,\frac{\mu_{2z}}{\mu_{2z}h_3+\mu_o h_2}\Big\{\sum_{\substack{m=3,4\\ k\neq m}}\frac{1-\frac{\mu_{2y}h_2+\mu_o h_3}{\mu_o}\delta_m}{\delta_m-\delta_k}\,I_4(\delta_m,k_{yo},L)$$

$$-\sum_{\substack{m=1,2\\ k\neq m}}\frac{1+\frac{\mu_{2z}h_2+\mu_o h_3}{\mu_o}\delta_m}{\delta_m-\delta_k}\,I_4(\delta_m,k_{yo},L)\Big\} \tag{3.47a}$$

$$\bar{F}_{y_2} \cong \mathrm{Re}\,\frac{-i\mu_o K_o^2}{\pi}\,\frac{\mu_{2z}}{\mu_{2z}h_3+\mu_o h_2}\sum_{\substack{m=3,4\\ k\neq m}}\frac{1-\dfrac{\mu_{2z}h_2+\mu_o h_3}{\mu_o}\delta_m}{\delta_m-\delta_k}\,I_5(\delta_5,k_{yo},L)$$

$$-\sum_{\substack{m=1,2\\ k\neq m}}\frac{1+\dfrac{\mu_{2y}h_2+\mu_o h_3}{\mu_o}\delta_m}{\delta_m-\delta_k}\,I_5(\delta_m,k_{yo},L)\Big\} \qquad (3.47b)$$

Here:

$$I_4(\delta_m,k_{yo},L) = \int_{-\infty}^{0}\frac{1}{k_y-\delta_m}\,\frac{\sin^2(k_y-k_{yo})L}{(k_y-k_{yo})^2}\,dk_y \qquad (3.48a)$$

$$I_5(\delta_m,k_{yo},L) = \delta_m I_4(\delta_m,k_{yo},L) + \int_{-\infty}^{0}\frac{\sin^2(k_y-k_{yo})L}{(k_y-k_{yo})^2}\,dk_y \qquad (3.48b)$$

I_4 can be evaluated in the same manner as $I_2(\delta_m,k_{yo},L)$ in Appendix D. Actually, for most practical cases, $k_{yo}L$ is large. $\dfrac{\sin^2(k_y-k_{yo})L}{(k_y-k_{yo})^2}$ is a fast varying function. And, thus by comparing to $|S_1(\delta_m,k_{yo},L)|$ (i.e., an integral whose limits are $-\infty$ and $+\infty$), $|I_4(\delta_m,k_{yo},L)|$ is relatively small. Also, the integral $I_4(\delta_m,k_{yo},L)$ can be approximated as:

$$I_4(\delta_m,k_{yo},L) \cong \frac{1}{2}\left[\frac{1}{(\delta_m-k_{yo})^2}\,\ell n\,\frac{\delta_m}{k_{yo}} - \frac{1}{(\delta_m-k_{yo})k_{yo}}\right] \qquad (3.49a)$$

and

$$\int_{-\infty}^{0}\frac{\sin^2(k_y-k_{yo})L}{(k_y-k_{yo})^2}\,dk_y \cong \frac{1}{2}\,\frac{1}{k_{yo}} \qquad (3.49b)$$

This approximation is basically similar to the neglect of I_3 in I_2 (see Appendix D). Now, we can begin to consider two extreme cases.

(i) $\gamma \gg 1$:

In this case, both equations $k_y^2 - i(\omega - k_y v)K_1 \pm \frac{\mu_{2z}}{\mu_{2z}h_3 + \mu_o h_2} k_y = 0$ can be approximated as $k_y^2 - i(\omega - k_y v)K_1 = 0$. That is, $\delta_1 \cong \delta_3$ and $\delta_2 \cong \delta_4$ can be considered as true. Thus,

$$\overline{P}_2 \cong \frac{-i\omega\mu_o K_o^2}{\pi} \frac{\mu_{2z}}{\mu_{2z}h_3 + \mu_o h_2} \frac{\mu_{2y}h_2 + \mu_o h_3}{\mu_o} \frac{-1}{\delta_1 - \delta_2} \left\{ \frac{\delta_1}{(\delta_1 - k_{yo})^2} \ln \frac{\delta_1}{k_{yo}} \right.$$

$$\left. - \frac{\delta_2}{(\delta_2 - k_{yo})^2} \ln \frac{\delta_2}{k_{yo}} - \frac{1}{\delta_1 - k_{yo}} + \frac{1}{\delta_2 - k_{yo}} \right\} \qquad (3.50a)$$

$$\overline{F}_{y_2} \cong \mathrm{Re} \frac{-i\mu_o K_o^2}{\pi} \frac{\mu_{2z}}{\mu_{2z}h_3 + \mu_o h_2} \frac{\mu_{2y}h_2 + \mu_o h_3}{\mu_o} \frac{-1}{\delta_1 - \delta_2} \left\{ \frac{\delta_1^2}{(\delta_1 - k_{yo})^2} \ln \frac{\delta_1}{k_{yo}} \right.$$

$$\left. - \frac{\delta_2^2}{(\delta_2 - k_{yo})^2} \ln \frac{\delta_2}{k_{yo}} - \frac{\delta_1^2}{(\delta_1 - k_{yo})k_{yo}} + \frac{\delta_2^2}{(\delta_2 - k_{yo})k_{yo}} + \frac{\delta_1 - \delta_2}{k_{yo}} \right\} \qquad (3.50b)$$

δ_1 and δ_2 are approximately given at (3.32), i.e., α_1 and α_2, respectively, so we have:

$$\ln \frac{\delta_1}{k_{yo}} \cong \ln \frac{1}{a_o} + i \frac{\omega}{K_1 v^2}$$

$$\ln \frac{\delta_2}{k_{yo}} \cong \ln \frac{1}{a_o} + \ln \frac{K_1 v^2}{\omega} - i\left(\frac{\pi}{2} + \frac{\omega}{K_1 v^2}\right)$$

The last two terms in $\bar{P}_2$ can be shown to have a small effect on the power factor (actually, $\bar{P}_2 \propto \frac{-1}{k_{yo}L}\bar{P}_o$). And the last three terms in $\bar{F}_{y_2}$ will give a drag force which is about $1/k_{yo}L$ of the ideal propulsion force. Now, we will begin to look at the effect due to the first terms in $\bar{P}_2$ and $\bar{F}_{y_2}$. The imaginary part in $\ell n \frac{\delta_1}{k_{yo}}$ can be seen to have an opposite effect compared to the corresponding terms in (3.45a), (3.45b), i.e., generally, it will ease the end effect. However, since $\frac{\pi}{2} >> \frac{\omega}{K_1 v^2}$, the influence is relatively small. The real part in $\ell n \frac{\delta_1}{k_{yo}}$ will also generally result in positive Re $\bar{P}_2$ and $\bar{F}_{y_2}$ and negative Im $\bar{P}_2$ for a_o which is not very small (e.g., $a_1 > \frac{1}{3}$ where $\ell n \frac{1}{a_o} < \frac{\pi}{2}$).

Thus, we can also say that it will make the overall end effect a little bit smaller. As for the remaining parts, the term $-i\frac{\pi}{2}$ in $\ell n \frac{\delta_2}{k_{yo}}$ will just cancel the corresponding term in $\bar{P}_1$ and $\bar{F}_{y_1}$. Due to the largeness of $|\delta_2 - k_{yo}|$ and $\frac{K_1 v^2}{\omega}$, the effect of the term $-i\frac{\omega}{K_1 v^2}$ in $\ell n \frac{\delta_2}{k_{yo}}$ is negligible. Unfortunately, for the real part of $\ell n \frac{\delta_2}{k_{yo}}$, both the power factor and the propulsion force will be decreased. However, the contribution due to this term is small too. By combining all other results we can conclude that the most serious degradation in the machine performance will occur at a_o where $1 - a_o \cong \frac{\omega}{K_1 v^2} < \gamma$.

(ii) $\gamma << 1$

Now the term $iK_1 k_{yo} v$ can be neglected in the equations

$k_y^2 - i(\omega - k_y v)K_1 \pm \frac{\mu_{2z}}{\mu_{2z}h_3 + \mu_o h_2} = 0$. And, we will have:

$$\delta_1 \cong -\delta_4 \cong \frac{K_1 v}{2\gamma}\left\{\left[\sqrt{\frac{b_3+1}{2}} - 1\right] + i\sqrt{\frac{b_3-1}{2}}\right\} = \frac{\omega}{v}\gamma\left[\frac{\omega\gamma^2}{K_1 v^2} + i\right]$$

$$\delta_2 \cong -\delta_3 \cong \frac{K_1 v}{2}\left\{-\left[\sqrt{\frac{b_3+1}{2}} + 1\right] - i\sqrt{\frac{b_3-1}{2}}\right\} \cong -\frac{K_1 v}{\gamma}\left[1 + i\frac{\omega\gamma^2}{K_1 v}\right]$$

By using the above relations $\delta_1 \cong -\delta_4$ and $\delta_2 \cong -\delta_3$, formulas (3.47a) and (3.47b) can be reduced to

$$\overline{P}_2 \cong \frac{-i\omega\mu_o K_o^2}{\pi}\frac{\mu_{2z}}{\mu_{2z}h_3 + \mu_o h_2}\frac{1}{2}\sum_{\substack{m=1,2\\ k\neq m}}\frac{-\left(1 + \frac{\mu_{2y}h_2 + \mu_o h_3}{\mu_o}\delta_m\right)}{\delta_m - \delta_k}$$

$$\times\left\{\frac{\ell n\,\frac{\delta_m}{k_{yo}}}{(\delta_m - k_{yo})^2} + \frac{\ell n\,\frac{-\delta_m}{k_{yo}}}{(\delta_m + k_{yo})^2} + \frac{1}{k_{yo}(\delta_m + k_{yo})} - \frac{1}{(\delta_m - k_{yo})k_{yo}}\right\} \qquad (3.51a)$$

$$\overline{F}_{y_2} \cong \mathrm{Re}\,\frac{-i\mu_o K_o^2}{\pi}\frac{\mu_{2z}}{\mu_{2z}h_3 + \mu_o h_2}\frac{1}{2}\sum_{\substack{m=1,2\\ k\neq m}}\frac{\ell n\,\frac{\delta_m}{k_{yo}}}{(\delta_m - k_{yo})^2} - \frac{\ell n\,\frac{-\delta_m}{k_{yo}}}{(\delta_m + k_{yo})^2}$$

$$- \frac{1}{(\delta_m + k_{yo})k_{yo}} - \frac{1}{(\delta_m - k_{yo})k_{yo}}\Bigg\} \qquad (3.51b)$$

where

$$\ell n\,\frac{\delta_1}{k_{yo}} \tilde{=} \ell n\,\frac{\gamma}{a_o} + i\left(\frac{\pi}{2} - \frac{\omega\gamma^2}{K_1 v^2}\right)$$

$$\ln \frac{-\delta_1}{k_{yo}} \cong \ln \frac{\gamma}{a_o} - i\left(\frac{\pi}{2} + \frac{\omega\gamma^2}{K_1 v^2}\right)$$

$$\ln \frac{\delta_2}{k_{yo}} \cong \ln \frac{K_1 v^2}{\omega\gamma a_o} - i\left(\frac{\pi}{2} - \frac{\omega\gamma^2}{K_1 v^2}\right)$$

$$\ln \frac{-\delta_2}{k_{yo}} \cong \ln \frac{K_1 v^2}{\omega\gamma a_o} + i\,\frac{\omega\gamma^2}{K_1 v^2}$$

Now, we will make a very rough approximation for the above formulas and hope that we can get some idea about the effects due to them. After some tedious algebraic manipulation and the neglect of the small terms, we get:

$$\overline{P}_2 \cong \frac{\omega\mu_o K_o^2}{\pi} \frac{\mu_{2z}}{\mu_{2z} h_3 + \mu_o h_2}$$

$$\times \frac{1}{2}\left\{ \frac{2\,\frac{\omega\gamma^2}{K_1 v^2}(a_o^2 - \gamma^2) - A_4 + i\left[A_4 + \frac{\mu_{2y} h_2 + \mu_o h_3}{\mu_o} \frac{\omega}{v} \frac{2\omega\gamma^2}{K_1 v^2}(a_o^2 - \gamma^2)\right]}{\frac{K_1 v}{\gamma}\frac{\omega^2}{v}(a_o^2 + \gamma^2)} \right.$$

$$\left. + \frac{\mu_{2y} h_2 + \mu_o h_3}{\mu_o} \frac{2(\ln \frac{K_1 v^2}{\omega\gamma a_o} - 1)i + \pi}{\frac{K_1^2 v^2}{\gamma^2}} \right\} \qquad (3.52a)$$

$$\overline{F}_{y_2} \cong \frac{\mu_o K_o^2}{\pi} \frac{\mu_{2z}}{\mu_{2z} h_3 + \mu_o h_2}$$

$$\times \frac{1}{2} \{ \frac{\gamma^2 [-4a_o\gamma \frac{\gamma}{K_1 v} \frac{\mu_o}{\mu_{2y} h_2 + \mu_o h_3} + 4a_o\gamma \ln \frac{\gamma}{a_o} + \pi(a_o^2 - \gamma^2) + \frac{2\gamma(a_o^2+\gamma^2)}{a_o}]}{(a_o^2 + \gamma^2)^2}$$

$$- \pi \} \frac{\mu_{2y} h_2 + \mu_o h_3}{\mu_o \frac{K_1 v}{\gamma}} \qquad (3.52b)$$

where

$$A_4 = \frac{\omega}{v} \gamma \frac{\mu_{2y} h_2 + \mu_o h_3}{\mu_o} [2(a_o^2 - \gamma^2) \ln \frac{\gamma}{a_o} - 2\pi a_o \gamma + 2(a_o^2 + \gamma^2)] \qquad (3.52c)$$

The last terms in $\overline{P}_2$ and $\overline{F}_{y_2}$ (i.e., with π involved) are going to be cancelled by the corresponding terms in $\overline{P}_1$ and $\overline{F}_{y_1}$, respectively. As for the remaining terms, their values largely depend on a_o. However, the maximum influence definitely will be observed at $a_o \cong \gamma$. And at that point, the contribution to $\overline{F}_{y_2}$ is found to be positive, i.e., it will ease the end effect. Especially if $\frac{\omega}{v} \gamma \frac{\mu_{2y} h_2 + \mu_o h_3}{\mu_o} > \pi$, there is even a possibility that the overall end effect will help to increase the propulsion force.

Some of the arguments given above can be observed from comparing the plots, Fig. 3.15 and Fig. 3.10.

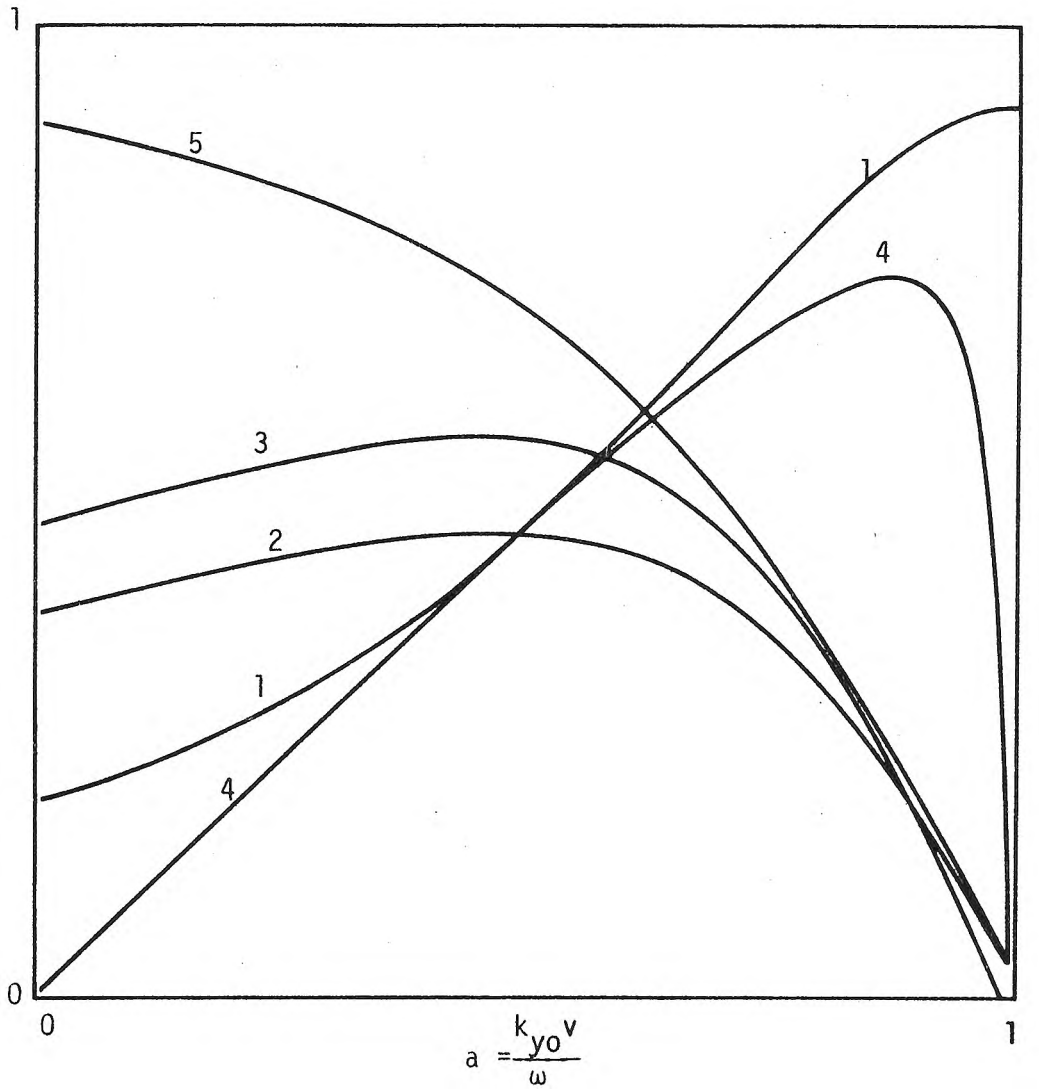

Fig. 3.15a Machine performance for geometry (B-i-1) with

$$|\tilde{K}_x|^2 = \frac{2K_o^2}{\pi} \frac{\sin^2(k_y-k_{yo})L}{(k_y-k_{yo})^2}$$

All parameters are the same as those of Fig. 3.10a; L = 1.256m. Curves (1), (2), (3) and (5) represent the same quantities as in Fig. 3.10a. Curve (4) is the machine efficiency.

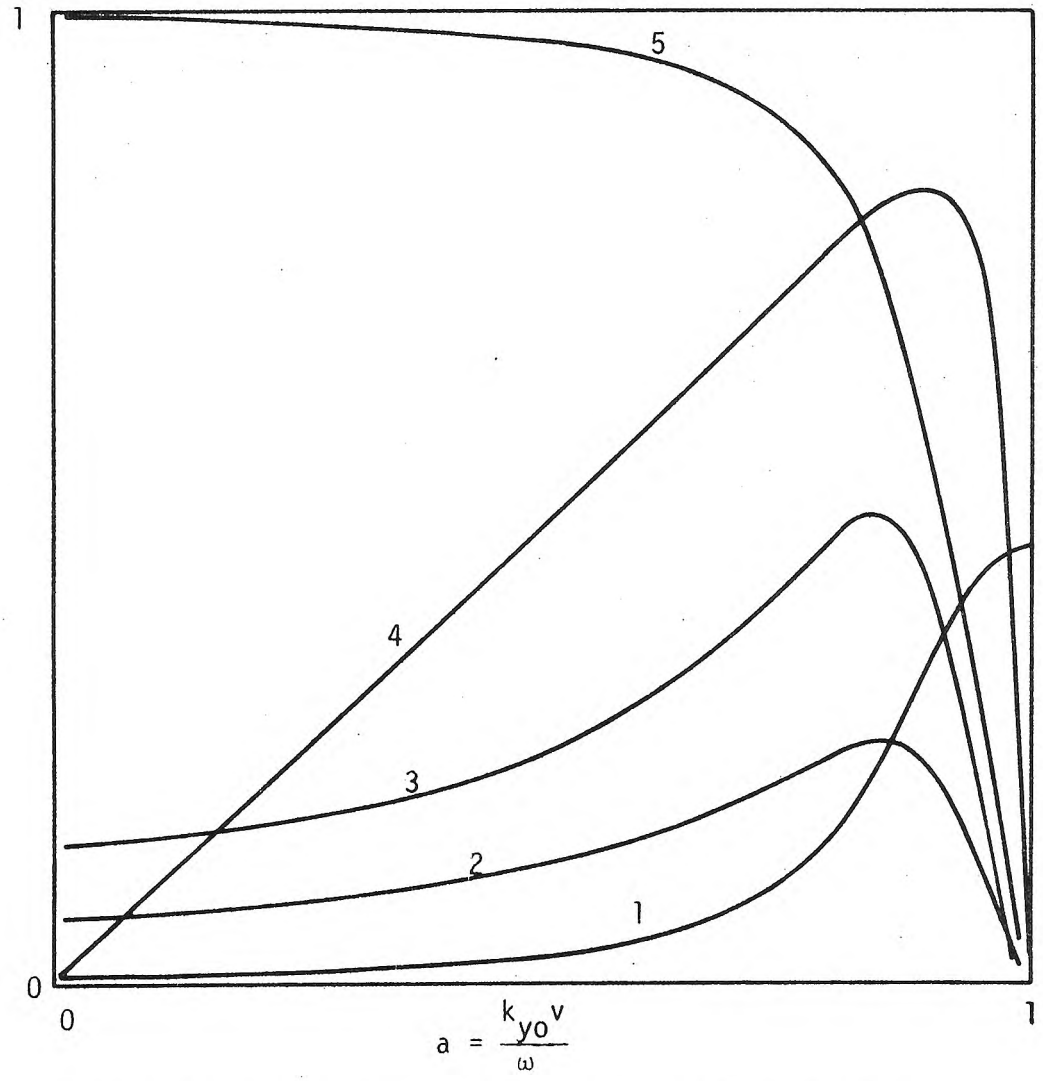

Fig. 3.15b Machine performance for geometry (B-i-1) with

$$|\tilde{K}_x|^2 = \frac{2K_o^2}{\pi} \frac{\sin^2(k_y - k_{yo})L}{(k_y - k_{yo})^2}$$

All parameters are the same as those of Fig. 3.10b; L = 1.256m. Curves (1), (2), (3) and (5) represent the same quantities as in Fig. 3.10b. Curve (4) is the machine efficiency.

CHAPTER IV

COMPOSITE TRACKS

From the previous discussion it follows that a composite track is highly recommended. Definitely, in order to satisfy different purposes, the LIM track configurations should be different also. It is obvious that a composite track will make region 2 inhomogeneous, and it thus makes the problem impossible to solve exactly. However, for practical analytical purposes, some approximations can always be made. If the track has a finely distributed inhomogeneity such that the relatively long wavelength travelling source field does not see the inhomogeneity, the track can be approximately considered as homogeneous with some effective uniaxial $\underset{\sim}{\sigma},\underset{\sim}{\mu}$. This idea was probably first suggested by Mishkin[21], Cullen and Barton[19] in analyzing rotary machines with slotted rotors. Experiments have already been made to check its applicability. It also gives the reason why we used uniaxial $\underset{\sim}{\sigma},\underset{\sim}{\mu}$ to represent the track properties from the very beginning of our analysis.

The values of the effective $\underset{\sim}{\sigma},\underset{\sim}{\mu}$ depend on the track configuration. Their values are determined from a homogeneous track for given uniformly distributed e.m.f. and m.m.f. in such a way that the same amounts of currents and fluxes are obtained. For example, for the general composite track shown in Fig. 4.1, we will get (assuming that within the track the material is uniformly distributed in the z direction):

$$\sigma_z = \frac{a_x a_y \sigma_a + (t_x t_y - a_x a_y)\sigma_b}{t_x t_y} \tag{4.1a}$$

$$\sigma_x = \frac{a_x b_y \sigma_b + (b_x b_y + a_y t_x)\sigma_a}{t_y} \quad \frac{\sigma_b}{a_x \sigma_b + b_x \sigma_a} \tag{4.1b}$$

$$\sigma_y = \frac{b_x a_y \sigma_b + (a_x t_y + b_x b_y)\sigma_a}{t_x} \quad \frac{\sigma_b}{a_y \sigma_b + b_y \sigma_a} \tag{4.1c}$$

To obtain $\underset{\sim}{\mu}$ we change σ_a into μ_a, σ_b into μ_b and σ_i into μ_i in the above formulas.

It should also be noticed that in the limit $b_x \to 0$ these expressions reduce to the familiar formulas given by Cullen and Barton[19].

As we mentioned earlier, this effective $\underset{\sim}{\mu},\underset{\sim}{\sigma}$ concept has already been experimentally verified. A theoretical proof, however, has never been attempted. There is no doubt that it is impossible to analyze this composite track geometry exactly. However, in order to gain some intuition about its validity, an extremely simplified geometry, specifically a finitely laminated iron, will be analyzed.

Due to the lamination, the problem basically becomes a 3-dimensional one. The transfer matrix method is thus not applicable. The most complete method for analyzing problems with laminated iron was previously given by Bondi and Mukherji[22] who evaluated the induced eddy current losses. Here we will use a similar formulation and extend it to the LIM problem. The finitely laminated iron is supposed to be used in region 2. Of course, for different LIM geometries, the situation will be different. Here we will consider the geometry (A-ii-2). The results for some of the other configurations are possibly obtained by some suitable substitutions.

The governing equations are the same as before. But now we have $\underset{\sim}{\sigma} = \sigma\underset{\sim}{I}$ and $\underset{\sim}{\mu} = \mu\underset{\sim}{I}$ in region 2. The source is still

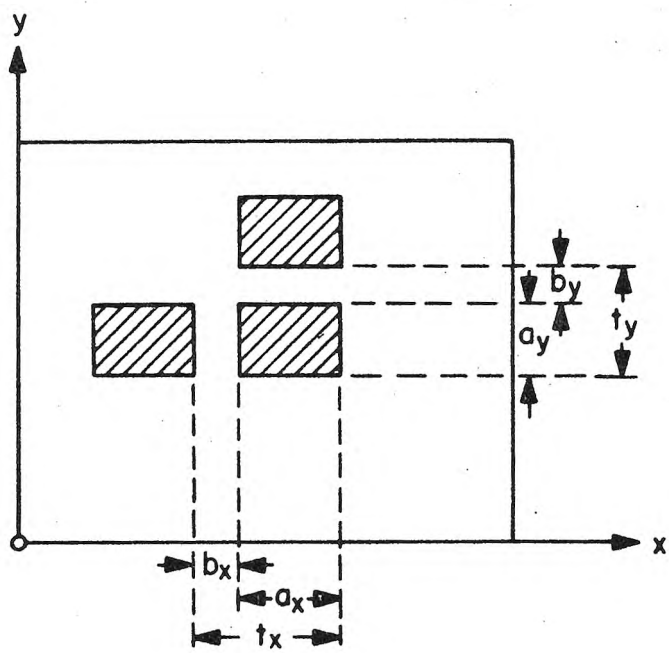

Fig. 4.1

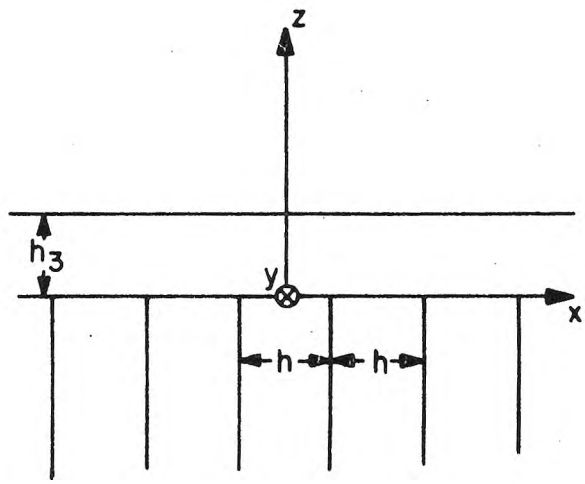

Fig. 4.2

infinitely extended in the x-direction. Due to the periodic character of the track, the field distribution will also be periodic in the x direction. A Fourier series expansion can be used to take care of the x variation. Thus, only one lamination (i.e., $|x| \leq h/2$) should be considered. For the y variation, the Fourier transform technique is employed. And, in the following, only one Fourier component is considered.

It can easily be seen that $\begin{pmatrix} \tilde{H}_x \\ \tilde{H}_y, \tilde{H}_z \end{pmatrix}$ are $\begin{pmatrix} \text{odd} \\ \text{even} \end{pmatrix}$ functions of x for the coordinate system shown in Fig. 4.2. The insulation regions (which make $\tilde{J}_x = 0$ at $x = \pm h/2$) are assumed to be very thin. $\tilde{B}_x$ and $\tilde{H}_x$ are thus continuous at the interfaces. Hence, it may be concluded that $\tilde{H}_x = 0$ at $x = h/2$. Using similar arguments as in Bondi and Mukherji[22], we can decompose the field in region 2 into three parts, namely:

(a) $\tilde{H}_x = 0$ everywhere but $\tilde{J}_x \neq 0$,

(b) $\tilde{J}_x = 0$ everywhere but $\tilde{H}_x \neq 0$,

(c) $\tilde{J}_x = 0$, $\tilde{H}_x = 0$ everywhere.

Part (c) is the so-called deeply penetrated field which will be found to be the most important. It plays a role in reducing the undesired skin effect.

The field components in each region are thus:

Region 2:

(a) $\tilde{H}_x = 0$

$$\tilde{J}_x = \sum_{\ell=0}^{\infty} a_\ell \cos\left[(2\ell+1)\frac{\pi x}{h}\right] e^{k_{z,\ell} z} \qquad (4.2a)$$

$$\tilde{H}_y = \sum_{\ell=0}^{\infty} \frac{-a_\ell k_{z,\ell}}{(2\ell+1)^2 \frac{\pi^2}{h^2} - \frac{i}{d^2}} \cos[(2\ell+1)\frac{\pi x}{h}]\, e^{k_{z,\ell} z} \tag{4.2b}$$

$$\tilde{H}_z = \sum_{\ell=0}^{\infty} \frac{ik_y a}{(2\ell+1)^2 \frac{\pi^2}{h^2} - \frac{i}{d^2}} \cos[(2\ell+1)\frac{\pi x}{h}]\, e^{k_{z,\ell} z} \tag{4.2c}$$

$$\tilde{J}_y = \sum_{\ell=0}^{\infty} \frac{a_\ell (2\ell+1)}{(2\ell+1)^2 \frac{\pi^2}{h^2} - \frac{i}{d^2}} \frac{ik_y \pi}{h} \sin[(2\ell+1)\frac{\pi x}{h}]\, e^{k_{z,\ell} z} \tag{4.2d}$$

$$\tilde{J}_z = \sum_{\ell=0}^{\infty} \frac{(2\ell+1)}{h} \frac{a_\ell k_{z,\ell}\, \pi}{(2\ell+1)^2 \frac{\pi^2}{h^2} - \frac{i}{d^2}} \sin[(2\ell+1)\frac{\pi x}{h}]\, e^{k_{z,\ell} z} \tag{4.2e}$$

(b) $\tilde{J}_x = 0$

$$\tilde{H}_x = \sum_{m=1}^{\infty} b_m \sin(\frac{2m\pi x}{h})\, e^{k_{z,m} z} \tag{4.3a}$$

$$\tilde{J}_y = \sum_{m=1}^{\infty} (-\frac{i}{d^2}) \frac{b_m k_{z,m}}{\frac{4m^2\pi^2}{h^2} - \frac{i}{d^2}} \sin(\frac{2m\pi x}{h})\, e^{k_{z,m} z} \tag{4.3b}$$

$$J_z = \sum_{m=1}^{\infty} (-\frac{k_y}{d^2}) \frac{b_m}{\frac{4m^2\pi^2}{h^2} - \frac{i}{d^2}} \sin(\frac{2m\pi x}{h})\, e^{k_{z,m} z} \tag{4.3c}$$

$$\tilde{H}_y = \sum_{m=1}^{\infty} \left(-\frac{2m\pi}{h}\right) \frac{ik_y b_m}{\frac{4m^2\pi^2}{h^2} - \frac{i}{d^2}} \cos\left(\frac{2m\pi x}{h}\right) e^{k_{z,m} z} \tag{4.3d}$$

$$\tilde{H}_z = \sum_{m=1}^{\infty} \left(\frac{2m\pi}{h}\right) \frac{-b_m k_{z,m}}{\frac{4m^2\pi^2}{h^2} - \frac{i}{d^2}} \cos\left(\frac{2m\pi x}{h}\right) e^{k_{z,m} z} \tag{4.3e}$$

(c) $$\tilde{J}_x = \tilde{H}_x = 0 \tag{4.4a}$$

$$\tilde{H}_z = k_z f \cosh\left(\frac{\sqrt{i}x}{id}\right) e^{k_z z} \tag{4.4b}$$

$$\tilde{H}_y = ik_y f \cosh\left(\frac{\sqrt{i}x}{id}\right) e^{k_z z} \tag{4.4c}$$

$$\tilde{J}_y = -k_z f \frac{\sqrt{i}}{id} \sinh\left(\frac{\sqrt{i}x}{id}\right) e^{k_z z} \tag{4.4d}$$

$$\tilde{J}_z = ik_y f \frac{\sqrt{i}}{id} \sinh\left(\frac{\sqrt{i}x}{id}\right) e^{k_z z} \tag{4.4e}$$

where

$$k_{z,\ell}^2 = k_y^2 + (2\ell+1)^2 \frac{\pi^2}{h^2} - \frac{i}{d^2} \tag{4.5a}$$

$$k_{z,m}^2 = k_y^2 + \frac{4m^2\pi^2}{h^2} - \frac{i}{d^2} \tag{4.5b}$$

$$\frac{1}{d^2} = (\omega - k_y v)\mu\sigma \tag{4.5c}$$

$$k_z^2 = k_y^2 \tag{4.5d}$$

A suitable Riemann surface sheet should be taken to give positive real parts for the $k_{z,\ell}$, $k_{z,m}$ and k_z

Region 3

$$\tilde{J} = 0 \tag{4.6a}$$

$$\tilde{H}_x = \sum_{m=0}^{\infty} \left[q_{m1} \exp\left[\left(-k_y^2 + \frac{4m^2\pi^2}{h^2}\right)^{1/2} z\right] + q_{m2} \right.$$

$$\left. \times \exp\left[\left(k_y^2 + \frac{4m^2\pi^2}{h^2}\right)^{1/2} z\right]\right] \sin\left(\frac{2m\pi x}{h}\right) \frac{2m\pi}{h} \tag{4.6b}$$

$$\tilde{H}_y = \sum_{m=0}^{\infty} \left[q_{m1} \exp\left[-\left(k_y^2 + \frac{4m^2\pi^2}{h^2}\right)^{1/2} z\right] + q_{m2} \exp\left[\left(k_y^2 + \frac{4m^2\pi^2}{h^2}\right)^{1/2} z\right]\right]$$

$$\times \cos\frac{2m\pi x}{h} (-ik_y) \tag{4.6c}$$

$$\tilde{H}_z = \sum_{m=0}^{\infty} \left[q_{m1} \exp\left[-\left(k_y^2 + \frac{4m^2\pi^2}{h^2}\right)^{1/2} z\right] - q_{m2} \exp\left[\left(k_y^2 + \frac{4m^2\pi^2}{h^2}\right)^{1/2} z\right]\right]$$

$$\times \cos\frac{2m\pi x}{h} \left(k_y^2 + \frac{4m^2\pi^2}{h^2}\right)^{1/2} \tag{4.6d}$$

Thus we have unknowns $\{q_{m1}\}$, $\{q_{m2}\}$, $\{b_m\}$, $\{\alpha_\ell\}$, f . In principle, they can be solved by matching the boundary conditions at $z = 0$ and $z = h_3$.

At $z = 0$: $\begin{pmatrix} \tilde{H}_t \\ \tilde{B}_z \end{pmatrix}$ are continuous (4.7a)

(Note: $J_z = 0$ at $z = 0$ is automatically satisfied from the boundary conditions given above.)

At $z = h_3$: $-\hat{e}_z \times \underline{\tilde{H}} = \underline{\tilde{K}} = \tilde{K}_x \hat{e}_x$ (4.7b)

i.e.,

$$q_{o2} = \frac{\tilde{K}_x e^{-k_z h_3}}{-ik_y} - q_{o1} e^{-2k_z h_3} \tag{4.7c}$$

$$q_{m2} = -q_{m1} e^{-2h_3\left(k_y^2 + \frac{4m^2\pi^2}{h^2}\right)^{1/2}} \qquad \text{for } m \neq 0 \tag{4.7d}$$

$$(q_{m1} + q_{m2}) \frac{2m\pi}{h} = b_m \tag{4.7e}$$

$$-ik_y(q_{m1} + q_{m2}) = -ik_y \frac{2m\pi}{h} \frac{b_m}{(2m\frac{\pi}{h})^2 - \frac{i}{d^2}} + ikf \frac{4}{h}\frac{\sqrt{i}}{di}\left(1 - \frac{1}{2}\delta_{mo}\right)$$

$$\cdot \frac{(-1)^m \sinh \frac{\sqrt{i}h}{2di}}{(2m\frac{\pi}{b})^2 - \frac{i}{d^2}} + \sum_{\ell} \frac{a_\ell k_{z,\ell}}{(2\ell+1)^2 \frac{2\pi^2}{b^2} - \frac{i}{d^2}} \frac{4}{\pi}\left(1 - \frac{1}{2}\delta_{mo}\right) \frac{(2\ell+1)(-1)^{\ell+m}}{4m^2 - (2\ell+1)^2} \tag{4.7f}$$

$$\mu_o(q_{m1} - q_{m2})\left(k_y^2 + \frac{4m^2\pi^2}{h^2}\right)^{1/2} = \frac{2m\pi}{h}\mu \frac{b_m k_{z,m}}{(2m\frac{\pi}{h})^2 - \frac{i}{d^2}}$$

$$+ k_z f \mu \frac{4}{h}\frac{\sqrt{i}}{di}\left(1 - \frac{1}{2}\delta_{mo}\right)(-1)^m \sinh \frac{\sqrt{i}h}{2di}$$

$$- ik\mu \sum_{\ell=0}^{\infty} \frac{a_\ell}{(2\ell+1)^2 \frac{\pi^2}{h^2} - \frac{i}{d^2}} \frac{4}{\pi}\left(1 - \frac{1}{2}\delta_{mo}\right) \frac{(-1)^{\ell+m}(2\ell+1)}{4m^2 - (2\ell+1)^2} \tag{4.7g}$$

Then, with

$$a_\ell = \frac{(-1)^\ell \left[(2\ell+1)^2 \frac{\pi^2 d^2}{k^2} - i\right]}{(2\ell+1)\, d^2 k_{z,\ell}} \frac{\pi}{2}\alpha_\ell \tag{4.8a}$$

$$f \frac{2}{b}\sqrt{i} \sinh \frac{\sqrt{i}h}{2di} = f' \tag{4.8b}$$

$$q_{ml} = q'_{ml}\, d(-1)^m \tag{4.8c}$$

This set of equations is manipulated to give:

$$i\mu_o \tilde{K}_x\, e^{-k_z h_3}\,(1 + \tanh k_z h_3) = \sum_{\ell=0}^{\infty} \alpha_\ell \left\{ \frac{\frac{4m^2\pi^2 d^2}{h^2} - i}{4m^2 - (2\ell+1)^2} (\mu_o + \mu \tanh k_z h_3) \right.$$

$$\cdot \frac{F(m) - \dfrac{i\mu k_y^2 d^2\,[1 - \exp\{-2h_3(k_y^2 + \frac{4m^2\pi^2}{h^2})^{1/2}\}]}{k_{z,\ell}\, d}}{F(m) - i\mu k_z d[1 - \exp\{-2h_3(k_y^2 + \frac{4m^2\pi^2}{h^2})^{1/2}\}]}$$

$$\left. - \frac{i}{(2\ell+1)^2} \left[\mu_o + \frac{\mu k_z d \tanh k_z h_3}{k_{z,\ell} d}\right] \right\} \tag{4.9a}$$

$$\tilde{K}_x\, e^{-k_z h_3}(\mu - \mu_o) = q'_{01}\, ik_y d(1 - e^{-2k_z h_3})(\mu + \mu_o \coth k_z h_3)$$

$$- \sum_{\ell=0}^{\infty} \frac{\mu \alpha_\ell}{(2\ell+1)^2} \left(1 - \frac{k_z d}{k_{z,\ell} d}\right) \tag{4.9b}$$

$$f' k_z d(\mu + \mu_o \coth k_z h_3) = -i\mu_o\, \mathrm{sgn}(k_y) \tilde{K}_x\, e^{-k_z h_3}\,(1 + \coth k_z h_3)$$

$$- \sum_{\ell=0}^{\infty} \frac{\alpha_\ell i}{(2\ell+1)^2} \left[\mu_o\, \mathrm{sgn}(k_y) \coth k_z h_3 + \frac{\mu k_y d}{k_{z,\ell} d}\right] \tag{4.9c}$$

$$q'_{ml} \{F(m) - i\mu k_z d[1 - \exp\{-2h_3(k_y^2 + \frac{4m^2\pi^2}{h^2})^{1/2}\}]\}$$

$$= \sum_{\ell=0}^{\infty} 2\alpha_\ell\, i\mu\, \mathrm{sgn}(k_y)\, \frac{[(4m^2\pi^2 d^2)/h^2] - i}{4m^2 - (2\ell+1)^2} \left(1 - \frac{k_z d}{k_{z,\ell} d}\right) \tag{4.9d}$$

$$F(m) = \mu_o\left(k_y^2 d^2 + \frac{4m^2\pi^2 d^2}{h^2}\right)^{1/2}\left(\frac{4m^2\pi^2 d^2}{h^2} - i\right)^{1/2}\left[1 + \exp\left\{-2h_3\left(k_y^2 + \frac{4m^2\pi^2}{h^2}\right)^{1/2}\right\}\right]$$

$$+ \mu \frac{4m^2\pi^2 d^2}{h^2} k_{z,m} d\left[1 - \exp\left\{-2h_3\left(k_y^2 + \frac{4m^2\pi^2}{h^2}\right)^{1/2}\right\}\right] \qquad (4.9e)$$

If (4.9a) can be solved for α_ℓ , all of the other unknowns can be obtained from the remaining equations. Then we can find the field distribution everywhere.

It is understood that the final results we want are machine performances such as forces, power, efficiency, etc. All of these can be expressed in terms of the field distribution at $z = h_3$ as given by (2.24), (2.25), (2.27). As far as the fields at $z = h_3$ are concerned, formulas (4.6), (4.7) can be used to give:

$$\tilde{H}_x = 0 \qquad (4.10a)$$

$$\tilde{H}_y = \tilde{K}_x \qquad (4.10b)$$

$$\tilde{H}_z = \sum_{m=0}^{\infty} 2q_{m1}\exp\left\{-h_3\left(k_y^2 + \frac{4m^2\pi^2}{h^2}\right)^{1/2}\right\}\cos\frac{2m\pi x}{h}\left(k_y^2 + \frac{4m^2\pi^2}{h^2}\right)^{1/2} \qquad (4.10c)$$

For average $\overline{F}_y$, $\overline{P}$ the $m \neq 0$ terms in H_z do not give any contribution. But for $\overline{F}_z$ these terms do have some effect. However, due to the fast decay of $\exp\left[-h_3\left(k_y^2 + \frac{4m^2\,2}{h^2}\right)^{1/2}\right]$, the contributions from $m \neq 0$ can be considered as negligible. (Note, generally $h \lesssim h_3$ is true.) So, for $\tilde{H}_z$, we probably need only to consider the term with $m = 0$. Thus q'_{01} is the most important unknown constant to evaluate.

Now, let us assume that α_ℓ can be solved for, except for a common factor α_∞ . Then we set

$$\sum_{\ell} \alpha_{\ell} \frac{\frac{4m^2\pi^2d^2}{h^2} - i \quad F(m) - \frac{i\mu k_y^2 d^2[1 - \exp\{-2h_3(k_y^2 + \frac{4m^2\pi^2}{h^2})^{1/2}\}]}{k_{z,\ell}d}}{4m^2 - (2\ell+1)^2} = i\alpha_\infty A$$

$$F(m) - i\mu k_z d[1 - \exp\{-2h_3(k_y^2 + \frac{4m^2\pi^2}{h^2})^{1/2}\}] \qquad (4.11a)$$

$$\sum_{\ell=0}^{\infty} \alpha_{\ell} \frac{1}{(2\ell+1)^2} = \alpha_\infty B \qquad (4.11b)$$

$$\sum_{\ell=0}^{\infty} \alpha_{\ell} \frac{1}{(2\ell+1)^2} \frac{k_z d}{k_{z,\ell} d} = \alpha_\infty C \qquad (4.11c)$$

It should be noticed that A, B, C, α_∞ are all ℓ,m independent. From (4.9),(4.11):

$$2q'_{01} ik_y d \cosh k_z h_3 = \tilde{K}_x \frac{\mu_0(B-A) + \mu(A-C)}{\mu_0(A-B) + \mu \tanh k_z h_3 (A-C)} \qquad (4.12)$$

And the $\underline{\tilde{H}}$-field at $z = h_3$ is thus:

$$\tilde{H}_x = 0 \qquad (4.13a)$$

$$\tilde{H}_y = \tilde{K}_x \qquad (4.13b)$$

$$\tilde{H}_z \cong -i \, \mathrm{sgn}(k_y) \, \tilde{K}_x \frac{1 + \frac{\mu_0(A-B)}{\mu(A-C)} \tanh k_z h_3}{\tanh k_z h_3 + \frac{\mu_0(A-B)}{\mu(A-C)}} \qquad (4.13c)$$

Here for $\tilde{H}_z$, only the $m = 0$ term is included. The corresponding $\underline{\tilde{E}}$ field is given by $\underline{\tilde{E}} = \hat{\ell}_x \frac{\omega\mu_0}{k_y} \tilde{H}_z$. Using (2.24), (2.25), (2.27), the expressions for $\underline{F}$,$\overline{P}$ are found to be exactly the same as those given in (A-ii-2), except that $\frac{\mu_0\gamma_2}{\mu_{2y}k_z}$ now should be replaced by

$$\frac{\mu_o(A-B)}{\mu(A-C)} \quad .$$

Now we come to the point where we have to evaluate A, B, C, i.e., we should solve (4.9a). Doing it exactly is a hopeless task. An approximation can be made by truncating this set of equations, considering only a limited number of equations with the same number of unknowns. However, this will lead only to some numerical data. In the problem we are considering it seems that an analytical solution is more desirable. Thus, an alternative approximation will be made. First, let us look at the term:

$$F(m) - \frac{i\mu k_y^2 d^2[1 - \exp\{-2h_3(k_y^2 + \frac{4m^2\pi^2}{h^2})^{1/2}\}]}{k_{z,\ell}d}$$

$$\overline{F(m) - i\mu k_z d[1 - \exp\{-2h_3(k_y^2 + \frac{4m^2\pi^2}{h^2})^{1/2}\}]}$$

It can be rewritten as:

$$1 + \frac{i\mu k_z d[1 - \exp\{-2h_3(k_y^2 + \frac{4m^2\pi^2}{h^2})^{1/2}\}][1 - \frac{k_z d}{k_{z,\ell}d}]}{F(m) - i\mu k_z d[1 - \exp\{-2h_3(k_y^2 + \frac{4m^2\pi^2}{h^2})^{1/2}\}]}$$

Now, if $\frac{k_{yo}h}{2\pi} << 1$ is assumed, $\frac{k_z d}{k_{z,\ell}d} << 1$ can be shown to hold in the region where $\tilde{K}_x$ is large. $\frac{k_z d}{k_{z,\ell}d}$ can thus be neglected in $1 - \frac{k_z d}{k_{z,\ell}d}$. Furthermore, even for m=1, if $(|4\pi^2 d^2|)/h_2 \gtrsim 1$, $|F(m)| >> uk_z d$ can always be obtained. Generally, the requirement $(|4\pi^2 d_o^2|)/h^2 \gtrsim 1$ is not difficult to meet in the LIM which we are now considering. Under these conditions, the following approximation is reasonable:

$$\frac{F(m) - \dfrac{i\mu k_y^2 d^2[1 - \exp\{-2h_3(k_y^2 + \frac{4m^2\pi^2}{h^2})^{1/2}\}]}{k_{z,\ell} d}}{F(m) - i\mu k_z d[1 - \exp\{-2h_3(k_y^2 + \frac{4m^2\pi^2}{h^2})^{1/2}\}]} \cong 1 \qquad (4.14)$$

The next step is then trying to find an explicit function of ℓ for α_ℓ to make $\sum_\ell \alpha_\ell \frac{(4m^2\pi^2d^2)/h^2 - i}{4m^2 - (2\ell+1)^2}$ independent of m. The only possibilities we can find are $\alpha_\ell = \alpha_\infty$ and $\alpha_\ell = \alpha_\infty / (2\ell+1)^2 - \frac{ih^2}{\pi^2 d^2}$. If $\alpha_\ell = \alpha_\infty$, then $\sum_\ell \alpha_\ell \frac{(4m^2\pi^2d^2)/h^2 - i}{4m^2 - (2\ell+1)^2} = 0 = A$. The magnitude of the error term in A will always be larger than 0. Also, we are expecting a set of α_ℓ which will decrease faster than α_∞ when ℓ increases. Thus, we must exclude this possibility. On the contrary, for $\alpha_\ell = \alpha_\infty / [(2\ell+1)^2 - \frac{ih^2}{\pi^2 d^2}]$, $\sum_{\ell=0}^{\infty} \alpha_\ell \frac{(4m^2\pi^2d^2)/h^2 - i}{4m^2 - (2\ell+1)^2}$ is no longer zero. And the error term will always be small. Thus, we may conclude that the assumption $\alpha_\ell \cong \alpha_\infty / [(2\ell+1)^2 - \frac{ih^2}{\pi^2 d^2}]$ will give a quite good approximation.

Now we use $\alpha_\ell \cong \alpha_\infty / [(2\ell+1)^2 - \frac{ih^2}{\pi^2 d^2}]$ in (4.11) to get:

$$A \cong \frac{\pi^2 d^2}{ih^2} \frac{\pi^2 d}{4\sqrt{i}h} \tan(\frac{\sqrt{i}h}{2d}) \qquad (4.15a)$$

$$B \cong \frac{\pi^4 d^3}{4i\sqrt{i}h^3} \tan(\frac{\sqrt{i}\,h}{2d}) - \frac{\pi^4 d^2}{8ih^2} \qquad (4.15b)$$

$$C \cong \frac{k_z h}{\pi} g_o(\frac{\pi d}{h}) \qquad (4.15c)$$

with

$$g_o(\frac{\pi d}{h}) = \sum_{\ell=0}^{\infty} \frac{1}{(2\ell+1)^2} \frac{1}{(2\ell+1)^2 - \frac{ih^2}{\pi^2 d^2}} \frac{1}{\sqrt{(2\ell+1)^2 - \frac{ih^2}{\pi^2 d^2} + \frac{k_y^2 h^2}{\pi^2}}} \qquad (4.15d)$$

Thus:

$$\frac{\mu_o(A-B)}{\mu(A-C)} \cong \frac{\mu_o \frac{\pi^4 d^2}{8ih^2}}{\mu[\frac{\pi^4 d^3}{4i\sqrt{i}\, h^3} \tan(\frac{\sqrt{i}h}{2d}) - \frac{k_z h}{\pi} g_o(\frac{\pi d}{h})]} \tag{4.16}$$

Now compare the above formula with $\frac{\mu_o \gamma_2}{\mu_{2y} k_z}$. If h is sufficiently small such that $h/2d_o << 1$ is true, then $\tan(\frac{\sqrt{i}h}{2d}) \cong \frac{\sqrt{i}h}{2d}$ and $|g_o(\frac{\pi d}{h})| \cong 1.005 << |\frac{\pi^4 d^2}{8h^2}|$. $\frac{\mu_o(A-B)}{\mu(A-C)}$ is thus reduced to μ_o/μ . This means that $\mu_{2y} \cong \mu$ and $\sigma \cong 0$ are the effective material constants. And they are consistent with the values given by empirical formulas (4.1). However, if $h/2d << 1$ is not met, then the above simplification is not valid any longer. Thus, we can conclude that the conditions under which formula (4.1) gives accurate values for the effective material constants are $k_y h << 1$ and $h/2d << 1$.

Up to now we only consider one Fourier component with $e^{ik_y y}$ variation. Eventually we have to take the Fourier inverse to get the machine performances. It is obvious that the assumptions which we make above cannot hold for all k_y . However, the source function will generally decay when it is away from k_{yo}. Thus, if the above assumptions are reasonable around k_{yo}, a good solution can still be obtained by applying this kind of approximation to all k_y .

In the geometry we are now considering, $\frac{\mu_o(A-B)}{\mu(A-C)} \cong \frac{\mu_o}{\mu}$ will give a zero propulsion force. Thus it is out of the question to use merely this kind of track as the LIM in HSGT vehicles. (Of course, it can be used for the levitation purpose.) Extra conductivity should be added. One example is shown in the LIM built by the Rohr Inc.[17] with

suitably arranged conducting bars inserted into the laminated iron. Definitely, if the requirements $k_{yo}h << 1$ and $h/2d_o << 1$ hold, the effective material constant concept is still valid. However, we are not going to give any further analyses of that kind. Instead, an alternative geometry is suggested. Now we will try to lift the criterion $h/2d_o << 1$ and introduce a track with a larger h such that $h/2d_o\pi$ approximately equals 1. Then the approximation $\tan(\frac{\sqrt{i}h}{2d}) \approx \frac{\sqrt{i}h}{2d}$ is not true any longer, nor is the effective material constant concept. Instead, the direct method, as introduced in this chapter, should be used. However, even for $h/2d\pi \sim 1$, "C" can still be shown to be small compared to "A". Thus, $\frac{\mu_o(A-B)}{\mu(A-C)} \approx \frac{\mu_o}{\mu}\frac{\sqrt{i}h}{2d}\cot(\frac{\sqrt{i}h}{2d})$. Now $h/2d_o\pi \sim 1$, so, except possibly in a very small region where $\omega/v \sim k_y$ such that $|\frac{\sqrt{i}h}{2d}| << 1$, $h/2d\pi$ is going to be of the order of "1" for most k_y around k_{yo}. And for $h/2d\pi \sim 1$, the argument of the cotangent function will be large enough to allow us to make the approximation that $\cot\frac{\sqrt{i}h}{2d} \approx -i$. Thus, $\frac{\mu_o(A-B)}{\mu(A-C)} \approx \frac{\mu_o}{\mu}\frac{-i\sqrt{i}h}{2d}$ and:

$$\tilde{Z}_L \approx \frac{-i\omega\mu_o}{k_z}\frac{1}{k_z h_3 + \frac{\mu_o}{\mu}\frac{-i\sqrt{i}h}{2d}} \tag{4.17a}$$

$$= \frac{-i\omega\mu_o}{k_z}\frac{k_z h_3 + \frac{\mu_o}{2\sqrt{2}\mu}\sqrt{(\omega-k_y v)\mu\sigma h^2} + i\frac{\mu_o}{2\sqrt{2}\mu}\sqrt{(\omega-k_y v)\mu\sigma h^2}}{k_y^2 h_3^2 + \frac{\mu_o^2}{4\mu^2}(\omega-k_y v)\mu\sigma h^2 + k_z h_3\frac{\mu_o}{\sqrt{2}\mu}\sqrt{(\omega-k_y v)\mu\sigma h^2}} \tag{4.17b}$$

$$\tilde{F}_y \approx \mathrm{Re}[\frac{-i\mu_o}{2}\frac{\mathrm{sgn}(k_y)}{k_z h_3 + \frac{\mu_o}{\mu}\frac{-i\sqrt{i}h}{2d}}|\tilde{K}_x|^2] \tag{4.17c}$$

$$= \frac{\mu_o}{2} \frac{\operatorname{sgn}(k_y) - \frac{\mu_o}{2\sqrt{2}\,\mu_o} \sqrt{(\omega - k_y v)\mu\sigma h^2}}{k_y^2 h_3^2 + \frac{\mu_o^2}{4\mu^2}(\omega - k_y v)\mu\sigma h^2 + k_z h_3 \frac{\mu_o}{\sqrt{2}\mu} \sqrt{(\omega - k_y v)\mu\sigma h^2}} \tag{4.17d}$$

$$\tilde{F}_z \cong \frac{\mu_o}{4} \operatorname{Re}\left[\frac{1 - \frac{\mu_o^2}{\mu^2} \frac{h^2}{4d^2}}{\left| k_z h_3 + \frac{\mu_o}{\mu} - \frac{i\sqrt{1}h}{2d} \right|^2} |\tilde{K}_x|^2 \right] \tag{4.17e}$$

$$= \frac{\mu_o}{4} \frac{1 - \frac{\mu_o^2}{4\mu^2}(\omega - k_y v)\mu\sigma h^2}{k_y^2 h_3^2 + \frac{\mu_o^2}{4\mu^2}(\omega - k_y v)\mu\sigma h^2 + k_z h_3 \frac{\mu_o}{\sqrt{2}\mu} \sqrt{(\omega - k_y v)\mu\sigma h^2}} |\tilde{K}_x|^2 \tag{4.17f}$$

Analyses can be made of these integrands. At $k_y = 0$, $\frac{\tilde{F}_z}{|\tilde{K}_x|^2}$ is no longer equal to zero. Actually, if $(\mu_o^2 \sigma h^2 v^2)/(16\omega\mu h_3^2) \lesssim 1$, $\tilde{F}_y/|\tilde{K}_x|^2$ is a monotonically decreasing function of k_y for $0 \le k_y \le \omega/v$. Its value will decrease from $\frac{\mu_o}{2} \frac{\sqrt{2}\mu}{\mu_o \sqrt{\omega\mu\sigma h^2}}$ at $k_y = 0$ to "0" at $k_y = \omega/v$. Also, in that same region, $\tilde{F}_z/|\tilde{K}_x|^2$ can be shown to be positive under the condition that $1 > \frac{\mu_o^2 \omega\sigma h^2}{4\mu}$.

For the ideal source, (4.17) can be used to evaluate the machine performances. However, this approximation will be good only under the conditions that $k_{yo} h_3 \ll 1$ and $h/2\pi d_o \sim 1$. Thus for the given source and track configurations, generally the approximation cannot satisfactorily cover the entire velocity range $0 \le v \le \omega/k_{yo}$. If the necessary conditions are satisfied, the maximum force will be found at $v = \frac{\omega}{k_{yo}} \left(2 \Big/ 1 + \sqrt{1 + \frac{16\omega\mu h_3^2}{\sigma v^2 \mu_o^2 h^2}} \right)$ with a corresponding force density of

$$\frac{\pi \mu_o k_o^2}{k_{yo} h_3 (2+2\sqrt{2})} .$$

Special care should be taken if (4.17) is applied to the more realistic source $|\tilde{K}_x|^2 = \frac{2K_o^2}{\pi} \frac{\sin^2(k_y - k_{yo})L}{(k_y - k_{yo})^2}$. It is obvious that the conditions $k_y h_3 \ll 1$ and $h/2\pi d \sim 1$ cannot be satisfied for a large region of k_y. Thus, for a source distribution $|\tilde{K}_x|^2 \propto \frac{\sin^2(k_y - k_{yo})L}{(k_y - k_{yo})}$ the additional condition that L is very large seems to be necessary to ensure the use of (4.17) a good approximation.

Now, if all the conditions for the approximations to be valid are satisfied, it can be seen that the examined geometry can offer forces of the same order of magnitude as those of geometry (A-i-1). Thus, if the geometry (A-i-1) can meet the force requirements for the LIMs, the studied geometry can also do it with source current magnitudes of the same order. However, it seems that the most important advantage which this geometry can offer is the "influences due to the end effect." From a remark given earlier, we know that now $\tilde{F}_y/|\tilde{K}_x|^2$ is a monotonically decreasing function. If the source function $\tilde{K}_x$ is not a δ-function, although part of it will spread into a region where $\tilde{F}_y/|\tilde{K}_x|^2$ is smaller, there always are other parts which will go into larger integrand regions. Thus, the net effect is generally small. Similarly, since $\tilde{F}_z/|\tilde{K}_x|^2$ is always positive, it is not necessary to worry about $|\tilde{K}_x|^2$ being pushed into the repulsive region.

In the above analyses, a LIM of geometry (A-ii-2) with region 2 consisting of laminated iron is considered. We would expect that a similar approach could be applied to other configurations. In some

cases this is found to be true indeed. Actually, similar formulas will hold with suitable substitution of $\frac{\mu_o\gamma_2}{\mu_{2y}k_z}$, $\frac{\mu_o\gamma_2}{\mu_{2y}k_z}\tanh\gamma_2 h_2$ by expressions A, B, C. However, generally these A, B, C's will be somewhat more complicated and the equations for them will be more difficult to solve. Especially for a thin reaction rail geometry, we shall find that we cannot use the same approximation any longer while solving for α_ℓ. Also, because less material is employed, a somewhat larger effective conductivity is always necessary to give a large enough propulsion force. Thus, laminated iron alone is not good enough to build a thin reaction rail LIM.(i.e., composite reaction rails with both ferro- and nonferro-magnetic material are necessary). Hence, we neglect further considerations of this kind of configuration.

As for (A-ii-1), we shall find (3.14), (3.15) and (3.16) to be still true with $\frac{\mu_o\gamma_2}{\mu_{2y}k_z}$ replaced by $\frac{\mu_o(A-B)}{\mu(A-C)}$. Here B,C are defined by the same formulas as in the previous case, i.e., (4.11b), (4.11c). However, for A and α_ℓ they are somewhat different. Now we have:

$$\sum_{\ell=0}^{\infty} \frac{\frac{4m^2\pi^2d^2}{h^2} - i}{4m^2-(2\ell+1)^2} \frac{F(m) - \frac{i\mu k_y^2 d^2}{k_{z,\ell} d}}{F(m) - i\mu k_z d} = i\alpha_\infty A \qquad (4.18a)$$

$$-i\mu_o e^{-k_z h_3} \tilde{K}_x = \sum_{\ell=0}^{\infty} \alpha_\ell \left\{ \frac{i}{(2\ell+1)^2}(\mu_o + \frac{\mu k_z d}{k_{z,\ell} d}) \right.$$
$$\left. - \frac{\frac{4m^2\pi^2d^2}{h^2} - i}{4m^2-(2\ell+1)^2}(\mu+\mu_o) \frac{F(m) - \frac{i\mu k_y^2 d^2}{k_{z,\ell} d}}{F(m) - i\mu k_z d} \right\} \qquad (4.18b)$$

$$F(m) = \mu_o(k_y^2 d^2 + \frac{4m^2\pi^2d^2}{h^2})^{1/2}(\frac{4m^2\pi^2d^2}{h^2} - i) + \mu \frac{4m^2\pi^2d^2}{h^2} k_{z,m} d \qquad (4.18c)$$

Equations (4.18b), (4.18c) are similar to (4.11a), (4.9e). Thus, the approximation given for the previous case can be used directly. And, for $h/2d \ll 1$, we shall obtain the same conclusion that the reaction rail works as if it is a nonconducting ferromagnetic material. Thus, it is not suitable for use in the LIM except for levitation purposes only. However, for $h/2\pi d_o \sim 1$, we can use the by now familiar approach to get:

$$\tilde{Z}_L \overset{\sim}{=} \frac{-i\omega\mu_o}{k_z} \frac{1}{1+\frac{\mu_o}{\mu}\frac{-i\sqrt{ih}}{2d}} \tag{4.19a}$$

$$= \frac{-i\omega\mu_o}{k_z} \frac{1+\frac{\mu_o}{2\sqrt{2}\mu}\sqrt{(\omega-k_y v)\mu\sigma h^2}+i\frac{\mu_o}{2\sqrt{2}\mu}\sqrt{(\omega-k_y v)\mu\sigma h^2}}{1+\frac{\mu_o^2}{4\mu^2}(\omega-k_y v)\mu\sigma h^2+\frac{\mu_o}{\sqrt{2}\mu}\sqrt{(\omega-k_y v)\mu\sigma h^2}} \tag{4.19b}$$

$$\tilde{F}_y \overset{\sim}{=} \mathrm{Re}\,\frac{-i\mu_o}{2}\,\mathrm{sgn}(k_y)\,\frac{1}{1+\frac{\mu_o}{\mu}\frac{-i\sqrt{ih}}{2d}}\,|\tilde{K}_x|^2 \tag{4.19c}$$

$$= \frac{\mu_o}{2}\,\mathrm{sgn}(k_y)\,\frac{\frac{\mu_o}{2\sqrt{2}\mu}\sqrt{(\omega-k_y v)\mu\sigma h^2}}{1+\frac{\mu_o^2}{4\mu^2}(\omega-k_y v)\mu\sigma h^2+\frac{\mu_o}{2\sqrt{2}\mu}\sqrt{(\omega-k_y v)\mu\sigma h^2}}\,|\tilde{K}_x|^2 \tag{4.19d}$$

$$\tilde{F}_z = \frac{\mu_o}{4}\,\mathrm{Re}\,\frac{1-\frac{\mu_o^2}{\mu^2}\frac{h^2}{4d^2}}{\left|1+\frac{\mu_o}{\mu}\frac{-i\sqrt{ih}}{2d}\right|^2}\,|\tilde{K}_x|^2 \tag{4.19e}$$

$$= \frac{\mu_o}{4} \frac{1 - \frac{\mu_o^2}{4\mu^2}(\omega - k_y v)\mu\sigma h^2}{1 + \frac{\mu_o^2}{4\mu_o^2}(\omega - k_y v)\mu\sigma h^2 + \frac{\mu_o}{\sqrt{2}\mu}\sqrt{(\omega - k_y v)\mu\sigma h^2}} |\tilde{K}_x|^2 \qquad (4.19f)$$

Again we observe that the magnitude of every term is relatively small compared to the case with $\alpha \cong 0$. It is also noticed that $\tilde{F}_y/|\tilde{K}_x|^2$ is a monotonically decreasing function of both k_y and v, provided that $[(\omega\mu\sigma h^2\mu_o^2)/\mu^2] < 1$ which is generally true. $\tilde{F}_z/|\tilde{K}_x|^2$ is also always positive. The arguments given in the previous case are applicable. The end effect is not serious for this geometry. However, the properties that the power factor and $|\tilde{Z}_L|$ are relatively low (so that the same amount of current can only draw a very small propulsion force) compared to the case with $\alpha \cong 0$ will make this geometry unfavorable.

In the above, we discussed the LIM which has a track with small scale inhomogeneity such that the source only sees an average effect as described above. Of course, different situations are possible. For example, in the LIM built by Rohr Inc., we can put the inserted conductor bars quite far away from each other such that the distances between them are larger than $2\pi/k_{yo}$. Then definitely, the effective $\underset{\sim}{\mu}$ and $\underset{\sim}{\sigma}$ concept fails. However, in this case, it seems that each bar operates independently of the others. This is, of course, a different problem and can be easily solved.

CHAPTER V

THREE-DIMENSIONAL CORRECTIONS

It is obvious that generally the current source and the reaction rail cannot be infinitely extended in the x-direction. Thus, a correction should be made, i.e., a more realistic geometry such as shown in Fig. 5.1a should be investigated. This is a tough three-dimensional problem and there are no simple methods available to handle it. Thus, instead of considering that geometry, we shall look into an alternative geometry as shown in Fig. 5.1b. With a suitable source arrangement, the boundary condition $J_x = 0$ at $x = \pm W_o$ can be satisfied. Thus, within $|x| \leq W_o$, this alternative geometry is supposed to be a good approximation for the original one.

With Maxwell's equations and material properties as introduced in Chapter 2, the Fourier transform method can be used to solve this boundary value problem. Due to the periodicity in the x-direction, in addition to the Fourier transform pair (2.4a),(2.4b), another Fourier series pair (5.1a),(5.1b) is necessary to take care of the x-variation:

$$g(x) = \sum_{n=-\infty}^{\infty} C_n \, e^{i \frac{n\pi x}{2W_o}} \tag{5.1a}$$

$$C_n = \frac{1}{4W_o} \int_{-2W_o}^{2W_o} g(x) \, e^{-i \frac{n\pi x}{2W_o}} \, dx \tag{5.1b}$$

For neither Fourier component can the transfer matrix method be applied any longer. A direct method should be used. First, we can solve the Maxwell's equations in each region, introducing certain unknowns which can be determined by matching the boundary conditions.

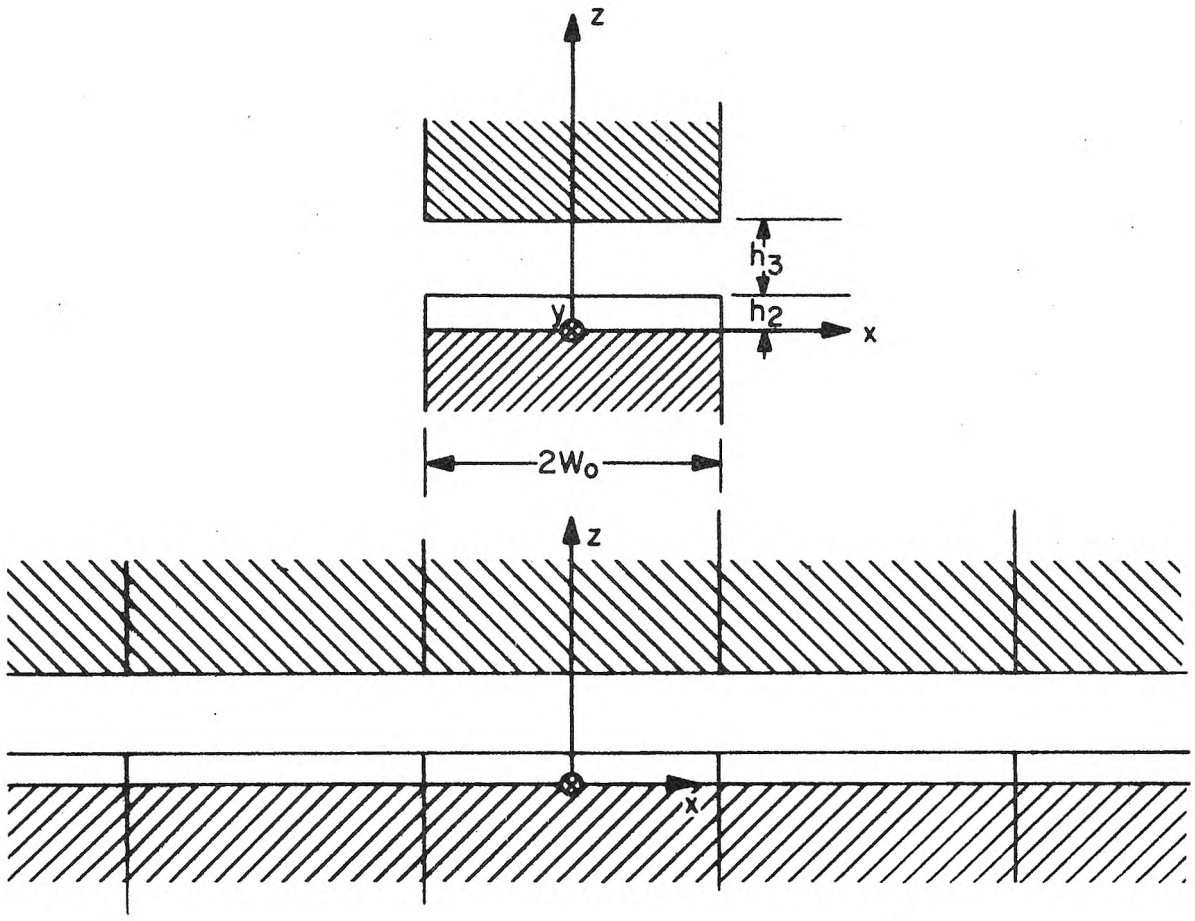

Fig. 5.1a,b

In order to make the problem simpler, only the case $\beta_1 \tilde{=} 0$ will be considered. We have:

Region (2): (i.e., $0 \leq z \leq h_2$)

$$\tilde{E}_{xn} = [\tilde{II}_{xn}^{(1)} \cosh k_{zn}^{(1)} z + \tilde{II}_{xn}^{(2)} \cosh k_{zn}^{(2)} z] \tag{5.2a}$$

$$\tilde{E}_{yn} = [\tilde{II}_{yn}^{(1)} \cosh k_{zn}^{(1)} z + \tilde{II}_{yn}^{(2)} \cosh k_{zn}^{(2)} z] \tag{5.2b}$$

$$\tilde{E}_{zn} = [\tilde{II}_{zn}^{(1)} \sinh k_{zn}^{(1)} z + \tilde{II}_{zn}^{(2)} \sinh k_{zn}^{(2)} z] \tag{5.2c}$$

Here, the following relation also holds:

$$\tilde{II}_{yn}^{(m)} = R_n^{(m)} \tilde{II}_{xn}^{(m)} \tag{5.2d}$$

with

$$R_n^{(m)} = \frac{X_n[\mu_{2y}k_y^2 - \mu_{2z}k_{zn}^{(m)2} - i(\omega - k_y v)\sigma_x\mu_{2y}\mu_{2z}] + \mu_{2x}\mu_{2z}k_{xn}^2 k_{zn}^{(m)2}}{\mu_{2y}\{(k_{xn}k_y + ik_{xn}\sigma_x v\mu_{2z})(\mu_{2x}\mu_{2y}X_n - \mu_{2z}k_{zn}^{(m)2}) - \mu_{2z}k_{zn}^{(m)2} \cdot ik_{xn}v(\mu_{2x}\sigma_z - \sigma_x\mu_{2z})\}} \tag{5.2e}$$

and

$$\tilde{II}_{zn}^{(m)} = \frac{-k_{zn}^{(m)}[i\mu_{2x}k_{xn} + (ik_y - v\mu_{2x}\sigma_z)\mu_{2y}R_n^{(m)}]\,\tilde{II}_{xn}^{(m)}}{\mu_{2x}\mu_{2y}X_n} \tag{5.2f}$$

where $m=1,2$ and $k_{xn} = \frac{n\pi}{2W_o}$

$$X_n = \frac{k_{xn}^2}{\mu_{2y}} + \frac{k_y^2}{\mu_{2x}} - i(\omega - k_y v)\,\sigma_z \tag{5.2g}$$

and $k_{zn}^{(m)2}$ are the roots of

$$k_{zn}^4 - \{[\frac{\sigma_x}{\sigma_z} k_{xn}^2 + \frac{\sigma_y}{\sigma_z} k_y^2 + \frac{\mu_{2y}}{\mu_{2z}} k_y^2 + \frac{\mu_{2x}}{\mu_{2z}} k_{xn}^2] - i(\omega - k_y v)(\sigma_x \mu_{2y} + \sigma_y \mu_{2x})\} k_{zn}^2$$

$$+ \frac{\mu_{2x}\mu_{2y}}{\mu_{2z}\sigma_z} \chi_n [\sigma_x k_{xn}^2 + \sigma_y k_y^2 - i(\omega - k_y v)\sigma_x \sigma_y \mu_{2z}] = 0 \qquad (5.2h)$$

From (5.2), (2.1), it follows:

$$i\omega \tilde{B}_{xn} = (ik_y \tilde{II}_{zn}^{(1)} - k_{zn}^{(1)} \tilde{II}_{yn}^{(1)}) \sinh k_{zn}^{(1)} z + (ik_y \tilde{II}_{zn}^{(2)} - k_{zn}^{(2)} \tilde{II}_{yn}^{(2)}) \sinh k_{zn}^{(2)} z \qquad (5.3a)$$

$$i\omega \tilde{B}_{yn} = (k_{zn}^{(1)} \tilde{II}_{xn}^{(1)} - ik_{xn} \tilde{II}_{zn}^{(1)}) \sinh k_{zn}^{(1)} z + (k_{zn}^{(2)} \tilde{II}_{xn}^{(2)} - ik_{xn} \tilde{II}_{zn}^{(2)}) \sinh k_{zn}^{(z)} z \qquad (5.3b)$$

$$i\omega \tilde{B}_{zn} = (ik_{xn} \tilde{II}_{yn}^{(1)} - ik_y \tilde{II}_{xn}^{(1)}) \cosh k_{zn}^{(1)} z + (ik_{xn} \tilde{II}_{yn}^{(2)} - ik_y \tilde{II}_{xn}^{(2)}) \cosh k_{zn}^{(2)} z \qquad (5.3c)$$

Using the boundary condition:

$$[\underset{\sim}{\sigma} \cdot (\underline{\tilde{E}}_n + \underline{v} \times \underline{\tilde{B}}_n)]_z = 0 \quad \text{at} \quad z = h_2$$

we obtain:

$$\frac{\tilde{II}_{xn}^{(2)}}{\tilde{II}_{xn}^{(1)}} = \frac{-k_{zn}^{(1)} \sinh k_{zn}^{(1)} h_2 [(\omega - k_y v)\mu_{2x} k_{xn} + R_n^{(1)} (\omega \mu_{2y} k_y + v\mu_{2x} k_{xn}^2)]}{k_{zn}^{(2)} \sinh k_{zn}^{(2)} h_2 [(\omega - k_y v)\mu_{2x} k_{xn} + R_n^{(2)} (\omega \mu_{2y} k_y + v\mu_{2x} k_{xn}^2)]} \qquad (5.4)$$

In region (3), (i.e., $h_2 \leq z \leq h_2 + h_3$):

$$\tilde{B}_{xn} = \tilde{\tilde{\tilde{III}}}^{(1)}_{xn} e^{-k_{zn}(z-h_2)} + \tilde{\tilde{\tilde{III}}}^{(2)}_{xn} e^{k_{zn}(z-h_2)} \tag{5.5a}$$

$$\tilde{B}_{yn} = \tilde{\tilde{\tilde{III}}}^{(1)}_{yn} e^{-k_{zn}(z-h_2)} + \tilde{\tilde{\tilde{III}}}^{(2)}_{yn} e^{k_{zn}(z-h_2)} \tag{5.5b}$$

$$\tilde{B}_{zn} = \tilde{\tilde{\tilde{III}}}^{(1)}_{zn} e^{-k_{zn}(z-h_2)} + \tilde{\tilde{\tilde{III}}}^{(2)}_{zn} e^{k_{zn}(z-h_2)} \tag{5.5c}$$

where $k_{zn}^2 = k_{xn}^2 + k_y^2$ and

$$\tilde{\tilde{\tilde{III}}}^{(1)}_{yn} = \frac{k_y}{k_{xn}} \tilde{\tilde{\tilde{III}}}^{(1)}_{xn} \tag{5.5d}$$

$$\tilde{\tilde{\tilde{III}}}^{(1)}_{zn} = i \frac{k_{zn}}{k_{xn}} \tilde{\tilde{\tilde{III}}}^{(1)}_{xn} \tag{5.5e}$$

$$\tilde{\tilde{\tilde{III}}}^{(2)}_{yn} = \frac{k_y}{k_{xn}} \tilde{\tilde{\tilde{III}}}^{(2)}_{xn} \tag{5.5f}$$

$$\tilde{\tilde{\tilde{III}}}^{(2)}_{zn} = - \frac{ik_{zn}}{k_{xn}} \tilde{\tilde{\tilde{III}}}^{(2)}_{xn} \tag{5.5g}$$

Now we match the boundary conditions at $z = h_2$. The continuity of $\tilde{H}_{xn}$ and the relations above give us:

$$\tilde{\tilde{\tilde{III}}}^{(1)}_{xn} + \tilde{\tilde{\tilde{III}}}^{(2)}_{xn} = - A_{2n} \tilde{\tilde{II}}^{(1)}_{xn} \tag{5.6a}$$

with

$$A_{2n} = \frac{\mu_o k_{zn}^{(1)} \sinh k_{zn}^{(1)} h_2 (k_{xn}) (R_n^{(1)} - R_n^{(2)})}{i[(\omega - k_y v)\mu_{2x} k_{xn} + R_n^{(2)} (\omega \mu_{2y} k_y + v \mu_{2x} k_{xn}^2)]} \tag{5.6b}$$

The continuity of $\tilde{B}_{zn}$ and the previous relations also give us:

$$\tilde{\tilde{\tilde{III}}}^{(1)}_{xn} - \tilde{\tilde{\tilde{III}}}^{(2)}_{xn} = - A_{1n} \tilde{\tilde{II}}^{(1)}_{x} \tag{5.7a}$$

with

$$A_{1n} = \frac{-k_{xn}}{\omega k_{zn}} [(ik_{xn}R_n^{(1)} - ik_y)\cosh k_{zn}^{(1)}h_2 - (ik_{xn}R_n^{(2)} - ik_y)\cosh k_{zn}^{(2)}h_z$$

$$+ \frac{k_z^{(1)}\sinh k_z^{(1)}h_2}{k_{zn}^{(2)}\sinh k_z^{(2)}h_z} \frac{(\omega-k_yv)\mu_{2x}k_{xn} + R_n^{(1)}(\omega\mu_{2y}k_y + v\mu_{2x}k_{xn}^2)}{(\omega-k_yv)\mu_{2x}k_{xn} + R_n^{(2)}(\omega\mu_{2y}k_y + v\mu_{2x}k_{xn}^2)}] \quad (5.7b)$$

so,

$$\tilde{\tilde{\tilde{\tilde{III}}}}_{xn}^{(1)} = - \frac{A_{1n} + A_{2n}}{A_{1n} - A_{2n}} \tilde{\tilde{\tilde{\tilde{III}}}}_{xn}^{(2)} \quad (5.8)$$

Furthermore, using $\hat{e}_z x[\tilde{\underline{H}}(h_2+ h_3+ \varepsilon) - \tilde{\underline{H}}(h_2+ h_3- \varepsilon)] = \tilde{\underline{K}}(h_2+ h_3)$, we get:

(i) $\beta_4 \tilde{=} 0$, i.e., $\tilde{\underline{H}}(h_2+ h_3+ \varepsilon) = 0$

$$\tilde{\tilde{\tilde{\tilde{III}}}}_{xn}^{(2)} = \frac{\mu_o k_{xn}}{k_y} \tilde{K}_{xn} e^{-k_{zn}h_3} \frac{1}{1 - \frac{A_{1n} + A_{2n}}{A_{1n} - A_{2n}} e^{-2k_{zn}h_3}} \quad (5.9a)$$

$$\tilde{B}_{zn}(h_2+ h_3) = \frac{-\mu_o k_{zn} i}{k_y} \frac{1 + \frac{A_{1n} + A_{2n}}{A_{1n} - A_{2n}} e^{-2k_{zn}h_3}}{1 - \frac{A_{1n} + A_{2n}}{A_{1n} - A_{2n}} e^{-2k_{zn}h_3}} \tilde{K}_{xn} \quad (5.9b)$$

$$\tilde{B}_{xn}(h_2+ h_3- \varepsilon) = \frac{k_{xn}}{k_y} \tilde{B}_{yn}(h_2+ h_3- \varepsilon) = \mu_o \frac{k_{xn}}{k_y} \tilde{K}_{xn} \quad (5.9c)$$

(ii) $\beta_4 = \beta_3$:

$$\tilde{\tilde{\tilde{III}}}^{(2)}_{xn} = \frac{\mu_o k_{xn}}{2k_y} e^{-k_{zn}h_3} \tilde{K}_{xn} \tag{5.10a}$$

$$\tilde{B}_{zn}(h_2+ h_3) = \frac{-i\mu_o k_{zn}}{2k_y} \left[1 + \frac{A_{1n}+ A_{2n}}{A_{1n}- A_{2n}} e^{-2k_{zn}h_3}\right] \tilde{K}_{xn} \tag{5.10b}$$

$$\tilde{B}_{xn}(h_2+ h_3- \varepsilon) = \frac{k_{xn}}{k_y} \tilde{B}_{yn}(h_2+ h_3- \varepsilon) = \frac{\mu_o k_{xn}}{2k_y} \times \left[1 - \frac{A_{1n}+ A_{2n}}{A_{1n}- A_{2n}} e^{-2k_{zn}h_3}\right] \tilde{K}_{xn} \tag{5.10c}$$

Now all of the field distributions can be obtained. The machine performances can be calculated by using (2.17), (2.27), (2.28), (2.29), etc. Among these we shall now consider only $\bar{F}_x$, $\bar{F}_y$ which are the simplest and the most important.

$$\bar{F}_x = \frac{1}{2} \mathrm{Re}\left\{ \sum_{n=-\infty}^{\infty} \sum_{m=-\infty}^{\infty} \frac{4W_o \sin(m-n)\frac{\pi}{2}}{(m-n)\pi} \int_{-\infty}^{\infty} \tilde{B}_z(h_2+h_3,n) \frac{k_{xm}}{k_y} \tilde{K}^*_{xm}(k_y)dk_y \right\} \tag{5.11a}$$

$$\bar{F}_y = \frac{1}{2} \mathrm{Re}\left\{ \sum_{n=-\infty}^{\infty} \sum_{m=-\infty}^{\infty} \frac{4W_o \sin(m-n)\frac{\pi}{2}}{(m-n)\pi} \int_{-\infty}^{\infty} B_z(h_2+h_3,n) \tilde{K}^*_{xm}(k_y)dk_y \right\} \tag{5.11b}$$

These formulas are still too complicated to evaluate. We shall simplify them even more by assuming the medium in region 2 to be isotropic; then,

$$\frac{A_{1n}+ A_{2n}}{A_{1n}- A_{2n}} = \frac{1 - \frac{\mu_o \gamma_{2n}}{\mu k_{zn}} \tanh \gamma_{2n}h_2}{1 + \frac{\mu_o \gamma_{2n}}{\mu k_{zn}} \tanh \gamma_{2n}h_2} \tag{5.12a}$$

with

$$\gamma_{2n}^2 = k_{zn}^2 - i(\omega - k_y v)\mu\sigma \tag{5.12b}$$

After some manipulations, it can be found that:

$$\bar{F}_x = \mathrm{Re}\Big\{ \sum_{n=-\infty}^{n=\infty} \sum_{m=-\infty}^{\infty} \frac{4W_o \sin\frac{(m-n)\pi}{2}}{(m-n)\pi} \int_{-\infty}^{\infty} \tilde{F}(n)\, \tilde{K}_{xn}(k_y)\, \tilde{K}_{xm}^*(k_y) \frac{k_{xm}}{k_y}\, dk_y \Big\} \tag{5.13a}$$

$$\bar{F}_y = \mathrm{Re}\Big\{ \sum_{n=-\infty}^{\infty} \sum_{m=-\infty}^{\infty} \frac{4W_o \sin\frac{(m-n)\pi}{2}}{(m-n)\pi} \int_{-\infty}^{\infty} \tilde{F}(n)\, \tilde{K}_{xn}(k_y)\, \tilde{K}_{xm}^*(k_y)\, dk_y \Big\} \tag{5.13b}$$

where

$$\tilde{F}(n) = -\frac{i\mu_o}{2} \frac{k_{zn}}{k_y} \frac{1 + \frac{\mu_o \gamma_{2n}}{\mu k_{zn}} \tanh \gamma_{2n} h_2 \tanh k_{zn} h_3}{\tanh k_{zn} h_3 + \frac{\mu_o \gamma_{2n}}{\mu k_{zn}} \tanh \gamma_{2n} h_2} \quad \text{for } \beta_4 \neq 0 \tag{5.13c}$$

$$+ \frac{-i\mu_o}{4} \frac{k_{zn}}{k_y} \left[1 + \frac{1 - \frac{\mu_o \gamma_{2n}}{\mu k_{zn}} \tanh \gamma_{2n} h_2}{1 + \frac{\mu_o \gamma_{2n}}{\mu k_{zn}} \tanh \gamma_{2n} h_2} e^{-2k_{zn} h_3}\right] \quad \text{for } \beta_4 = \beta_3 \tag{5.13d}$$

Here $\tilde{F}(n)$ is an even function of n.

Now we take the source distribution into account. In order to make $J_x = 0$ at $x = \pm W_o$ within the reaction rail, the following extended periodic source current distribution $J_x^{\ell}(x,y)$ is necessary:

$$J_x^{\ell}(x,y) = J_x(x,y) \quad \text{for } |x| \leq W_o \tag{5.14a}$$

$$-J_x(2W_o - x, y) \quad \text{for } W_o \leq x \leq 2W_o \tag{5.14b}$$

$$-J_x(-2W_o - x, y) \quad \text{for } -W_o \geq x \geq -2W_o \tag{5.14c}$$

Thus, $$\tilde{K}_{xn}(y) = \frac{1}{4W_o} \int_{-2W_o}^{2W_o} J_x^{\ell}(x,y)\, e^{-\frac{i\pi nx}{2W_o}}\, dx$$

$$= \frac{1}{4W_o} \left\{ \int_{-W_o}^{W_o} J_x(x,y)\, e^{-\frac{in\pi x}{2W_o}}\, dx - (-1)^n \int_{-W_o}^{W_o} J_x(x,y) e^{i\frac{n\pi x}{2W_o}}\, dx \right\}$$

$$= \frac{1}{4W_o}\, 2 \int_{-W_o}^{W_o} J_x(x,y) \cos \frac{n\pi x}{2W_o}\, dx \qquad \text{for n odd} \qquad (5.15a)$$

$$(-2i) \int_{-W_o}^{W_o} J_x(x,y) \sin \frac{n\pi x}{2W_o}\, dx \qquad \text{for n even} \qquad (5.15b)$$

$$0 \qquad \text{for } n = 0 \qquad (5.15c)$$

Applying (5.15) to (5.13), we have:

$$\bar{F}_x = \mathrm{Re} \sum_{n\neq 0} \sum_{\substack{n+m \\ \text{odd}}} \frac{4W_o \sin \frac{(m-n)\pi}{2}}{(m-n)\pi} \int_{-\infty}^{\infty} \tilde{F}(n)\, \tilde{K}_{xn}(k_y) \tilde{K}_{xm}^*(k_y) \frac{k_{xm}}{k_y}\, dk_y \qquad (5.16a)$$

$$\bar{F}_y = \mathrm{Re} \sum_{n\neq 0} 2W_o \int_{-\infty}^{\infty} \tilde{F}(n)\, \tilde{K}_{xn}(k_y) \tilde{K}_{xn}^*(k_y)\, dk_y \qquad (5.16b)$$

So, if $J_x(x,y)$ is neither even nor odd, there is a possibility that a lateral force exists.

Now let us consider one example. The case $\beta_4 \tilde{=} 0$ will be analyzed. We shall assume that the reaction rail is thin such that, for small n, $|\gamma_{2n} h_2| \ll 1$ and $k_{zn} h_3 \ll 1$ are true. Then, for small n:

$$\tilde{F}(n) \cong \frac{-i\mu_o}{2} \frac{1}{k_y} \frac{\mu k_{zn}^2}{\mu k_{zn}^2 h_3 + \mu_o \gamma_{2n}^2 h_2} \tag{5.17}$$

Also, in order to compare this with the two-dimensional case, we shall assume that $J_x(x,y)$ is uniformly distributed for $|x| \leq a$. Then,

$$\tilde{K}_{xn}(k_y) = \begin{cases} \frac{2}{n\pi} \sin \frac{n\pi a}{2W_o} \tilde{K}_x(k_y) & n \text{ odd} \\ 0 & \text{otherwise} \end{cases} \tag{5.18}$$

Here $\tilde{K}_x(k_y)$ is introduced to take care of the y-variation. Of course, we get a zero lateral force. As for $\bar{F}_y$, we have:

$$\bar{F}_y \cong \sum_{\text{odd}} 2W_o \int_{-\infty}^{\infty} \frac{1}{2} \frac{1}{k_y} \frac{(k_y^2 + \frac{n^2\pi^2}{4W_o^2})(\omega - k_y v)}{(k_y^2 + \frac{n^2\pi^2}{4W_o^2})^2 + (\omega - k_y v)^2 K_1^2} \frac{K_1^2}{\sigma h_2}$$

$$\cdot \frac{4}{n^2\pi^2} \sin^2 \frac{n\pi a}{2W_o} |\tilde{K}_x(k_y)|^2 \, dk_y \tag{5.19}$$

The "n" summation can be evaluated by using several series summation formulae

$$\bar{F}_y \cong \int_{-\infty}^{\infty} \frac{2a}{2} \frac{\omega - k_y v}{\sigma k_y} \frac{K_1^2}{h_2} \text{Re}\left\{\frac{1}{\gamma_2^2}\left[1 - \frac{1}{\gamma_2 a} \frac{\tanh \gamma_2 a}{1 + \tanh \gamma_2 a \tanh \gamma_2 (W_o - a)}\right]\right\}$$

$$\cdot |\tilde{K}_x(k_y)|^2 dk_y \tag{5.20a}$$

where

$$\gamma_2^2 = k_y^2 - i(\omega - k_y v) K_1 \tag{5.20b}$$

A remark should be made here. Obviously, for large n the conditions $|\gamma_{2n}h_2| << 1$, $k_{zn}h_3 << 1$ are not satisfied and the approximation (5.17) is not valid any more. However, for large n the force contribution as given by (5.13) is small and so is the invalid approximation (5.17). Hence, using (5.17) for large n (which was derived using the thin reaction rail approximation) will only introduce a small error in the expression of the total force and we may conclude that (5.17) is a fairly good approximation for all n .

If the y-variation of J_x is the same as that of the idealistic source for the two-dimensional case, $\tilde{K}_x(k_y)$ will be given by $\sqrt{2\pi}\,\delta(k_y-k_{yo})$. Of course, (5.20) will give us an infinite force. However, for the force of unit length in the y-direction, we go back to the original force equation in real space to get:

$$\frac{\bar{F}_y}{\text{unit length}} \cong \frac{2a}{2}\,\frac{\omega-k_{yo}v}{k_{yo}}\,\frac{K_1^2}{\sigma h_2}\,\mathrm{Re}\Big\{\frac{1}{\gamma_{20}^2}\Big[1-\frac{1}{\gamma_{20}\,a}\times\frac{\tanh\gamma_{20}a}{1+\tanh\gamma_{20}a\,\tanh\gamma_{20}(W_o-a)}\Big]\Big\}\,K_o^2 \qquad (5.21a)$$

where

$$\gamma_{20}^2 = k_{yo}^2 - i(\omega-k_{yo}v)K_1 \qquad (5.21b)$$

If, furthermore, we assume $(\omega-k_{yo}v)K_1 << k_{yo}^2$, then (5.21) reduces to:

$$\frac{\bar{F}_y}{\text{unit length}} \cong \frac{2a}{2}\,\frac{\omega-k_{yo}v}{k_{yo}}\,\frac{K_1^2}{\sigma h_2}\,\frac{1}{k_{yo}^2}\Big[1-\frac{1}{k_{yo}a}\,\frac{\tanh k_{yo}a}{1+\tanh k_{yo}a\,\tanh k_{yo}(W_o-a)}\Big]K_o^2 \qquad (5.22)$$

Comparing this to (3.8), we can say the finite width reaction rail has an effective conductivity of

$$\sigma[1 - \frac{1}{k_{yo}a} \frac{\tanh k_{yo}a}{1 + \tanh k_{yo}a \tanh k_{yo}(W_o-a)}]$$

This is exactly the same conclusion as Russell and Norsworthy[23] made, using another approach. Also, it is observed that the propulsion force is reduced. The increase of "a" will generally reduce this so-called lateral end effect.

Of course, the above condition $(\omega-k_{yo}v)\ K_1 << k_{yo}^2$ is generally not true. Then, we cannot introduce the effective conductivity concept any more. However, by comparing with (3.8), we can see the lateral end effect will change the propulsion force by an amount:

$$\frac{-2(\omega-k_{yo}v)}{k_{yo}} \frac{K_1^2}{2\sigma h_2} \mathrm{Re}\{\frac{1}{\gamma_{20}^3} \frac{\tanh \gamma_{20}a}{1 + \tanh \gamma_{20}a \tanh \gamma_{20}(W_o-a)}\} \qquad (5.23)$$

From this complicated expression we cannot conclude whether this term will decrease or increase the propulsion force. Assuming $|\gamma_{20}a| \gtrsim \pi$ and $|\gamma_{20}(W_o-a)| << 1$, (5.23) becomes:

$$\frac{-2(\omega-k_{yo}v)}{k_{yo}} \frac{K_1^2}{2\sigma h_2} \mathrm{Re} \frac{1}{[k_{yo}^2 - i(\omega-k_{yo}v)K_1]^{3/2}} \qquad (5.24a)$$

Or, we can assume both $|\gamma_{20}a|$ and $|\gamma_{20}(W_o-a)| \gtrsim \pi$ to get:

$$- \frac{2(\omega-k_{yo}v)}{k_{yo}} \frac{K_1^2}{2\sigma h_2} \mathrm{Re} \frac{1}{2[k_{yo}^2 - i(\omega-k_{yo}v)K_1]^{3/2}} \qquad (5.24b)$$

Thus, if $\frac{(\omega-k_{yo}v)K_1}{k_{yo}^2} > \sqrt{3}$, (5.24) will be positive, i.e., the lateral end effect will increase the propulsion force. Unfortunately, at the maximum force point, $\frac{\omega-k_{yo}v}{k_{yo}^2} K_1 = 1$. Thus, the lateral end effect will reduce the propulsion force at that point.

For the more general source $|\tilde{K}_x(k_y)|^2 = \frac{2}{\pi} \frac{\sin^2(k_y-k_{yo})L}{(k_y-k_{yo})^2}$, we can try to evaluate the integral (5.20). However, due to the presence of the term γ_{20}^3, the integral is too tough to evaluate. However, a change of propulsion force can always be observed, namely

$$-\mathrm{Re}\int_{-\infty}^{\infty} \frac{\omega-k_y v}{k_y} \frac{2K_1^2}{2\sigma h_2} \frac{1}{\gamma_2^3} \frac{\tanh \gamma_2 a}{1+\tanh \gamma_2 a \tanh \gamma_2(W_o-a)} \frac{2K_o^2}{\pi} \times \frac{\sin^2(k_y-k_{yo})L}{(k_y-k_{yo})^2}\, dk_y \qquad (5.25)$$

(The main term is just given by (3.30b) except for a factor of "a").

Now, again using the assumptions $|\gamma_2 a| \gtrsim \pi$, $|\gamma_2(\omega_o-a)| \ll 1$, we simplify (5.25) and get (5.26). The same expression (5.26) can also be used for another situation with both $|\gamma_2 a|$ and $|\gamma_2(W_o-a)| \gtrsim \pi$, except that now a factor 1/2 should be introduced:

$$-\mathrm{Re}\int_{-\infty}^{\infty} \frac{\omega-k_y v}{k_y} \frac{2K_1^2}{\sigma_x h_2} \frac{K_o^2}{\pi} \frac{1}{\gamma_2^3} \frac{\sin^2(k_y-k_{yo})L}{(k_y-k_{yo})^2}\, dk_y \qquad (5.26)$$

Note that, if the source function is not suitably constructed the singularity at $k_y = 0$ will possibly give an infinite force and also infinite power input, which is not practical. Thus $\sin k_{yo}L = 0$ is always necessary to get rid of this singularity.

As for the idealized source case, the integrand will be positive in the region where $\frac{(\omega-k_y v)K_1}{k_y^2} > \sqrt{3}$ and negative in the remaining region, $0 < \frac{(\omega-k_y v)K_1}{k_y^2} < \sqrt{3}$. Thus, if k_{yo} belongs to the negative region, a smaller propulsion force than in the two-dimensional case will be obtained. Because an odd power of γ_{20} appears in the above integral, two extra branch points in the complex k_y plane should be introduced, making the integral extremely hard to evaluate. In order to obtain an explicit formula for the force, we shall go back to the original series formulation (5.19). For each "n", an integral of the following form should be computed:

$$\int_{-\infty}^{\infty} \frac{\omega-k_y v}{k_y} \frac{k_y^2 + \frac{n^2\pi^2}{4W_o^2}}{(k_y^2 + \frac{n^2\pi^2}{4W_o^2})^2 + (\omega-k_y v)^2 K_1^2} \frac{\sin^2(k_y-k_{yo})L}{(k_y-k_{yo})^2} \, dk_y \qquad (5.27)$$

We know that for the two-dimensional case, the F_y force is proportional to the above integral with $n=0$. Now for $n \neq 0$, suppose that $K_1 \frac{\omega-k_{yo}v}{k_{yo}^2} < 1$; then the integral will generally be smaller than the two-dimensional case (corresponding to $n=0$). Thus, this lateral end effect will reduce the propulsion force even more. However, if $\frac{\omega-k_{yo}v}{k_{yo}^2} K_1 > 1$, there is a possibility that the lateral end effect will compensate the longitudinal end effect. Actually, it had already been found that the overall critical point should be around $\frac{(\omega-k_{yo}v)}{k_{yo}^2} K_1 = \sqrt{3}$.

The factorization of

$$\frac{\omega-k_y v}{k_y}\,\frac{k_y^2+\dfrac{n^2\pi^2}{4W_o^2}}{\left(k_y^2+\dfrac{n^2\pi^2}{4W_o^2}\right)^2+(\omega-k_y v)^2\,K_1^2}$$

will lead to integrals of the form

$$\int_{-\infty}^{\infty}\frac{1}{p-p_o}\,\frac{\sin^2 p}{p^2}\,dp\ .$$

In Appendix C this integral is worked out.

Also, integrals of the form

$$\int_{-\infty}^{\infty}\frac{1}{k_y}\,\frac{\sin^2(k_y-k_{yo})L}{(k_y-k_{yo})^2}\,dk_y$$

will appear. These integrals need further consideration. They will give an infinite result unless $\sin k_{yo}L = 0$. If this condition is satisfied, we easily get from Appendix C:

$$\int_{-\infty}^{\infty}\frac{1}{k_y}\,\frac{\sin^2(k_y-k_{yo})L}{(k_y-k_{yo})^2}\,dk_y = \frac{L}{k_{yo}} \tag{5.28}$$

Finally, we have

$$\overline{F}_y \cong \sum_{n=1,3,5} \frac{8W_o}{n^2\pi^2}\sin^2\frac{n\pi a}{2W_o}\,\frac{2K_1^2}{\pi\sigma h_2}\,\mathrm{Re}\left\{\frac{\pi L}{k_{yo}}\,\frac{\omega}{\alpha_1\alpha_2}+\frac{\omega-\alpha_1 v}{\alpha_1(\alpha_1-\alpha_2)}\,S_1(\alpha_1,k_{yo},L)\right.$$

$$\left.+\frac{\omega-\alpha_2 v}{\alpha_2(\alpha_2-\alpha_1)}\,S_1(\alpha_1,k_{yo},L)\right\} \tag{5.29a}$$

where α_1,α_2 are roots of $k_y^2+\dfrac{n^2\pi^2}{4W_o^2}-i(\omega-k_y v)K_1 = 0$.

or:

$$\alpha_1 = \frac{-i(K_1 v - b) + c}{2} \tag{5.29b}$$

$$\alpha_2 = \frac{-i(K_1 v + b) - c}{2} \tag{5.29c}$$

with

$$c = \sqrt{\frac{K_1^2 v^2 + \frac{n^2\pi^2}{W_o^2}}{2}} \left[-1 + \sqrt{1 + \frac{16\omega^2 K_1^2}{(K_1^2 v^2 + \frac{n^2\pi^2}{W_o^2})^2}} \right]^{1/2}$$

$$b = \sqrt{\frac{K_1^2 v^2 + \frac{n^2\pi^2}{W_o^2}}{2}} \left[1 + \sqrt{1 + \frac{16\omega^2 K_1^2}{(K_1^2 v^2 + \frac{n^2\pi^2}{W_o^2})^2}} \right]^{1/2}$$

Now, let us consider the case that the originally symmetrical source is shifted over a distance ε to the right, i.e., we consider a source current distribution:

$$J_x(x,y) = \begin{cases} J_x(y) & \text{for } -a+\varepsilon \leq x \leq a+\varepsilon \\ 0 & \text{elsewhere} \end{cases} \tag{5.30a}$$

The corresponding Fourier components are then found to be:

$$\tilde{K}_{xn}(y) = \begin{cases} \frac{2}{n\pi} \sin \frac{n\pi a}{2W_o} \cos \frac{n\pi\varepsilon}{2W_o} \tilde{K}_x(y) & \text{for n odd} \\ \frac{2}{n\pi} \sin \frac{n\pi a}{2W_o} \sin \frac{n\pi\varepsilon}{2W_o} \tilde{K}_x(y) & \text{for n even} \end{cases} \tag{5.30b}$$

By using (5.16), the force components for the idealized source will be given as:

$$\frac{\bar{F}_y}{\text{unit length}} = \sum_{n=1,3,5} \frac{16W_o K_o^2}{n^2\pi^2} \sin^2 \frac{n\pi a}{2W_o} \cos^2 \frac{n\pi\varepsilon}{2W_o} \tilde{F}_r(n)$$

$$+ \sum_{n=2,4,6} \frac{16W_o K_o^2}{n^2\pi^2} \sin^2 \frac{n\pi a}{2W_o} \sin^2 \frac{n\pi\varepsilon}{2W_o} \tilde{F}_r(n) \qquad (5.31a)$$

$$\frac{\bar{F}_x}{\text{unit length}} = \sum_{n=2,4,6} \sum_{m=1,3,5} \frac{-8(-1)^{n/2}(1)^{\frac{m-1}{2}} K_o^2}{(m^2-n^2)\pi^2 k_{yo}}$$

$$\times \left(4 \sin \frac{n\pi a}{2W_o} \sin \frac{n\pi\varepsilon}{2W_o} \sin \frac{m\pi a}{2W_o} \cos \frac{m\pi\varepsilon}{2W_o}\right) [\tilde{F}_r(n) + \tilde{F}_r(m)] \qquad (5.31b)$$

Here $\tilde{F}_r(n)$ represents the real part of $\tilde{F}(n)$:

$$\tilde{F}_r(n) \cong \frac{K_1^2}{2\sigma h_2} \frac{\omega - k_{yo}v}{k_{yo}} \frac{k_{yo}^2 + \frac{n^2\pi^2}{4W_o^2}}{(k_{yo}^2 + \frac{n^2\pi^2}{4W_o^2})^2 + (\omega - k_{yo}v)^2 K_1^2} \qquad (5.31c)$$

Going through complicated series summation procedures, we get the explicit forms for $\tilde{F}_y$ and $\tilde{F}_x$:

$$\frac{\bar{F}_y}{\text{unit length}} \cong \frac{aK_1^2 K_o^2}{\sigma h_2} \frac{\omega - k_{yo}v}{k_{yo}} \text{Re}\{\frac{1}{\gamma_{20}^2} [1 - \frac{\cosh^2 \gamma_{20}\varepsilon}{\gamma_{20}a}$$

$$\times \frac{\tanh \gamma_{20}a}{1 + \tanh \gamma_{20}a \tanh \gamma_{20}(W_o - a)} + \frac{\sinh^2 \gamma_{20}\varepsilon}{\gamma_{20}a} \frac{\tanh \gamma_{20}a}{1 + \tanh \gamma_{20}a \coth \gamma_{20}(W_o - a)}]\} \qquad (5.32a)$$

$$\frac{\bar{F}_x}{\text{unit length}} \simeq \frac{K_0^2 K_1^2}{\sigma h_2} \frac{(\omega - k_{yo} v)}{k_{yo}^2} \text{Re}\{\frac{1}{\gamma_{20}^2} [\sinh^2 \gamma_{20}\varepsilon - \frac{\sinh 2\gamma_{20}\varepsilon \tanh \gamma_{20} a}{1 + \tanh \gamma_{20} a \coth \gamma_{20}(2W_o - a)}]\} \quad (5.32b)$$

If $\gamma_{20}(W_o - a) \gtrsim \pi$, then $\tanh \gamma_{20}(W_o - a) \simeq \coth \gamma_{20}(W_o - a)$, and (5.32a) reduces to (5.21a); i.e., when the region which is not covered by the source is large, the influence of the shift on $\bar{F}_y$ will be small. Let us now look at the more practical case of $|\gamma_2(W_o - a)| \ll 1$, $|\gamma_{20}\varepsilon| \ll 1$. Then, after retaining only first order terms in the hyperbolic functions, we have:

$$\frac{\bar{F}_y}{\text{unit length}} \simeq \frac{K_1^2 a K_o^2}{\sigma h_2} \frac{\omega - k_{yo} v}{k_{yo}} \text{Re}\{\frac{1}{\gamma_{20}^2} [1 - \frac{1}{\gamma_{20} a} + \frac{\gamma_{20}^2 \varepsilon^2}{a} (W_o - a)]\} \quad (5.33)$$

By comparing this with formula (5.21), it is seen that there is always an increase of the propulsion force by the amount of $\frac{K_1^2 K_o^2}{2\sigma h_2} \frac{\omega - k_{yo} v}{k_{yo}} \varepsilon^2 (W_o - a)$.

As for the lateral force, because $|\gamma_{20} a| \gtrsim \pi$ and $|\gamma_{20} W_o| \gtrsim \pi$ generally hold, (5.32b) reduces to:

$$\frac{\bar{F}_x}{\text{unit length}} \simeq \frac{-K_1^2 K_o^2}{\sigma h_2} \frac{\omega - k_{yo} v}{k_{yo}^2} \text{Re}\{\frac{1}{2\gamma_{20}^2} (1 - e^{-2\gamma_{20}\varepsilon})\} \quad (5.34)$$

Thus, if $|\gamma_{20}\varepsilon|$ is large enough, there is a possibility that a huge lateral force in the same order as that of the propulsion force is obtained. Of course, for the practical machine operation, this

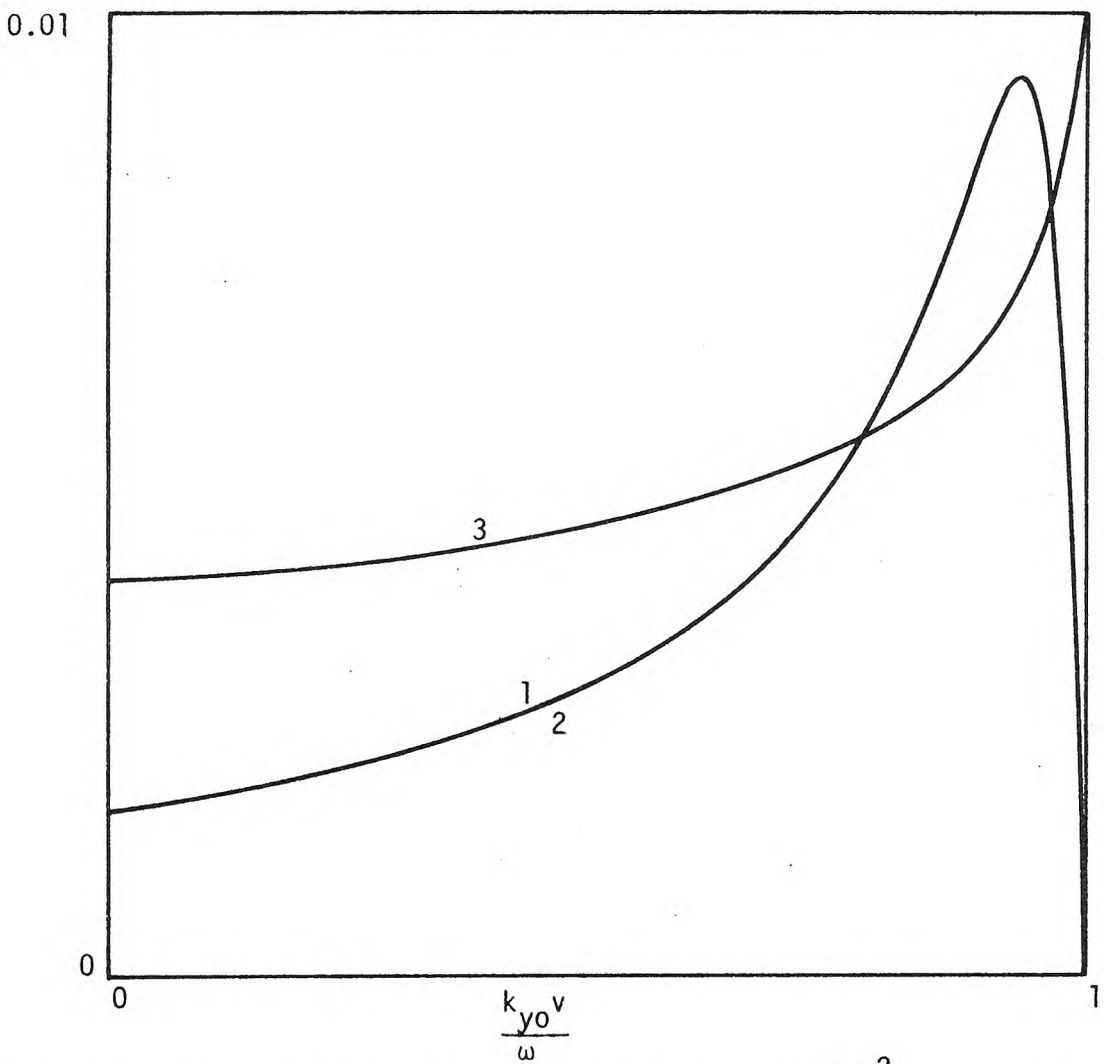

Fig. 5.2 Curves (1) and (2) represent $(5.31a)/(\frac{5K_1K_o^2}{2\ x h_2})$ for $\varepsilon = 0$ and $\varepsilon = 0.01$m, respectively;

Curve (3) represents $[(5.31b)/(\frac{K_1K_o^2}{\sigma_x h_2})] + 1$ for $\varepsilon = 0.01$m.

Here $W_o = 0.3$m and $a = 0.28$m. All parameters except ε are the same as those of Fig. 3.2.

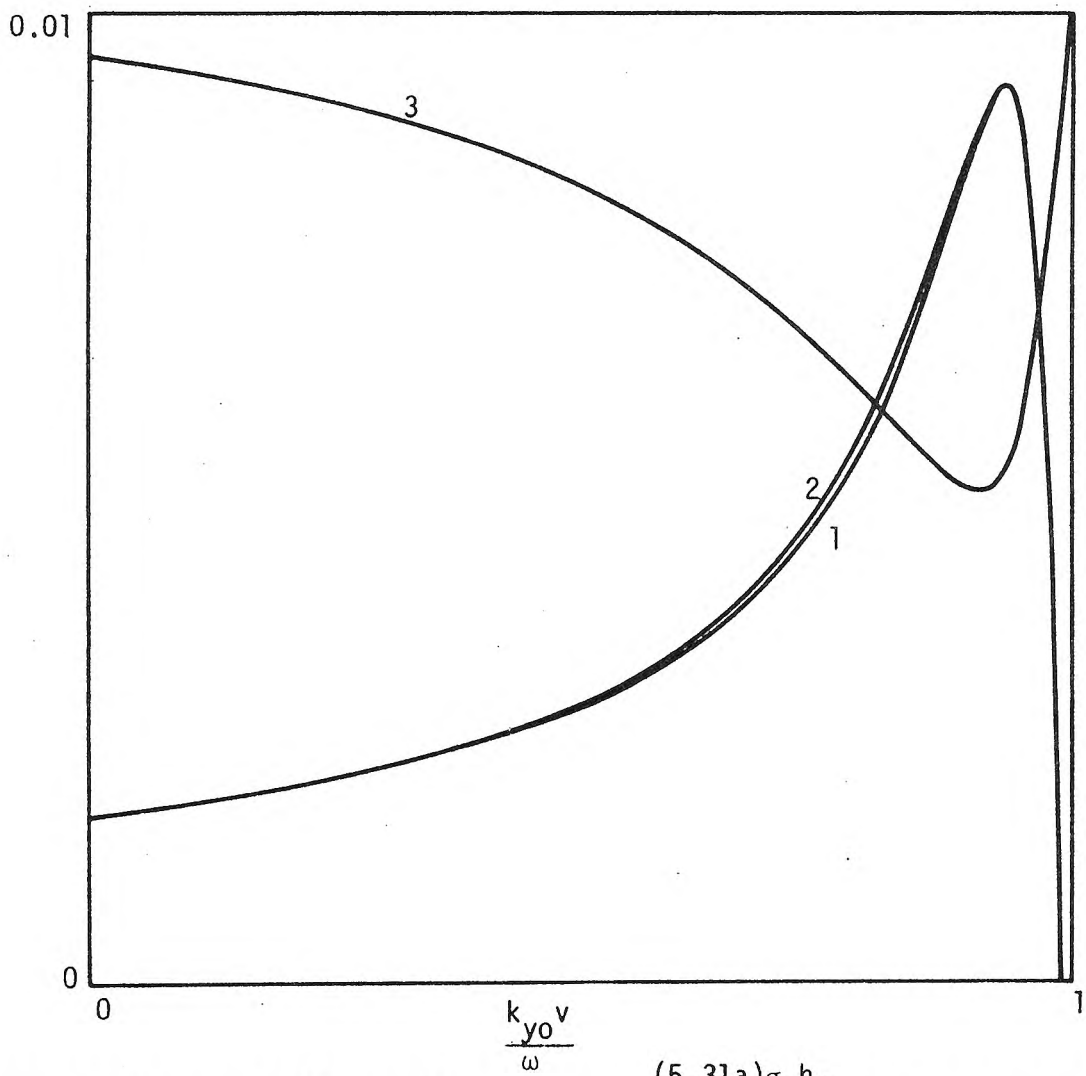

Fig. 5.3 Curves (1) and (2) represent $\frac{(5.31a)\sigma_x h_2}{2.5\ K_1 K_o^2}$ for $\varepsilon = 0$ and $\varepsilon = 0.05$, respectively;
Curve (3) represents $\frac{(5.31b)\sigma_x h_2}{2.5 K_1 K_o^2} + 1$ for $\varepsilon = 0.05$.

Here $W_o = 0.3m$, $a = 0.2m$.

All parameters except ε are the same as those of Fig. 3.2.

cannot happen. A small displacement from the symmetrical position will introduce a restoring force to push the source back to the original position. This force is given by

$$\frac{\bar{F}_x}{\text{unit length}} \cong \frac{-K_1^2 a\, K_o^2}{\sigma h_2}\ \frac{\omega - k_{yo} v}{k_{yo}^2}\ \mathrm{Re}\{\frac{\varepsilon}{\gamma_{20}}\}$$

It can easily be seen that $\bar{F}_x$ always has the opposite sign of ε. Thus, as far as the lateral displacement is concerned, the system is stable. Also, for small displacements, these extra forces are relatively small. For $\bar{F}_y$ it is of the order of ε^2, while for $\bar{F}_x$ it is of the order of ε.

For the more general source $|\tilde{K}_x|^2 = \frac{2}{\pi} \frac{\sin^2(k_y - k_{yo})L}{(k_y - k_{yo})^2}$, a formula similar to (5.20) can be obtained by using (5.16), (5.30), (5.31), and some series summations. Actually, we have:

$$\bar{F}_y \cong \mathrm{Re} \int_{-\infty}^{\infty} \frac{2aK_o^2\, K_1^2}{\sigma h_2 \pi} \frac{\omega - k_y v}{k_y} \{\frac{1}{\gamma_2^2} [1 - \frac{\cosh^2 \gamma_2 \varepsilon}{\gamma_2 a} \frac{\tanh \gamma_2 a}{1 + \tanh \gamma_2 a \tanh \gamma_2 (W_o - a)} + \frac{\sinh^2 \gamma_2 \varepsilon}{\gamma_2 a} \frac{\tanh \gamma_2 a}{1 + \tanh \gamma_2 a \coth \gamma_2 (W_o - a)}]\} \frac{\sin^2(k_y - k_{yo})L}{(k_y - k_{yo})} dk_y \quad (5.35a)$$

$$\bar{F}_x \cong \mathrm{Re} \int_{-\infty}^{\infty} \frac{2K_o^2\, K_1^2}{\sigma h_2 \pi} \frac{\omega - k_y v}{k_y^2} \frac{1}{\gamma_2^2} [\sinh^2 \gamma_2 \varepsilon - \frac{2 \sinh 2\gamma_2 \varepsilon \tanh \gamma_2 a}{1 + \tanh \gamma_2 a \coth \gamma_2 (2W_o - a)}] \times \frac{\sin^2(k_y - k_{yo})L}{(k_y - k_{yo})^2} dk_y \quad (5.35b)$$

It is difficult to evaluate these integrals. The assumptions $|\gamma_{20}\varepsilon| << 1$, $|\gamma_{20} a| >> 1$ and $|\gamma_{20}(W_o - a)| << 1$ are then used to

simplify (5.35) to:

$$\bar{F}_y \cong \mathrm{Re}\int_{-\infty}^{\infty} \frac{2K_o^2 K_1^2 a}{\sigma h_2 \pi} \frac{\omega - k_y v}{k_y} \{\frac{1}{\gamma_2^2} - \frac{1}{\gamma_2^3 a} + \varepsilon^2(\frac{W_o}{a} - 1)\} \frac{\sin^2(k_y - k_{yo})L}{(k_y - k_{yo})^2} dk_y \tag{5.36a}$$

$$\bar{F}_x \cong \mathrm{Re}\int_{-\infty}^{\infty} \frac{-2K_o^2 K_1^2}{\pi\sigma h_2} \frac{(\omega - k_y v)}{k_y^2} \frac{\varepsilon}{\gamma_2} \frac{\sin^2(k_y - k_{yo})L}{(k_y - k_{yo})^2} dk_y \tag{5.36b}$$

Thus, the unsymmetrical case will introduce one more term in the $\bar{F}_y$ integral, which can be easily evaluated to be:

$$\frac{2K_1^2 a}{\sigma h_2} \frac{K_o^2}{} \varepsilon^2(\frac{W_o}{a} - 1) [\frac{(\omega - k_{yo} v)}{k_{yo}} L] \tag{5.37}$$

(5.37) is always positive in the normal operating region, i.e., the unsymmetrical position generally increases the propulsion force. Also, (5.36b) can be seen to have the opposite sign of ε in most of the practical cases where $k_{yo}L$ is large.

The branch points at $\gamma_2 = 0$ (also poles) make (5.36) very difficult to evaluate. Thus, similar to the previous case, we go back to the original series formulation to get explicit expressions. Due to the factors $1/n^2$, $1/m^2$ and $1/(m^2-n^2)$, the total forces are mainly generated by small n,m terms. Going through all the factorization and integration procedures we get:

$$\bar{F}_y \cong \sum_{n=1,3,5} \frac{8W_o}{n^2\pi^2} \sin^2 \frac{n\pi a}{2W_o} \cos^2 \frac{n\pi\varepsilon}{2W_o} \frac{2K_o^2 K_1^2}{\pi\sigma h_2} \mathrm{Re}\{G(n)\}$$

$$+ \sum_{n=2,4,6} \frac{8W_o}{n^2\pi^2} \sin^2 \frac{n\pi a}{2W_o} \sin^2 \frac{n\pi\varepsilon}{2W_o} \frac{2K_o^2 K_1^2}{\pi\sigma h^2} \mathrm{Re}\{G(n)\} \tag{5.38a}$$

$$\bar{F}_x \cong \sum_{n=2,4,6} \sum_{m=1,3,5} \frac{(-8)(-1)^{n/2}(-1)^{\frac{m-1}{2}}}{(m^2-n^2)\pi^2} \left[4 \sin \frac{n\pi a}{2W_o} \sin \frac{n\pi\varepsilon}{2W_o}\right.$$

$$\left. \times \cos \frac{m\pi\varepsilon}{2W_o} \sin \frac{m\pi a}{2W_o}\right] \frac{K_o^2 K_1^2}{\pi\sigma h_2} \mathrm{Re}\{H(n) + H(m)\} \tag{5.38b}$$

where

$$G(n) = \frac{\pi L}{k_{yo}} \frac{\omega}{\alpha_1\alpha_2} + \frac{\omega_1 - \alpha_1 v}{\alpha_1(\alpha_1-\alpha_2)} S_1(\alpha_1, k_{yo}, L)$$

$$+ \frac{\omega - \alpha_2 v}{\alpha_2(\alpha_2-\alpha_1)} S_1(\alpha_2, k_{yo}, L) \tag{5.38c}$$

$$H(n) = \frac{\pi L}{k_{yo}} \frac{\omega(\alpha_1+\alpha_2) - v\alpha_1\alpha_2}{\alpha_1^2\alpha_2^2} + \frac{\omega}{\alpha_1\alpha_2} \frac{2\pi L}{k_{yo}^2} + \frac{\omega - \alpha_1 v}{\alpha_1^2(\alpha_1-\alpha_2)} S_1(\alpha_1, k_{yo}, L)$$

$$+ \frac{\omega - \alpha_2 v}{\alpha_2^2(\alpha_2-\alpha_1)} S_1(\alpha_2, k_{yo}, L) \tag{5.38d}$$

with α_1, α_2 being defined in (5.29).

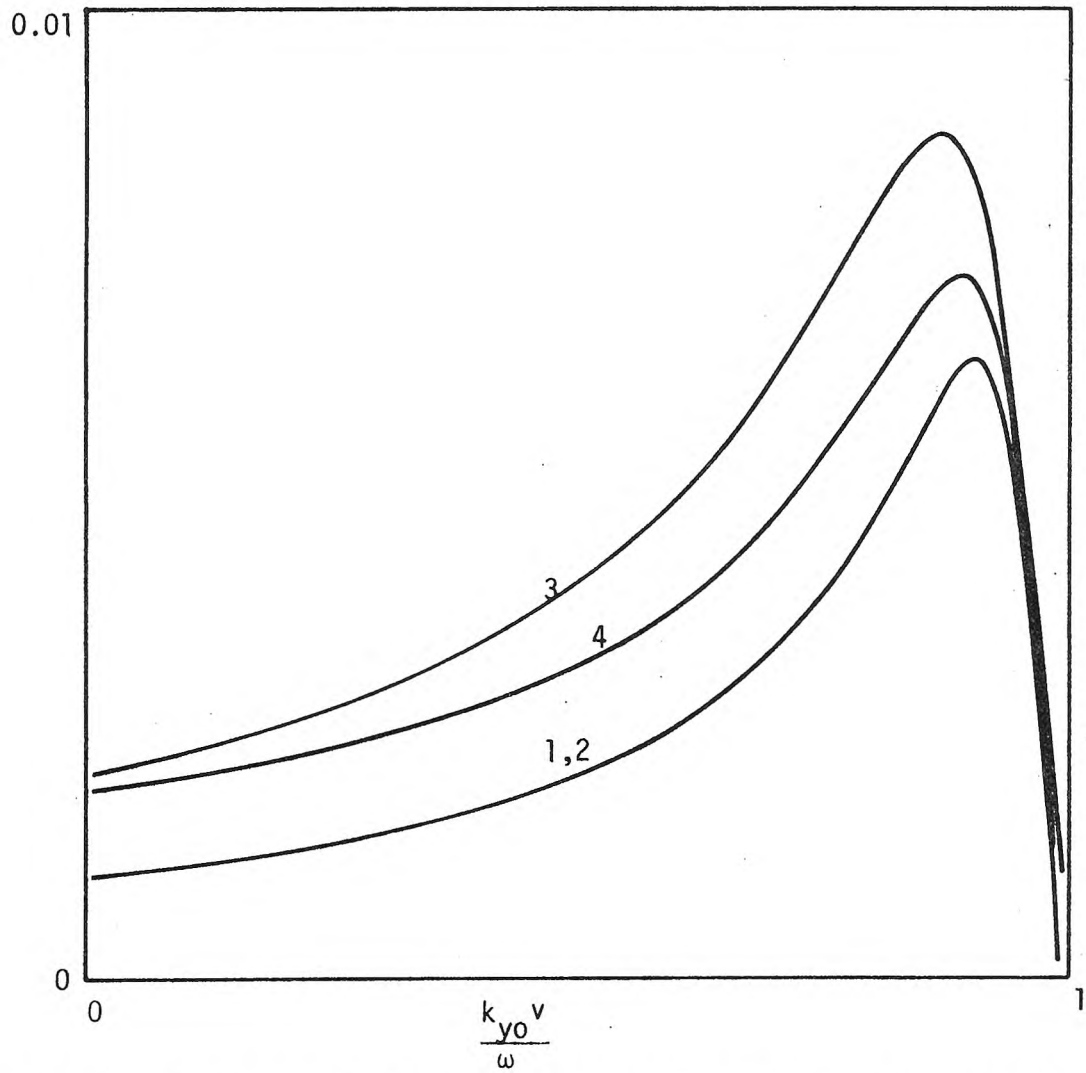

Fig. 5.4 Different force components of series expressions (5.38a) and (5.38b).

(1) $(\bar{F}'_y)_1$ with $\varepsilon = 0$; (2) $(\bar{F}'_y)_1$ with $\varepsilon = 0.01m$;

(3) $10^4 x\ (\bar{F}'_y)_2$ with $\varepsilon = 0.01m$; (4) $50(\bar{F}'_x)_{1,2}$ with $\varepsilon = 0.01m$

where $(\bar{F}'_y)_n = \dfrac{0.8(\bar{F}_y)_n\ \sigma_x h_2}{K_1 K_o^2}$, $(\bar{F}'_x)_{m,n} = \dfrac{0.8(\bar{F}_x)_{m,n}\sigma_x h_2}{K_1 K_o^2}$

All of the parameters defined in the same way as in Fig. 3.2.

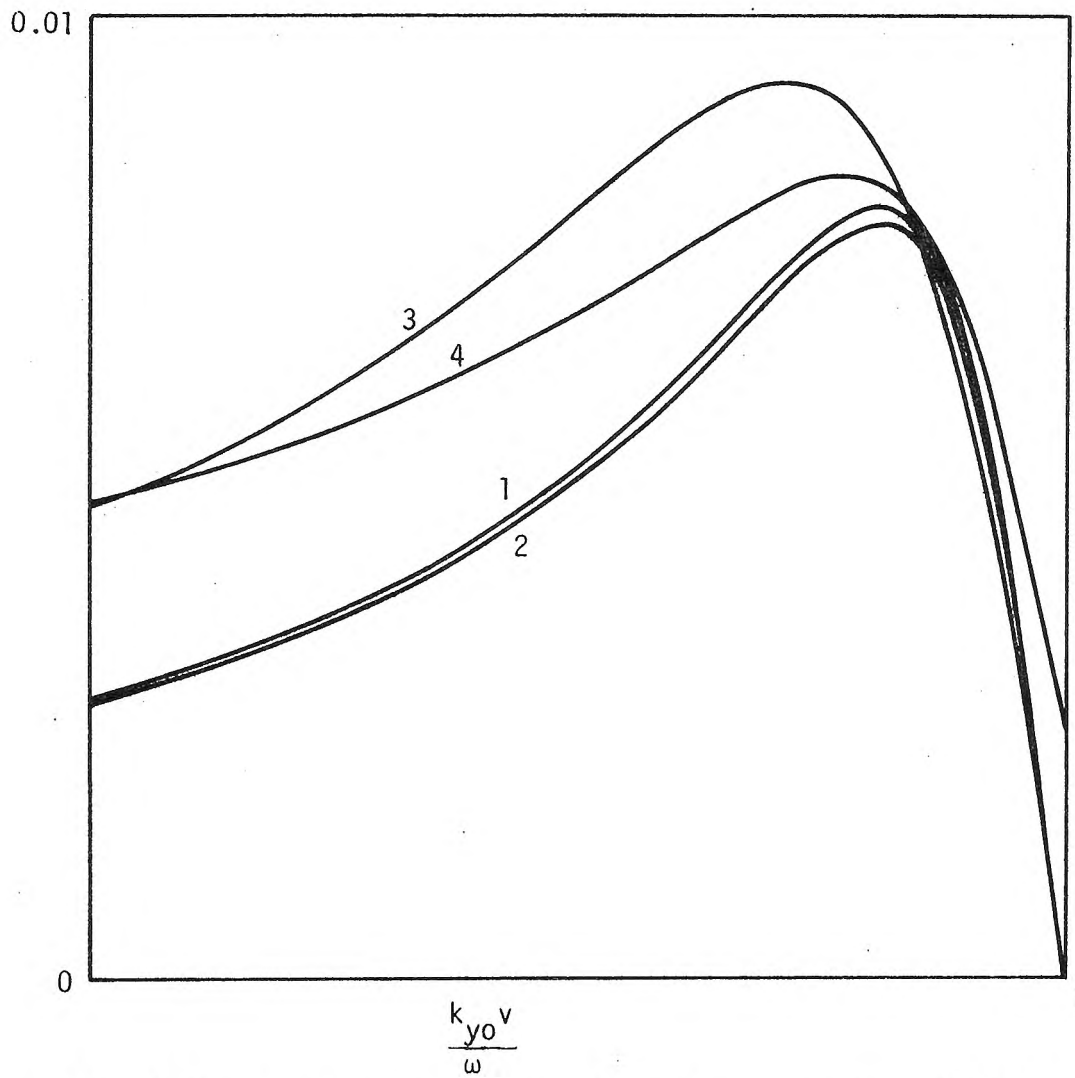

Fig. 5.5 Different force components of series expressions (5.38a) and (5.38b).

(1) $(\bar{F}'_y)_3$, with $\varepsilon = 0$; (2) $(\bar{F}'_y)_3$, with $\varepsilon = 0.01$m ;

(3) $250(\bar{F}'_y)_4$, with $\varepsilon = 0.01$m; (4) $2.5(\bar{F}'_x)_{3,4}$, with $\varepsilon = 0.01$m

where $(\bar{F}'_y)_n = \dfrac{8(\bar{F}_y)_n \sigma_x h_2}{K_1 K_o^2}$, $\bar{F}'_x)_{m,n} = \dfrac{8(\bar{F}_x)_{m,n} \sigma_x h_2}{K_1 K_o^2}$.

All of the parameters defined in the same way as in Fig. 3.2.

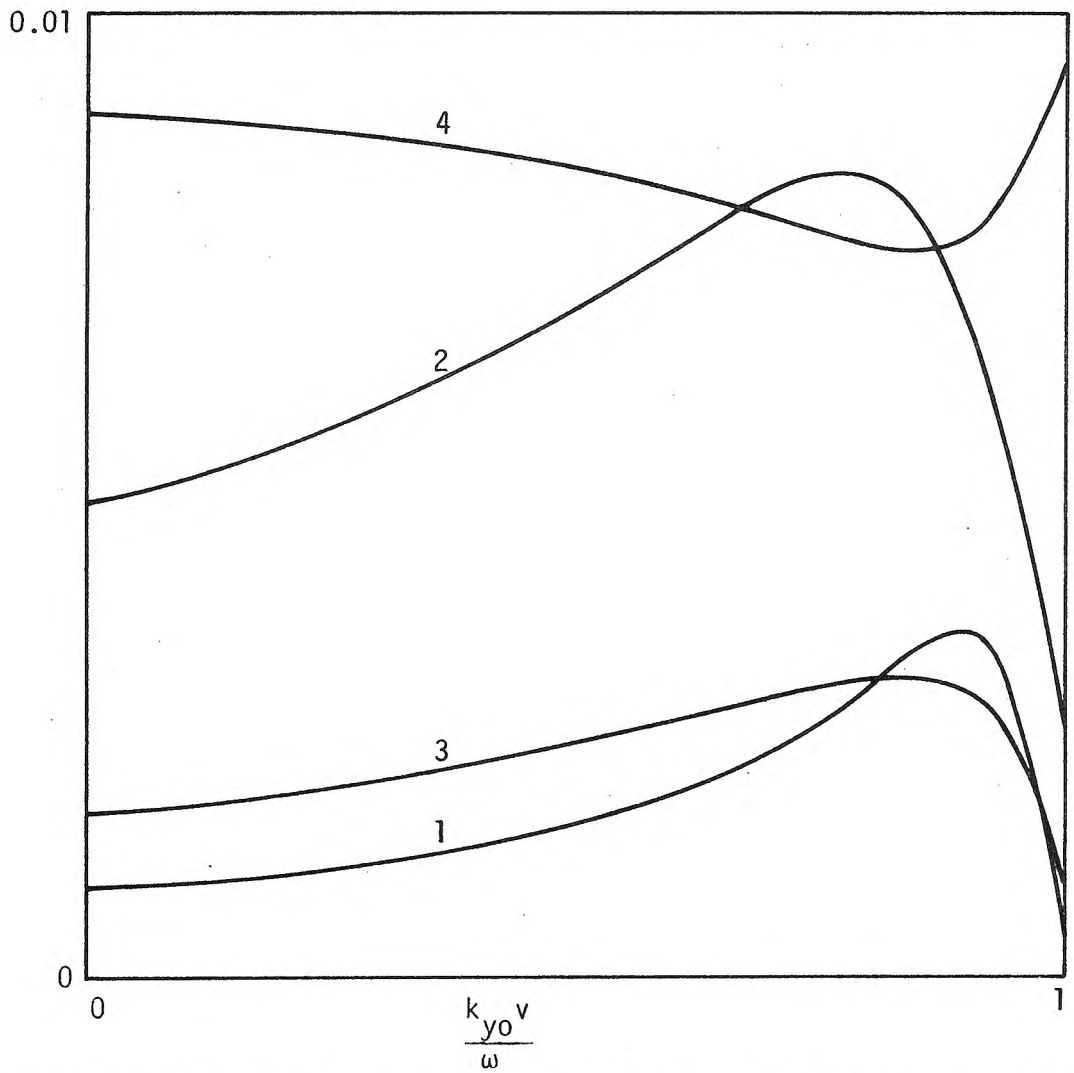

Fig. 5.6 Different lateral force components in the series expression (5.38b). (1) $(\bar{F}'_x)_{1,2}$

(2) $(\bar{F}'_x)_{3,4}$

(3) $(\bar{F}'_x)_{1,4}$

(4) $(\bar{F}'_x)_{3,2}$

where $(\bar{F}'_x)_{m,n} = \dfrac{20(\bar{F}_x)_{m,n}\sigma_x h_2}{K_1 K_o^2}$

ϵ = 0.0/m and all of the other parameters are the same as those of Fig. 5.2.

The analysis is essentially completed. For the ideal source some results are shown in Figs. 5.2 and 5.3. Comparing these to Fig. 3.2, we notice the influence of the 3-dimensional corrections we made in this chapter. As for the more realistic source, we only gave the series representation. Several components with small n,m are shown in Figs. 5.4, 5.5 and 5.6. When ε/W_o and ε/a are very small, it is seen that the series representation for $\bar{F}_y$ converges very fast. However, it seems that we need many terms to give a fairly good approximation for $\bar{F}_x$.

In the above, we mainly considered the three-dimensional corrections for geometry (A-i-1). Similar approaches can be used to other configurations.

CONCLUSION

In this work we studied the four-layer single-sided LIM used for propulsion and suspension of magnetically levitated vehicles. The moving track is assumed to be made of a conductor with uniaxial $\tilde{\mu}$ and $\tilde{\sigma}$. The source rigidly attached to the bottom of the vehicle has a given current distribution. Fourier transform techniques in conjunction with the transfer matrix method are used to solve this two-dimensional boundary value problem. The machine performance in terms of forces, efficiency, and power factor is given in integral form. The results for the ideal source $\tilde{K}_x \propto \delta(k_y - k_{y0})$ are obtained. (Here $\tilde{K}_x$ is the Fourier component of the given current suorce). In addition to this the analysis of the integrands under the assumption of thin or thick reaction rails gives us the following conclusions:

(a) Comparing with the case that the source has back iron, the geometry with region "4" being free space gives much smaller forces and power, more serious end effect at the velocity where the propulsion force is maximum.

(b) If region "1" is laminated iron, the effect of the permeability of the reaction rail is small when the reaction rail is thin.

(c) If region "1" is free space or the reaction rail is thick, the induction motor can only give repulsive supporting forces when the reaction rails are non-ferromagnetic. And the forces are large only in the low efficiency region. On the contrary, large attractive supporting forces are obtained in the high

efficiency region when the reaction rails are ferromagnetic. Thus, the attractive scheme is preferable, and ferromagnetic tracks are recommended.

(d) Small σv and $1/k_{yo}L$ are required to reduce the degrading of the machine performance due to the end effect. However, σ is not allowed being too small, otherwise a sufficient propulsion force can not be obtained. A suitable compromise is necessary and the composite track is recommended.

From the above information, unsuitable configurations are discarded. The machine performance integrals are evaluated for the promising geometries and source distribution

$$K_x \propto \frac{\sin(k_y - k_{yo})L}{(k_y - k_{yo})}$$

The composite track seems most promising. A possible way of computing the effective $\tilde{\mu}$ and $\tilde{\sigma}$ for a composite track is sketched. From the analysis of an extremely simplified geometry, the conditions for the validity of the effective $\tilde{\mu}$ and $\tilde{\sigma}$ concepts are determined to be $k_{yo}h \ll 1$ and $h/2d_o \ll 1$. Using a parallel approach, another possible LIM configuration with relatively thick lamination satisfying $h/2d_o \approx \pi$ is analyzed. It is found that this geometry has a very small end effect.

Finally, a three-dimensional correction is introduced to take care of the finite width of the LIM. Fourier transform and Fourier series techniques are used to solve this periodic 3-dimensional boundary value problem. A general analysis is given. The propulsion

force and the lateral force are calculated for several special cases. For a geometry similar to (A-i-1), this so-called lateral end effect generally increases the propulsion forces in the small velocity region. In the high velocity region (i.e., v is close to ω/k_{yo}), an effective conductivity concept can be developed and a decrease in the propulsion force is observed. As for the lateral displacement of the source, it is found to be stable.

In this theses, we only consider the case with series connected source. With minor changes, the results for the parallel or series-parallel hybrid connected sources can be obtained. The machine performance is expected to be drastically different when the end effect is taken into consideration. Further analysis of this kind is thus highly recommended.

Here, we mainly consider a LIM which has a track with a finely distributed inhomogeneity (i.e., $k_{yo}h<<1$, with h being the period of the structure). It appears that large supporting forces exist only within a narrow velocity range and change largely with the velocity. Control systems are thus difficult to construct. It is suspected that the opposite situation with $k_{yo}h \gtrsim 1$ can possibly overcome this difficulty. Further analysis of tracks of this kind is suggested.

REFERENCES

1. J. R. Reitz, et al., "Technical feasibility of magnetic levitation as a suspension system for HSGT vehicles", Ford Motor Co., Tech. Rep. FRA-RT-72-40, produced under Contract DOT-FR-10026 with the U.S. Dept. of Transportation, Feb. 1972.

2. H. T. Coffey et al., "The feasibility of magnetically levitating high speed ground vehicles", SRI Tech. Rep. DOT-FR-10001, Feb. 1972.

3. Robert H. Bocherts, et al., "Baseline specifications for a magnetically suspended high-speed vehicle", Proc. IEEE 61, 569 (1973).

4. Michel Poloujadoff, "Linear induction machines: I. History and theory of operation", IEEE Spectrum 8, 72 (1971).

5. Ibid, Part II, "Applications", IEEE Spectrum 8, 79 (1971).

6. E. R. Laithwaite and S. A. Nasar, "Linear-motion electrical machines", Proc. IEEE 58, 531 (1970).

7. E. R. Laithwaite, Induction Machines for Special Purposes (London: George Newms, 1966).

8. E. R. Laithwaite and F. T. Barwell, "Application of linear induction motors to high-speed transport systems", Proc. IEE 116, 713 (1969).

9. D. F. Wilkie, "Dynamics, control, and ride quality of a magnetically levitated high-speed ground vehicle", Transport Research 1972.

10. E. R. Laithwaite, "The goodness of a machine", Proc. IEE 112, 538 (1965).

11. T. C. Wang, "Linear induction motor for high-speed ground transportation", IEEE Trans. IGA7, 632 (1971).

12. B. T. Ooi and D. C. White, "Traction and normal forces in the linear induction motor", IEEE Trans. PAS-89, 638 (1970).

13. T. C. Wang, J. W. Smylie and R. Y. Pei, "Single-sided linear induction motor", in IEEE Conference Record of 1971 6th Annual Mtg. of the IEEE Industry & General Applications Group, p. 1-10.

14. S. A. Nasar, L. Del Cid, Jr., "Propulsion and levitator forces in a single-sided linear induction motor for high-speed ground transportation, Proc. IEEE 61, 638 (1973).

15. J. K. Dukowicz, "Analysis of linear induction machines in the discrete windings and finite iron length", G.M. research publication GMR-1426 (1973).

16. S. Yamamura, H. Ito, and Y. Ishikawa, "Theories of the linear induction motor and compensated linear induction motor", IEEE Trans. PAS-91, 1700 (1972).

17. H. H. Kolm and R. D. Thornton, "Electromagnetic flight", Scientific American 229, 17 (1973).

18. E. M. Freeman, "Travelling waves in induction machines; input impedance and equivalent circuits", Proc. IEE 115, 1772 (1968).

19. A. L. Cullen and T. H. Barton, "A simplified electromagnetic theory of the induction motor using the concept of wave impedance", Proc. IEE 105C, 331 (1958).

20. R. M. Fano, L. Chu, and R. Adler, "Electromagnetic Fields, Energy, and Forces (John Wiley & Sons, Inc., 1960).

21. E. Mishkin, "Theory of the squirrel-cage induction motor derived directly from Maxwell's field equations", Quant. J. Mech. Appl. Math 7, 472 (1954).

22. H. Bondi, K. C. Mukherji, "An analysis of tooth ripple phenomenon in smooth laminated pole shoes", Proc. IEE (London) 104, 349 (1957).

23. R. L. Russell, K. H. Norsworthy, "Eddy currents and wall losses in screened-rotor induction motors", Proc. IEE 105A, 163 (1958).

APPENDIX A

Let K and K' be the coordinate systems which are at rest with respect to the source and the reaction rail, respectively. Then, after neglecting the relativistic effect and the displacement current, Maxwell's equations within the reaction rail are given as

K: $$\nabla \times \underline{H} = \underline{J} \tag{A-1a}$$

$$\nabla \times \underline{E} = -\frac{\partial \underline{B}}{\partial t} \tag{A-1b}$$

K': $$\nabla' \times \underline{H}' = \underline{J}' \tag{A-1c}$$

$$\nabla' \times \underline{E}' = -\frac{\partial \underline{B}'}{\partial t} \tag{A-1d}$$

$$\underline{B}' = \underset{\sim}{\mu} \cdot \underline{H}' \tag{A-1e}$$

$$\underline{J}' = \underset{\sim}{\sigma} \cdot \underline{E}' \tag{A-1f}$$

We also know:

$$\underline{J} = \underline{J}' \tag{A-2a}$$

$$\underline{H} = \underline{H}' \tag{A-2b}$$

$$\underline{B} = \underline{B}' \tag{A-2c}$$

$$\underline{E} + \underline{v} \times \underline{B} = \underline{E}' \tag{A-2d}$$

So, finally, we have Maxwell's equations in K :

$$\nabla \times \underline{H} = \underline{J} \tag{A-3a}$$

$$\nabla \times \underline{E} = -\frac{\partial \underline{B}}{\partial t} \tag{A-3b}$$

$$\underline{J} = \underset{\sim}{\sigma} \cdot (\underline{E} + \underline{v} \times \underline{B}) \tag{A-3c}$$

$$\underline{B} = \underset{\sim}{\mu} \cdot \underline{H} \tag{A-3d}$$

This is the familiar Minkowski's formulation. However, because there is moving magnetic material present, as far as those quantities such as force density, energy, etc. are concerned, this formulation is not clear enough to explain everything. Thus, an alternative called E-H formulation introduced by Chu[20] is preferable, i.e., we have:

$$\nabla \times \underline{H}_c = \underline{J}_c \tag{A-4a}$$

$$\nabla \times \underline{E}_c + \mu_o \frac{\partial \underline{H}_c}{\partial t} = -\mu_o \frac{\partial \underline{M}_c}{\partial t} - \nabla \times (\mu_o \underline{M}_c \times \underline{v}) \tag{A-4b}$$

with

$$\underline{J}_c = \underset{\sim}{\sigma} \cdot (\underline{E}_c + \underline{v} \times \mu_o \underline{H}_c) \tag{A-4c}$$

$$\mu_o \underline{M}_c = (\underset{\sim}{\mu} - \mu_o \underset{\sim}{I}) \cdot \underline{H}_c \tag{A-4d}$$

The subscript "c" is introduced to distinguish those fields from the ordinary fields in Minkowski's formulation. Actually, with a suitable transformation, it can be found that these two formulations are equivalent.

$$\underline{E} = \underline{E}_c + \mu_o \underline{M}_c \times \underline{v} \tag{A-5a}$$

$$\underline{H} = \underline{H}_c \tag{A-5b}$$

$$\underline{B} = \mu_o (\underline{H}_c + \underline{M}_c) \tag{A-5c}$$

$$\underline{J} = \underline{J}_c \tag{A-5d}$$

In the E-H formulation, the force density can be expressed as:

$$\underline{f} = \underline{J}_c \times \mu_o \underline{H}_c - (\nabla \cdot \mu_o \underline{M}_c)\, \underline{H}_c \tag{A-6a}$$

And the input power density is given as:

$$P = \underline{E}_c \cdot \underline{J}_c + \underline{H}_c \cdot \mu_o[\frac{\partial \underline{M}_c}{\partial t} + \nabla \times (\underline{M}_c \times \underline{v})] \qquad \text{(A-6b)}$$

Then the total force and the total power input can be obtained by suitable volume integrations within the reaction rail. Further information about machine performance can thus also be obtained. Unfortunately, those integrations are tedious. A simpler integration can generally be obtained by introducing a stress energy tensor $\underset{\sim}{T}$ to transform the volume integral into a surface integral.

$$\underline{F} = \int_S \underset{\sim}{T}_c \cdot d\underline{s} \qquad \text{(A-7a)}$$

with

$$T_{cij} = \mu_o[H_{ci}H_{cj} - \frac{1}{2}\delta_{ij}|\underline{H}_c|^2] + \varepsilon_o[E_{ci}E_{cj} - \frac{1}{2}\delta_{ij}|\underline{E}_c|^2] \qquad \text{(A-7b)}$$

It should be noticed that except at the free space where $\underline{D} = \varepsilon_o\underline{E}$ and $\underline{B} = \mu_o\underline{H}$, this stress energy tensor is different from the familiar Minkowski's tensor. As for the power input, it seems to be much simpler to evaluate it directly at the source which is located in free space, i.e.,

$$\underline{P} = \underline{E} \cdot \underline{J} \qquad \text{(A-7b)}$$

APPENDIX B

Conditions for Thin and Thick Reaction Rails

Here we will say a reaction rail is thin when the condition that $|\gamma_2 h_2| \ll 1$ is satisfied around a region where the source function is most significant. Similarly, the condition $|\gamma_2 h_2| \gg 1$ is required for the thick reaction rail. Now that we know that the source function is generally concentrated within the region $\omega/v \geq k_y \geq 0$, we will first consider this region. Now

$$\gamma_2 = \sqrt{\frac{\mu_{2y}}{\mu_{2z}}} \sqrt{k_y^2 - i(\omega - k_y v)\sigma_x \mu_{2z}} \tag{B-1a}$$

$$|\gamma_2| = \sqrt{\frac{\mu_{2y}}{\mu_{2z}}} [k_y^4 + (\omega - k_y v)^2 \sigma_x^2 \mu_{2z}^2]^{1/4} \tag{B-1b}$$

With $k_y = a \frac{\omega}{v}$, the only minimum of $|\gamma_2|$ will occur at:

$$a_m = (\frac{R}{2})^{1/3} \{[(1 + \frac{4R}{27})^{1/2} + 1]^{1/3} - [(1 + \frac{4R}{27})^{1/2} - 1]^{1/3}\} \tag{B-2a}$$

where

$$R = \frac{\omega^2 \sigma_x^2 \mu_{2z}^2}{2 \frac{\omega^4}{v^4}} \tag{B-2b}$$

And the corresponding minimum value is

$$|\gamma_{2m}| = \frac{\omega}{v} a_m [1 + \frac{2a_m^2}{R})^{1/4} \sqrt{\frac{\mu_{2y}}{\mu_{2z}}} \tag{B-3a}$$

or

$$= \sqrt{\frac{\mu_{2y}}{\mu_{2z}}} \sqrt{\omega \sigma_x \mu_{2z}} [(1 - \frac{a_m}{2})(1 - a_m)]^{1/4} \tag{B-3b}$$

or

$$= \sqrt{\frac{\mu_{2y}}{\mu_{2z}}}\ \frac{\omega}{v}\left[a_m^4 + 2R(1 - a_m)^2\right]^{1/4} \qquad \text{(B-3c)}$$

Now let us consider two different cases:

(i) $R \geq \frac{1}{4}$, then $a_m > \frac{1}{2}$, and

$$\sqrt{\omega\sigma_x \mu_{2y}}\ (0.78) > |\gamma_{2m}| > \frac{\omega}{v} a_m > \frac{1}{2}\frac{\omega}{v} \qquad \text{(B-4a)}$$

(ii) $R \leq \frac{1}{4}$, then $4R/27$ can be considered as small. Thus

$$a_m \cong R^{1/3} - \frac{R^{2/3}}{3}$$

$$\sqrt{\frac{\mu_{2y}}{\mu_{2z}}}\ \frac{\omega}{v}\ (0.86) > |\gamma_{2m}| \cong \sqrt{\omega\sigma_x\mu_{2y}}\ \left[1 - \frac{3}{2}R^{1/3} + R^{2/3} - \frac{R}{3}\right]$$

$$> 0.78\ \sqrt{\omega\sigma_x\mu_{2y}} \qquad \text{(B-4b)}$$

Thus, the condition for $|\gamma_2 h_2| >> 1$ (i.e., thick reaction rails) can be rewritten as:

$$\text{smaller of } \left[\frac{1}{2}\frac{\omega}{v} h_2,\ 0.78\ \sqrt{\omega\sigma_x\mu_{2y}}\ h_2\right] >> 1 \qquad \text{(B-5a)}$$

Similarly, the condition for $|\gamma_2 h_2| << 1$ (i.e., thin reaction rails) is

$$\text{larger of } \left[\sqrt{\frac{\mu_{2y}}{\mu_{2z}}}\frac{\omega}{v} h_2\ ,\ \sqrt{\omega\mu_{2y}\sigma_x}\ h_2\right] << 1 \qquad \text{(B-5b)}$$

Actually, for the left-handed sides of $\binom{\text{B-5a}}{\text{B-5b}}$, values of the order of $\left(\frac{\pi}{1/\pi}\right)$ are generally good enough to give accurate approximations.

However, in some cases, even relatively relaxed conditions are difficult to be met. And, conditions cannot be satisfied for the whole range of $0 \leq k_y \leq \frac{\omega}{v}$. Under this situation, generally these conditions

can be further relaxed. As we understand, the source function is generally concentrated around k_{yo}. It seems that we need only to consider $|\gamma_2 h_2|$ around k_{yo}, i.e., $|\gamma_{20} h_2|$. And, the conditions $|\gamma_{20} h_2| << 1$ and $|\gamma_{20} h_2| >> 1$ can thus be used as the criteria to determine whether a reaction rail is thin or thick. And definitely, those conditions are much easier to be satisfied. For example, we can consider a case with $\sqrt{\omega \mu_{2z} \sigma_x} \sim 60$, $\omega/v \sim 300$. Then, it can be shown that even the value of $h_2 = 5 \times 10^{-3}$ cannot satisfy condition (B-5b). However, as we know, in most of the practical cases k_{yo} is about 15. Thus, the region for which we are most concerned corresponds to k_y around 15. For those k_y , $|\gamma_2 h_2|$ is about 0.3 for $h_2 = 5 \times 10^{-3}$, which is good enough to say that the plate is thin for this more relaxed criterion.

APPENDIX C

The Evaluation of the Integral $s_1(\alpha,k_{yo},L) = \int_{-\infty}^{\infty} \frac{1}{k_y-\alpha} \frac{\sin^2(k_y-k_{yo})L}{(k_y-k_{yo})^2} dk_y$ with a complex α

Using a suitable variable change, we have

$$s_1(\alpha,k_{yo},L) = L^2 \int_{-\infty}^{\infty} \frac{1}{k_y-\alpha'} \frac{\sin^2 k_y}{k_y^2} dk_y \tag{C-1a}$$

with

$$\alpha' = (\alpha - k_{yo})L \tag{C-1b}$$

Further, $s_1(\alpha,k_{yo},L)$ can be rewritten as:

$$s_1(\alpha,k_{yo},L) = \lim_{\varepsilon \to 0} \frac{1}{2} \int_{-\infty}^{\infty} \frac{1}{k_y-\alpha'} \frac{1}{k_y^2+\varepsilon^2} [1 - \frac{e^{i2k_y}}{2} - \frac{e^{-2ik_y}}{2}]dk_y \tag{C-1c}$$

$$= \lim_{\varepsilon \to 0} \frac{1}{2} (I_o - \frac{I_+}{2} - \frac{I_-}{2}) \tag{C-2b}$$

Now we will assume $\text{Im}\ \alpha > 0$. Then, by the using of Jordan's lemma and residue theorem, it can be shown that:

$$I_+ = \frac{\pi}{\varepsilon} [(\frac{e^{2i\alpha'}}{\alpha'-i\varepsilon} - \frac{e^{2i\alpha'}}{\alpha'+i\varepsilon}) + \frac{e^{-2\varepsilon}}{i\varepsilon-\alpha'}] \tag{C-3a}$$

$$I_- = \frac{\pi}{\varepsilon} \frac{e^{-2\varepsilon}}{-i\varepsilon-\alpha'} \tag{C-3b}$$

$$I_o = \frac{\pi}{\varepsilon} \frac{1}{-i\varepsilon-\alpha'} \tag{C-3c}$$

So, finally, we have

$$s_1(\alpha,k_{yo},L) = \frac{i\pi L^2}{2\alpha'^2}\,(1 - e^{2i\alpha'} + 2i\alpha') \qquad \text{(C-4a)}$$

or

$$s_1(\alpha,k_{yo},L) = \frac{\pi i}{2}\,\frac{1}{(\alpha-k_{yo})^2}\,[1 + 2i(\alpha-k_{yo})L - e^{2i(\alpha-k_{yo})L}] \qquad \text{(C-4b)}$$

A similar procedure can be used to evaluate the integral with $\mathrm{Im}\,\alpha < 0$ to get:

$$s_1(\alpha,k_{yo},L) = \frac{-\pi i}{2}\,\frac{1}{(\alpha-k_{yo})^2}\,[1 - 2i(\alpha-k_{yo})L - e^{-2i(\alpha-k_{yo})L}] \qquad \text{(C-4c)}$$

APPENDIX D

The Evaluation of the Integral

$$s_2(\alpha,k_{yo},L) = \int_{-\infty}^{\infty} \frac{|k_y|}{k_y-\alpha} \frac{\sin^2(k_y-k_{yo})L}{(k_y-k_{yo})^2} dk_y \tag{D-1}$$

with a complex α .

$s_2(\alpha,k_{yo},L)$ can be rewritten as:

$$\int_{-\infty}^{\infty} \frac{k_y}{k_y-\alpha} \frac{\sin^2(k_y-k_{yo})L}{(k_y-k_{yo})^2} dk_y - 2\int_{-\infty}^{0} \frac{k_y}{k_y-\alpha} \frac{\sin^2(k_y-k_{yo})L}{(k_y-k_{yo})^2} dk_y \tag{D-2a}$$

$$= I_1 - 2I_2 \tag{D-2b}$$

Using Appendix C, we have

$$I_1 = L\pi + \alpha \begin{cases} \frac{i\pi}{2(\alpha-k_{yo})^2}\left[1 + 2i(\alpha-k_{yo})L - e^{2i(\alpha-k_{yo})L}\right] \text{ for Im } \alpha > 0 \quad \text{(D-3a)} \\ \frac{-i\pi}{2(\alpha-k_{yo})^2}\left[1 - 2i(\alpha-k_{yo})L - e^{-2i(\alpha-k_{yo})L}\right] \text{ for Im } \alpha < 0 \quad \text{(D-3b)} \end{cases}$$

For I_2 , changes of variables will give us:

$$I_2 = \int_0^{\infty} \frac{k_y}{k_y+\alpha} \frac{\sin^2(k_y+k_{yo})L}{(k_y+k_{yo})^2} dk_y$$

$$= L\int_{k_{yo}L}^{\infty} \frac{k_y - k_{yo}L}{k_y + (\alpha-k_{yo})L} \frac{1-\cos 2k_y}{2k_y^2} dk_y$$

$$= \frac{L}{2}\left\{\frac{-1}{(\alpha-k_{yo})L} + \frac{\alpha L}{(\alpha-k_{yo})^2L^2} \ln\frac{\alpha}{k_{yo}} - I_3\right\} \tag{D-4a}$$

where

$$I_3 = \int_{k_{yo}L}^{\infty} \frac{k_y - k_{yo}L}{k_y + (\alpha - k_{yo})L} \frac{\cos 2k_y}{k_y^2} dk_y$$

$$= \int_{k_{yo}L}^{\infty} \left[\frac{C_1}{k_y + (\alpha - k_{yo})L} + \frac{C_2}{k_y} + \frac{C_3}{k_y^2}\right] \cos 2k_y \, dk_y$$

$$= C_1 \{\cos(2k_{yo}L)[-\sin 2\alpha L \, S_i(2\alpha L) - \cos 2\alpha L \, C_i(2\alpha L)]$$

$$- \sin(2k_{yo}L)[\sin 2\alpha L \, C_i(2\alpha L) - \cos 2\alpha L \, S_i(2\alpha L)]\}$$

$$- C_2 \, C_i(2k_{yo}L) + C_3\left[\frac{\cos(2k_{yo}L)}{k_{yo}L} + 2S_i(2k_{yo}L)\right] \qquad \text{(D-4b)}$$

with

$$C_1 = \frac{-\alpha L}{(\alpha - k_{yo})^2 L^2}, \quad C_2 = -C_1, \quad C_3 = \frac{-k_{yo}L}{(\alpha - k_{yo})L}$$

In (D.4b), the sine and cosine integrals $S_i(x)$ and $C_i(x)$ have been used with

$$S_i(pq) = -\int_p^{\infty} \frac{\sin tq}{t} dt \qquad \text{(D-5a)}$$

$$C_i(pq) = -\int_p^{\infty} \frac{\cos tq}{t} dt \qquad \text{(D-5b)}$$

I_3 is complicated; however, for many practical cases where $k_{yo}L$ is large, I_3 is relatively small compared to the remaining part of (D.4a). Thus it can generally be neglected.

APPENDIX E

The evaluation of the integral

$$S_3(\alpha,k_{yo},L) = \int_{-\infty}^{\infty} \frac{\sqrt{(k_y-\beta_1)(k_y-\beta_2)}}{k_y-\alpha} \frac{\sin^2(k_y-k_{yo})L}{(k_y-k_{yo})^2}\, dk_y \qquad \text{(E-1)}$$

α,β_1,β_2 are all complex.

The branch cuts are chosen as shown in Fig. (E.1). Thus, with the definition of $-3\pi/2 < \theta_1 < \pi$, $-\pi/2 < \theta_2 < 2\pi$ and $\sqrt{(k_y-\beta_1)(k_y-\beta_2)}$ $= \sqrt{\ell_1\ell_2}\, \exp[(i/2)(\theta_1+\theta_2)]$, the positiveness of Re $\sqrt{(k_y-\beta_1)(k_y-\beta_2)}$ is insured. (Note: To obtain the branch cut I, an arbitrary straight line is drawn from β_1 with $0 < \eta_1 < \pi/2$. Then another straight line can be drawn from β_2 with $\eta_2 = \pi/2 - \eta_1$. These lines will meet at the point P_1 . The branch cut I is just the loci of P_1 . A similar method can be used to get branch cut II.)

Now, using a change of variable, we have:

$$S_3(\alpha,k_{yo},L) = L \int_{-\infty}^{\infty} \frac{\sqrt{(k_y-\beta_1')(k_y-\beta_2')}}{k_y-\alpha'} \frac{\sin^2 k_y}{k_y^2}\, dk_y \qquad \text{(E-2a)}$$

where

$$\beta_1' = (\beta_1-k_{yo})L$$

$$\beta_2' = (\beta_2-k_{yo})L$$

$$\alpha' = (\alpha-k_{yo})L$$

$S_3(\alpha,k_{yo},L)$ can be further rewritten as:

$$S_3(\alpha,k_{yo},L) = L \lim_{\varepsilon \to 0} \int_{-\infty}^{\infty} \frac{\sqrt{(k_y-\beta_1')(k_y-\beta_2')}}{k_y-\alpha'} \frac{1}{k_y^2+\varepsilon^2}$$

$$\times \left[\frac{1}{2} - \frac{e^{2ik_y}}{4} - \frac{e^{-2ik_y}}{4}\right] dk_y \qquad \text{(E-2b)}$$

$$= L \lim_{\varepsilon \to 0} \left[\frac{1}{2} I_o(\varepsilon) - \frac{1}{4} I_{+L}(\varepsilon) - \frac{1}{4} I_{-L}(\varepsilon)\right] \qquad \text{(E-2c)}$$

Here ε is introduced to take care of the pole at $k_y = 0$.

First, let us consider $I_+(\varepsilon)$. By using Jordan's lemma:

$$I_{+L}(\varepsilon) = \sum \text{residues (at } i\varepsilon \text{ and possibly at } \alpha')$$

$$+ \int_{C_1+C_2} \frac{\sqrt{(k_y-\beta_1')(k_y-\beta_2')}}{k_y-\alpha'} \frac{e^{2ik_y}}{k_y^2} dk_y \qquad \text{(E-3a)}$$

$$= \sum \text{residues} + 2 \int_{C_1} \frac{\sqrt{(k_y-\beta_1')(k_y-\beta_2')}}{k_y-\alpha'} \frac{e^{2ik_y}}{k_y^2} dk_y \qquad \text{(E-3b)}$$

It should be noticed that ε^2 has been neglected in the contour integrals along C_1 and C_1+C_2. This is justified because along C_1 and C_2, ε^2 is always small compared to k_y^2 provided β_1' is not too close to the origin.

Applying Jordan's lemma again, we have

$$\int_{C_1} \frac{\sqrt{(k_y-\beta_1')(k_y-\beta_2')}}{(k_y-\alpha')} \frac{e^{2ik_y}}{k_y^2} dk_y = \int_{C} \frac{\sqrt{(k_y-\beta_1')(k_y-\beta_2')}}{(k_y-\alpha')} \frac{e^{2ik_y}}{k_y^2} dk_y$$

$$- \text{possible residue at } \alpha' \qquad \text{(E-4)}$$

Now:

$$\int_C \frac{\sqrt{(k_y-\beta_1')(k_y-\beta_2')}}{(k_y-\alpha')} \frac{e^{2ik_y}}{k_y^2}\, dk_y = \int_{\beta_1'}^{\infty} \frac{\sqrt{(k_y-\beta_1')(k_y-\beta_2')}}{(k_y-\alpha')} \frac{e^{2ik_y}}{k_y^2}\, dk_y \quad \text{(E-5a)}$$

$$= \int_{-\infty}^{\infty} \frac{e^{i(\beta_1'-\beta_2')\cosh t}(\cosh^2 t - 1)}{(\cosh t + \eta_1)(\cosh t + \eta_2)^2}\, dt\, \frac{e^{i(\beta_1' + \beta_2')}}{(\beta_2' - \beta_2')} \quad \text{(E-5b)}$$

To derive (E-5b), changes of variables have been used. Also, in (E-5b),

$$\eta_1 = \frac{\beta_1' + \beta_2' - 2\alpha'}{\beta_1' - \beta_2'}$$

$$\eta_2 = \frac{\beta_1' + \beta_2'}{\beta_1' - \beta_2'}$$

In (E-5b), factorization can be applied to the integrand. Thus, we need only consider integrals

$$I = \int_{-\infty}^{\infty} \frac{e^{i\beta \cosh t}}{\cosh t + \eta}\, dt \qquad \text{and} \qquad I' = \int_{-\infty}^{\infty} \frac{e^{i\beta \cosh t}}{(\cosh t + \eta)^2}\, dt = -\frac{\partial I}{\partial \eta}$$

"I" is still too difficult to evaluate. However, in most of the situations we now have, β is large. Thus, asymptotic expansions can always give us quite reasonable approximations, i.e.,

$$I \cong \frac{e^{i(\beta + \frac{\pi}{4})}}{\sqrt{\beta}} \sqrt{2\pi}\, \frac{1}{1+\eta} \left[1 + \frac{i}{2\beta(1+\eta)}\right] \quad \text{(E-6a)}$$

$$I' \cong \frac{\sqrt{2\pi}\, e^{i(\beta + \frac{\pi}{4})}}{\sqrt{\beta}} \frac{1}{(1+\eta)^2} \left[1 + \frac{i}{\beta(1+\eta)}\right] \quad \text{(E-6b)}$$

Combining (E-3), (E-4), (E-5), and (E-6), finally we have

$$I_{+L}(\varepsilon) \cong \sum \text{residues} - \frac{i}{4}\sqrt{2\pi}\, e^{i\frac{\pi}{4}} e^{2i(\beta_1 - k_{yo})L} \frac{\sqrt{\beta_1 - \beta_2}}{L^{5/2}(\beta_1 - k_{yo})^2(\beta_1 - \alpha)} \tag{E-7a}$$

A similar procedure will give us:

$$I_{-L}(\varepsilon) \cong \sum \text{residues} - \frac{i}{4}\sqrt{2\pi}\, e^{i\frac{\pi}{4}} e^{-2i(\beta_2 - k_{yo})L} \frac{\sqrt{\beta_1 - \beta_2}}{L^{5/2}(\beta_1 - k_{yo})^2(\beta_1 - \alpha)} \tag{E-7b}$$

As for $I_0(\varepsilon)$, we can follow the same procedure as either $I_+(\varepsilon)$ or $I_-(\varepsilon)$. Now a contour similar to $I_-(\varepsilon)$ is chosen to take care of $I_0(\varepsilon)$, i.e.

$$I_0(\varepsilon) = \sum \text{residues} - \int_1^\infty \frac{\sqrt{k_y^2 - 1}}{(k_y - \eta_1)(k_y - \eta_2)^2}\, dk_y \; \frac{4}{\beta_1' - \beta_2'} \tag{E-8a}$$

$$= \sum \text{residues} - \int_1^\infty \frac{k_y^2 - 1}{(k_y - \eta_1)(k_y - \eta_2)^2} \; \frac{1}{\sqrt{k_y^2 - 1}}\, dk_y \; \frac{4}{\beta_1' - \beta_2'} \tag{E-8b}$$

Factorization can be applied to the integrand in (E-8b). Thus, we need only consider integrals

$$J = \int_1^\infty \frac{dk_y}{(k_y - \eta)\sqrt{k_y^2 - 1}} \quad \text{and} \quad J' = \int_1^\infty \frac{dk_y}{(k_y - \eta)^2\sqrt{k_y^2 - 1}} = +\frac{\partial J}{\partial \eta}$$

Now the asymptotic expansion cannot be used any longer. We have to try to evaluate it exactly. After changing the variables, we get:

$$J = \int_0^\infty \frac{dx}{(x^2 - 2\eta + 1)}$$

$$= \int_0^\infty \frac{dx}{[(x-\eta) - \sqrt{\eta^2-1}\,][x-\eta) + \sqrt{\eta^2-1}]}$$

$$= \frac{1}{\sqrt{\eta^2-1}} \ln [-\eta + \sqrt{\eta^2-1}] \qquad \text{(E-9a)}$$

$$J' = \frac{-1}{\eta^2 - 1} \left[\frac{\eta}{\sqrt{\eta^2-1}} \ln(-\eta + \sqrt{\eta^2-1}) + 1\right] \qquad \text{(E-9b)}$$

So, finally we have

$$I_o(\varepsilon) = \sum \text{residues} + \frac{4}{\beta_1' - \beta_2'} \left\{ - \frac{\sqrt{\eta_1^2 - 1}}{(\eta_2 - \eta_1)^2} \ln(-\eta_1 + \sqrt{\eta_1^2 - 1}) - \frac{1}{\eta_1 - \eta_2} \right.$$

$$\left. + \frac{1}{\sqrt{\eta_2^2 - 1}} \frac{\eta_1\eta_2 - 1}{(\eta_1 - \eta_2)^2} \ln(-\eta_2 + \sqrt{\eta_2^2 - 1}) \right\}$$

$$= \sum \text{residues} + \left\{ - \frac{2\sqrt{(\beta_1 - \alpha)(\beta_2 - \alpha)}}{(\alpha - k_{yo})^2 L} \ln \left[\frac{-(\beta_1 + \beta_2 - 2\alpha) + 2\sqrt{(\beta_1 - \alpha)(\beta_2 - \alpha)}}{\beta_1 - \beta_2} \right] \right\}$$

$$- \frac{2}{(\alpha - k_{yo})L} + \frac{2(\beta_1 - k_{yo})(\beta_2 - k_{yo}) - (\alpha - k_{yo})(\beta_1 + \beta_2 - 2k_{yo})}{(\alpha - k_{yo})^2 \sqrt{(\beta_1 - k_{yo})(\beta_2 - k_{yo})}}$$

$$\times \ln \frac{-(\beta_1 + \beta_2 - 2k_{yo}) + 2\sqrt{(\beta_1 - k_{yo})(\beta_2 - k_{yo})}}{\beta_1 - \beta_2} \qquad \text{(E-9c)}$$

Now we can go back to consider those contributions due to the residues. Of course, depending on where α is, the result will be different. For the case we are considering, branch cuts I and II are in the regions I and III respectively. And α is found to be either in region II or IV. Thus, these are the regions we are going to discuss. We can use the same procedure as in Appendix C to get:

α in region II:

$$\sum \text{residues} = \frac{i\pi}{(\alpha-k_{yo})^2 L}\left\{\frac{\sqrt{(\beta_1-k_{yo})(\beta_2-k_{yo})}}{i}\left[-(\alpha-k_{yo})L + \frac{i}{2} - \frac{i(\alpha-k_{yo})(\beta_1+\beta_2-2k_{yo})}{4(\beta_1-k_{yo})(\beta_2-k_{yo})}\right] - \sqrt{(\alpha-\beta_1)(\alpha-\beta_2)}\,\frac{e^{2i(\alpha-k_{yo})L}}{2}\right\} \tag{E-10a}$$

α in region IV:

$$\sum \text{residues} = \frac{i\pi}{(\alpha-k_{yo})^2 L}\left\{\frac{\sqrt{(\beta_1-k_{yo})(\beta_2-k_{yo})}}{i}\left[-(\alpha-k_{yo})L + \frac{i}{2} - \frac{i(\alpha-k_{yo})(\beta_1+\beta_2-2k_{yo})}{4(\beta_1-k_{yo})(\beta_2-k_{yo})}\right] - \sqrt{(\alpha-\beta_1)(\alpha-\beta_2)}\left[1 - \frac{e^{-2i(\alpha-k_{yo})L}}{2}\right]\right\} \tag{E-10b}$$

Finally, we can combine (E-3), (E-7), and (E-10) to give the expression for $S_3(\alpha,k_{yo},L)$.

Of course, we can also use a contour similar to that for $I_+(\varepsilon)$ to evaluate (E-8). Then, although the results for either the branch cut part or the residue part will be somewhat different, the total result should be the same. However, in most of the examples which we are considering, $|\beta_2| >> |\beta_1|$ is generally true. The use of a contour similar to that for $I_-(\varepsilon)$ will make the contribution due to the branch cut negligible. And thus, further analyses can be significantly simplified.

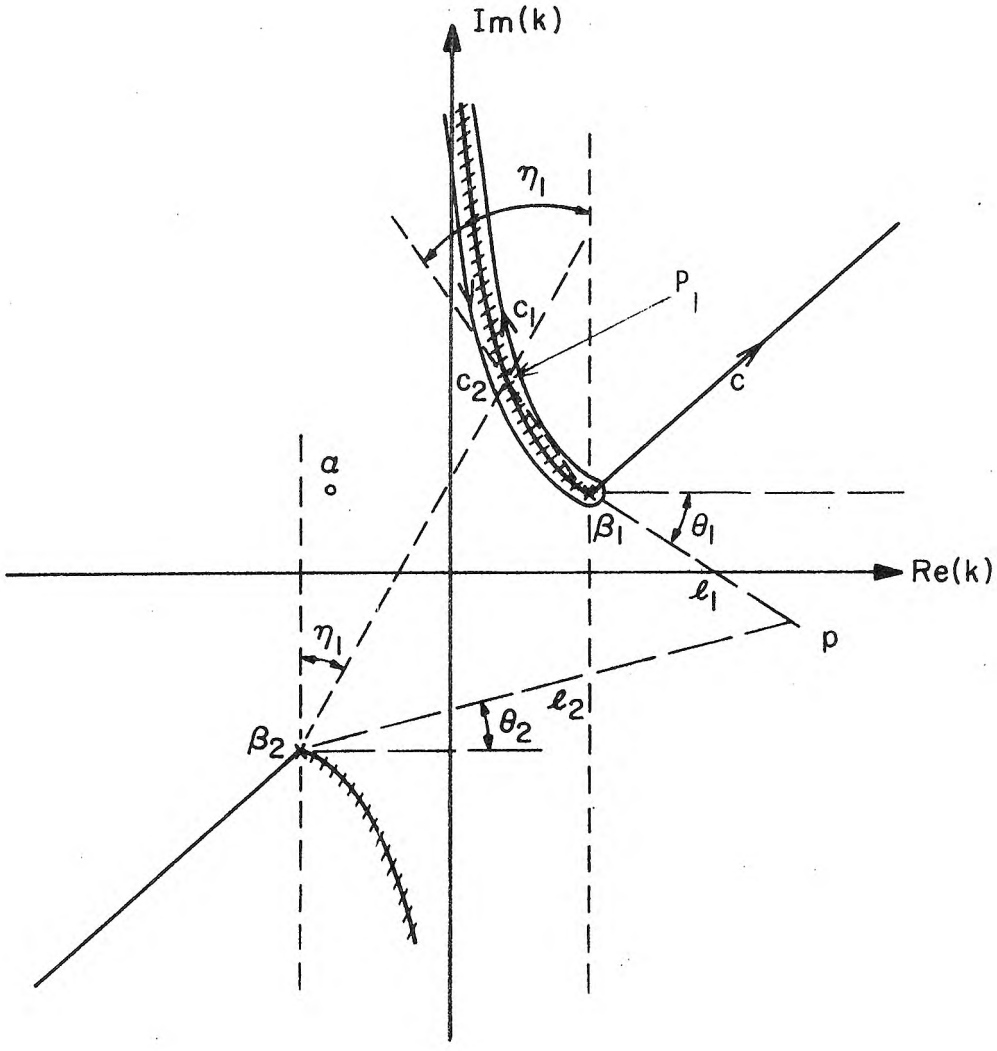
Im(k)
Re(k)
η_1
P_1
c_1
c_2
c
a
β_1
θ_1
ℓ_1
p
η_1
β_2
θ_2
ℓ_2

Fig. E-1

APPENDIX F

Results for Geometry (A-ii-2) with $|\tilde{K}_x|^2 = \frac{2}{\pi} \frac{\sin^2(k_y - k_{yo})L}{(k_y - k_{yo})^2}$

We apply Appendices C and E to (3.20a) and (3.21a) to get:

$$\overline{P} \cong \frac{-i\omega\mu_o}{2} \frac{2K_o^2}{\pi h_3} \left\{ \sum_{i=1,2,3,4} \left[\beta_i S_1(\alpha_i, k_{yo}, L) - \frac{\mu_o}{\sqrt{\mu_{2y}\mu_{2z}}\, h_3} \eta_i S_3(\alpha_i, k_{yo}, L) \right] \right\}$$

$$\overline{F}_y = \text{Re} \frac{-i\mu_o}{2} \frac{2K_o^2}{\pi h_3} \sum_{i=1,2,3,4} \left[\alpha_i \beta_i S_1(\alpha_i, k_{yo}, L) - \frac{\mu_o}{\sqrt{\mu_{2y}\mu_{2z}}\, h_3} \alpha_i \eta_i S_3(\alpha_k, k_{yo}, L) \right.$$

Here α_i are roots of $k_y^4 - \frac{\mu_o^2 k_y^2}{\mu_{2y}\mu_{2z} h_3^2} - i \frac{\mu_o^2 \sigma_x V}{\mu_{2y} h_3^2} k_y + i \frac{\mu_o^2 \sigma_x}{\mu_{2z} h_3^2} \omega = 0$

and $\beta_i = \prod_{j=1,2,3,4} \frac{\alpha_i^2}{(\alpha_i - \alpha_j)}$

$$\eta_i = \prod_{\substack{j=1,2,3,4 \\ j \neq i}} \frac{1}{(\alpha_i - \alpha_j)}$$

As for $\overline{F}_z$, it is much more complicated. However, the ideal source result can be used as a good approximation provided that $k_{yo}L$ is large.